NOVEL PHENYLAMINOTETRALIN (PAT) ANALOGS: MULTIFUNCTIONAL SEROTONIN 5HT2 RECEPTOR DRUGS FOR NEUROPSYCHIATRIC DISORDERS

By

ZHUMING SUN

A DISSERTATION PRESENTED TO THE GRADUATE SCHOOL
OF THE UNIVERSITY OF FLORIDA IN PARTIAL FULFILLMENT
OF THE REQUIREMENTS FOR THE DEGREE OF
DOCTOR OF PHILOSOPHY

UNIVERSITY OF FLORIDA

2010

To my mom and dad

ACKNOWLEDGMENTS

I thank Dr. Raymond Booth, as my mentor, who directed me through my graduate study. I thank Dr. Margaret James, Dr. Kenneth Sloan and Dr. Drake Morgan, for their effort as my committee members. I thank Dr. Neil Rowland and Dr. Joanna Peris for their collaboration on my research projects. I thank my colleagues who taught me bench work skills, gave me helpful suggestions and valuable information, provided me with necessary material for my experiments, and worked with me during my graduate study: Dr. Lijuan Fang, Dr. Adam Vincek, Dr. Myong Sang Kim, Dr. Clint Canal, Dr. Tania Cordova-Sintjago, Dr. Nancy Villa, Dr. Sashi Sivendren, Dr. Andrzej Wilczynski, Sean Travis, and Kondabolu Krishnakanth.

TABLE OF CONTENTS

page

LIST OF TABLES

LIST OF FIGURES

LIST OF ABBREVIATIONS

5HT	5-hydroxytryptamine, serotonin
αMSH	α-Melanocortin stimulating hormone
BAC	bovine adrenal chromaffin
cAMP	Adenosine 3',5'-cyclic monophosphate
CAR	Conditioned avoidance response
CMTB	8,9-dichloro-1-methyl-2,3,4,5-tetrahydro-1H-benzo[d]azepine
DAG	Diacylglycerol
DOI	2,5-dimethoxy-4-iodoamphetamine
EE	enantiomeric excess
GPCR	G protein-coupled receptor
IP3	Inositol trisphosphate
LSD	*D*-lysergic acid diethylamide
MCR	Melanocortin receptors
M-CPP	M-chlorophenyl piperazine
NAPT	(*R*,*R*)-*N*-(2-amino-1,2-diphenylethyl)-*p*-toluenesulfonamide
OCD	Obsessive-compulsive disorder
PAT	Phenylaminotrtralin; (–)-*Trans*-*N,N*-dimethyl-4-phenyl-1,2,3,4-tetrahydro-2-naphth-alenamine, (–)-*trans*-PAT.
PCC	pyridinium chlorochromate
PLC	Phospholipase C
PPA	polyphosphoric acid
R.T.	room temperature
TBDMS	tert-butyldimethylsilyl chloride
TMD	Transmembrane domain

Abstract of Dissertation Presented to the Graduate School
of the University of Florida in Partial Fulfillment of the
Requirements for the Degree of Doctor of Philosophy

NOVEL PHENYLAMINOTETRALIN (PAT) ANALOGS: MULTIFUNCTIONAL SEROTONIN 5HT2 RECEPTOR DRUGS FOR NEUROPSYCHIATRIC DISORDERS

By

Zhuming Sun

August 2010

Chair: Raymond Booth
Major: Pharmaceutical Science – Medicinal Chemistry

This Ph.D. thesis research describes drug discovery targeting serotonin 5HT2 G protein-coupled receptor (GPCR) subtypes. Brain 5HT2C receptor activation in humans leads to anti-obesity effects, antipsychotic effects, attenuation of psychostimulant addiction, and other psychotherapeutic effects. Meanwhile, brain 5HT2A receptor activation produces hallucinogenic effects and activation of peripheral 5HT2B receptors produces cardiac valvulopathy and pulmonary hypertension. Until our recent publication, there was no report of a 5HT2C receptor agonist that does not also activate 5HT2A and/or 5HT2B receptors. Thus, clinical 5HT2C receptor-based pharmacotherapy was hampered. We reported (-)-*trans*-*N,N*-dimethyl-4-phenyl-1,2,3,4-tetrahydro-2-naphthalenamine (phenylaminotetralin; PAT) as a full-efficacy agonist at human 5HT2C receptors and inverse agonist at 5HT2A and 5HT2B receptors. In addition to selective activation of the 5HT2C receptor, the pharmacotherapeutic potential of (-)-*trans*-PAT is promising given that 5HT2A inverse agonists are used clinically as antipsychotic drugs. Thus, the general goals of these Ph.D. thesis studies included facile routes for scale-up synthesis of (–)-*trans*-PAT for preclinical *in vivo* studies in rodents, as well as, design

and synthesis of PAT analogs with enhanced selective 5HT2C agonist potency and/or more potent 5HT2A and/or 5HT2B inverse agonist activity. In addition to development of pharmacotherapy for neuropsychiatric disorders and obesity, results are expected to help delineate 5HT2 GPCR structure and molecular requirements for activation for drug design purposes.

CHAPTER 1
BACKGROUND AND SIGNIFICANCE

5HT2 Receptors as Drug Targets

The biogenic amine Serotonin (5-hydroxytryptamine, 5HT, **Fig. 1-1**) regulates a wide range of central and peripheral psychological and physiological effects through activation of fourteen mammalian 5HT receptor subtypes that are grouped into the 5HT1–5HT7 families. The 5HT2 receptor class has three subtypes: 5HT2A, 5HT2B and 5HT2C (Roth et al.,1998; Sanders-Bush et al.,2006). They associate with $G\alpha_q$ before activate phospholipase (PL) C. This enzyme hydrolyses phospholipids, yielding inositol phosphates and diacylglycerol (DAG). Inositol trisphosphate (IP3) acts to liberate Ca^{2+} from intracellular stores, resulting in depolarization of the neuron. In addition, DAG activates protein kinase C, which can indirectly modulate the activity of ion channels (Raymond et al., 2001; Turner & Raymond, 2006, Lam et al., 2007).

5HT2A, 5HT2B and 5HT2C Receptors Physiological Roles

5HT2A receptors are broadly distributed in CNS. Hallucinogens such as *D*-lysergic acid diethylamide (LSD) exert their psychedelic effect mainly by activation of 5HT2A receptors (Glennon, 1990; Sanders-Bush et al., 2006). Meanwhile, 5HT2A antagonist/inverse agonist activity is shared by most atypical antipsychotics (e.g., clozapine, olanzapine, ziprazidone) and is thought to partially explain their therapeutic properties in schizophrenia (Weiner et al., 2001; Shapiro et al., 2003; Roth et al., 2004; Davies et al., 2004). 5HT2B receptor mRNA and protein are also present in human brain (Kursar et al., 1994) although its role in the CNS remains unclear. Peripherally, 5HT2B activation can lead to valvular heart disease (Fitzgerald et al., 2000; Rothman et al., 2000; Roth, 2007) and pulmonary hypertension (Launay et al., 2002). 5HT2B

receptor was first identified in rat stomach fundus (Foguet et al., 1992). In the 1990's 5HT2B selective antagonists were regarded as tool for the treatment of irritable bowel syndrome (IBS) but recent publications on this field are limited (Wainscott et al., 2004, Giorgioni et al., 2005). The human 5HT2C receptor (Lubbert et al., 1987,Saltzman et al., 1991) is found exclusively in the central nervous system where it is widely expressed and putatively involved in several (patho)- physiological and psychological processes i.e. ingestive behavior (Tecott et al., 1995), psychosis and response to schizophrenia pharmacotherapy (Reynolds et al., 2005; Siuciak et al., 2007; Marquis et al., 2007), motor function (Heisler and Tecott, 2000; Segman et al., 2000), cocaine addiction (Bubar and Cunningham, 2006; Muller and Huston, 2006), anxiety (Sard et al., 2005,Heisler et al., 2007), depression (Palvimaki et al., 1996; Rosenzweig-Lipson et al., 2007), epilepsy (Heisler et al., 1998), and sleep homeostasis (Frank et al., 2002).

Contemporary receptor theory classifies ligands as agonists, inverse agonists and antagonists. Constitutive activity of a receptor is defined as its ability to activate cellular signaling pathways in the absence of an agonist (Leff et al., 1997). In several *in vitro* systems 5HT2A and 5HT2C receptors demonstrate constitutive activities and inverse agonism (Aloyo et al., 2009), but the role of constitutive activity *in vivo* is not clear (Li et al., 2009).

5HT2C Receptors in Obesity

There are many studies documenting the importance of 5HT2C receptor regulation of body weight in rodents and humans (Bickerdike et al., 1999). Non-selective 5HT2 agonists **(Fig. 1-1)** such as *m*-CPP and RO 600175 are known to reduce food intake and lead to weight loss in rodents (Halford et al., 2005) and the anti-obesity effects are diminished if a 5HT2C antagonist is pre-administered (Schreiber et al., 2002). The

5HT2C knockout mouse demonstrates increased feeding and obesity, and, resistance to the anorectic effects of *S*-(+)-fenfluramine (Tecott et al., 1995; Vickers et al., 1999; 2001; Heisler et al., 2002). The now banned weight-loss drug, *S*-(+)-fenfluramine (*d*-fenfluramine), produces sustained weight loss of about 10% in humans (Tecott et al., 1995; Mccann et al., 1997; Vickers et al., 2001). *S*-(+)- and (±)-Fenfluramine promote serotonin release (Rothman et al., 1999) and both were banned by the US Food and Drug Administration in 1997 because fenfluramines and the metabolite *S*-(+)-norfenfluramine cause activation of 5HT2B receptors that can lead to valvular heart disease (Fitzgerald et al., 2000; Setola et al., 2005) and/or pulmonary hypertension (Launay et al., 2002)–fatalities have resulted. Other 5HT2C agonists continue to be developed as weight-loss drugs, including lorcaserin (Smith et al., 2008; Thomsen et al., 2008).

Mechanistic Model for Serotonergic Regulation of Food Intake

The 5HT2C receptor is highly expressed in the arcuate nucleus of the hypothalamus, an area known to be important for appetite and feeding. The 5HT2C receptor exerts regulatory control of melanocortin signaling. Stimulation of 5HT2C receptors by indirect agonists such as *S*-(+)-fenfluramine induce α-melanocortin stimulating hormone (αMSH) release. αMSH interacts with melanocortin receptors (MCR) 3 and 4 to alter energy homeostasis. This circuit is modeled in **Fig. 1-2** (Heisler et al., 2002, 2007).

5HT2A and 5HT2C Receptors in Psychiatric Disorders

Serotonergic neurons innervate virtually all parts of the central nervous system. In the ventral tegmental area and substantia nigra, dopamine (DA) neurons receive projections from serotonin-containing cell bodies (Herve et al, 1987; Hoyer et, al., 1994).

The precise elucidation of the interaction between 5HT and DA systems, as well as the pharmacological evaluation is an ongoing task, some recent reviews are listed here (Esposito 2006; Fink et al., 2007; Gruender et al, 2009).

Antagonist/inverse agonist activity at 5HT2A receptor is shared by most atypical antipsychotics (e.g., clozapine, olanzapine, ziprazidone) and partially contributes to their therapeutic properties in schizophrenia (Weiner et al., 2001; Schapiro et al., 2003; Roth et al., 2004; Davies et al., 2004). In contrast, agonist activity at 5HT2A receptors is displayed by hallucinogenic drugs such as lysergic diethylamide (LSD), psilocybin and mescaline.The 5HT2A receptor signaling is necessary for their psychotomimetic properties (Nichols, 2004). It is proposed that antipsychotic drugs with enhanced 5HT2A receptor antagonist/inverse agonist activity compared to dopamine D2 antagonist activity may cause less extrapyramidal movement disorder side effects (Horacek et al., 2006).

Historically, little attention was paid to specific interactions of 5HT2C receptors and antipsychotic clinical agents. It was revealed later that some atypical as well as some conventional antipsychotics, in fact, have high affinity at 5HT2C receptors (Horacek et al., 2006). Research on 5HT2A/2C receptors as potential antipsychotic drug targets currently is focused on 5HT2A inverse agonists, 5HT2C agonists, and ligands with both 5HT2A/2C inverse agonist activities.

Ligands with 5HT2A Inverse Agonism and/or 5HT2C Agonism for Psychoses, Depression, and Psychostimulant Abuse

The mRNA for 5HT2C receptors is abundant in the nucleus accumbens and ventral tegmentum which are limbic system structures that integrate emotional function.

Recent literature suggests 5HT2C receptors in the limbic system may be involved in symptoms of psychosis, depression, and psychostimulant addiction (Eltayb et al., 2007; Marquis et al., 2007). For example, non-selective 5HT2C receptor agonists such as *m*-chlorophenyl piperazine (*m*-CPP, **10**) and RO 60–0175 (**7**) have been reported to show antipsychotic-like effects in animal models of schizophrenia (Browning et al.,1999; Grauer et al.,2004). Recently, WAY163909 (**16**), a 5HT2C agonist, showed antipsychotic and anti-depressant activity in several rodent models (Dunlop et al., 2006; Marquis et al., 2007). Another 5HT2C agonist CP809-101 (**12**) also was reported to improve cognitive function associated with schizophrenia in animal models (Siuciak et al., 2007).

Some conventional antipsychotics (chloropromazine, mesoridazine and loxapine) have high affinities for 5HT2C receptors (Horacek et al., 2006). Blockade of 5HT2 receptors along with dopamine D2 receptors has been proposed as a strategy for antipsychotic drug design (Meltzer et al., 2003, 2004). However, studies have revealed that 5HT2C antagonism or inverse agonism elevates limibic dopamine levels. In animal models (Di Matteo et al., 2001), 5HT2C antagonism that increases dopamine concentration in brain produces hyperlocomotion that correlates with psychotic-type activity. Also, animals receiving 5HT2C antagonists show disfunction in information processing (Hutson et al., 2000). Predictably, 5HT2C blockade also is directly associated with weight gain as an adverse effect of some antipsychotics (Ellingrod et al., 2005; Miller et al., 2005; 2009).

Nevertheless, some drugs with inverse activity at both 5HT2A and 2C receptors have demonstrated efficacy for certain psychoses. For example, the 5HT2A/2C inverse

agonist ACP-103 (pimavanserin) entered Phase III trials for the treatment of psychoses associated with Parkinson's disease. However, results did not meet expectations (not specified) and the study was discontinued (Clinical trials, 2009).

There is also preclinical evidence that 5HT2C receptors modulate psychostimulant effects. For example, cocaine- and amphetamine-induced locomotor activity in rats is blocked by 5HT2C agonists (Grottick et al, 2000). In contrast, 5HT2C antagonists enhance locomotor stimulant effects induced by amphetamine and other drugs that release and/or inhibit reuptake of dopamine (Fletcher, 2006) .The effect of 5HT2C antagonists on psychostimulant effects and baseline locomotion correlates with their effect on dopamine efflux and dopamine neuronal firing. On the other hand, 5HT2C receptor agonists produce the opposite effect–suppressing dopamine release and dopamine neuronal firing (Weiner, 2001).

In other studies, the non-selective 5HT2 agonist RO60175 (Porter et al., 1999), reduces the rate of cocaine self-administration in rats and this effect is blocked selectively by the 5HT2C antagonist SB242084 (Bromidge et al., 1997). Correspondingly, SB242084 increases the rate of cocaine self-administration in rats in a dose-dependent manner (Fletcher et al., 2002).

Targeting the 5HT2C Receptor in Drug Discovery

As indicated above, it has been recognized for about 10-years that the 5HT2C receptor holds great promise as a pharmacotherapeutic target for neuropsychiatric disorders and obesity. However, 5HT2C receptor-selective drugs still are not available. The biggest challenge regarding drug discovery targeting the 5HT2C receptor is that this GPCR shares a transmembrane domain (TMD) sequence identity of about 80% with the 5HT2A receptor and about 70% with the 5HT2B receptor (Julius et al., 1988;

1990). The highly conserved TMDs and similar second messenger coupling has made development of ligands selective for the 5HT2C receptor especially difficult. As mentioned, activation of 5HT2A receptors induces LSD (d-lysergic acid diethylamide)-like hallucination and stimulant effects. Activation of peripheral 5HT2B receptors leads to valvular heart disease and pulmonary hypertension, as is the case of the indirect and nonselective 5HT agonist *S*-(+)-fenfluramine. Thus, for clinical purposes, there is no tolerance for activation of 5HT2A and/or 5HT2B receptors—absolutely selective activation of 5HT2C is required.

Design of Selective 5HT2C Agonists: A Brief Review of Ligand Structures and Their 5HT2-Type Activity

In the absence of X-ray crystal structure data for any of the serotonin 5HT2 GPCRs, 5HT2C agonist drug design has focused on a ligand-based approach. This section includes a brief summary of the compounds reported in the literature as the candidate selective 5HT2C agonists over the last 10-years. Structures are shown in **Fig. 1-3 – 1-10** and *in vitro* pharmacological data are summarized in **Table 1-1 – 1-2.** The discussion focuses on comparing the structures of putative 5HT2C agonists described in the literature with (–)-*trans*-*N,N*-dimethyl-4-phenyl-1,2,3,4-tetrahydro-2-naphthalenamine (1-phenyl-3-dimethylaminotetralin; PAT; **30**), the only ligand reported so-far that demonstrates full-efficacy agonist activity at human 5HT2C receptors while showing inverse agonist activity at 5HT2A and 5HT2B receptors i.e., (–)-*trans*-PAT is an absolutely selective 5HT2C agonist (Booth et al., 2009).

Classic Nonselective 5HT2 Agonists

The endogenous agonist 5HT (**1**), of course, is non-selective and activates all 5HT receptors. Meanwhile, DOI (2,5-dimethoxy-4-iodoamphetamine, **2**) is the archetype of

agonist molecules that target 5HT2 receptors, albeit, nonselectively. As mentioned, *S*-(+)-norfenfluramine (**3)** is the major metabolite of the indirect 5HT agonist *S*-(+)-fenfluramine, and, shows highest agonist potency at 5HT2B compared to 5HT2A and 5HT2C receptors. These agonist ligands all possess the highly flexible arylethylamine motif. The amine moiety of (–)-*trans*-PAT (**30**) and its analogs, however, is attached equatorially to the tetrahydronaphthalene (Wyrick et al 1993), that greatly restricts flexibility.

3-Substituted Indole Analogues

Tryptamine (**4**) is a non-selective 5HT2 agonist and the structural analog BW723C86 (**5**) also activates all three 5HT2 receptor types (Porter et al; 1999). The tryptamine analog 1-methylpsilocin (**6**), is a member of a group of derivatives called psilocins. It is a partial agonist at 5HT2A and 5HT2C receptors. In a mouse model of obsessive-compulsive disorder (OCD), 1-methylpsilocin reduced scratching after IP administration, an effect attributed to *in vivo* 5HT2C agonism (Sard et al.,2005).

Molecular modeling was performed to closely compare the structural similarities between 1-methylpsilocin and (–)-*trans*-PAT (**Fig. 1-5**, Wilczynski and Booth, unpublished data, 2009). 1-Methylpsilocin and (–)-*trans*-PAT share structural overlap when the flexible amine side chain of 1-methylpsilocin is in the energy minimized conformation. The absence of a pendant phenyl group in the 1-methylpsilocin compound may explain its partial agonist activity at 5HT2C receptors in comparison to (–)-*trans*-PAT, which, is a full efficacy agonist at 5HT2C receptors (Booth et al., 2009).

N-substituted Indole Analogues

RO600175 (**7**) was originally reported as a selective 5HT2C agonist (Martin et al., 1998). Subsequently, it has been determined that RO600175 also is a 5HT2B full

efficacy agonist (Porter et al., 1999). Pyrroloisoquinoline-type derivatives of RO600175 having an *N*-propylamine -substituted indole core structure recently were synthesized and reported (Adams et al., 2006). Ver 2692 (**8**), was reported as a potent 5HT2C agonist. However, it also activates 5HT2A and 5HT2B receptors. In the original report, Ver 2692 was orally administered to rats, and the author observed significant food intake reduction, but, no data was presented (Adams et al., 2006).

The amine moiety of Ver 2692 in the energy minimized conformation and the dimethylamine moiety of (–)-*trans*-PAT superimposed very closely (**Fig. 1-7**; Wilczynski and Booth, unpublished data, 2009). Given the very high affinity of Ver 2692 for the 5HT2C receptor (Ki=2nM), the preliminary molecular modeling data suggests the PAT amine moiety already is at the optimal orientation held fixed by the tetrahydronaphthyl scaffold. Although Ver 2692 has high 5HT2C affinity and efficacy, it does not have 5HT2 subtype selectivity—the notable absence of a pendant phenyl ring in the Ver 2692 molecule that is equivalent to the PAT phenyl ring may account for the lack of 5HT2 selectivity of Ver 2692. Also, the Ver 2692 flexible propylamino sidechain may interact with 5HT2 receptors in a conformation different than the global energy minimum conformation, perhaps, contributing to relatively poor 5HT2 selectivity profile in comparison to the more rigid (–)-*trans*-PAT.

Another series of indole derivates related to RO600175 includes YM348 (**9)** where the indole core is replaced by bioisostere indazole ring system (Shimada et al., 2008). YM348 is a 5HT2A and 5HT2B agonist and a 5HT2C partial agonist. After oral administration in rats, it produces penile erection, hypo-locomotion, and a transient decrease in food intake—these effects are blocked by a 5HT2C antagonist (Kimura et

al., 2004; Hayashi et al., 2005). YM348 is not selective and activates 5HT2A and 5HT2B receptors as well as 5HT2C receptors. In summary, the *N*-substituted indole ring and its bioisostere systems are not suitable as scaffolds for development of selective 5HT2C agonists.

M-CPP and Piperazine Analogues

Meta-chlorophenylpiperazine (*m*-CPP **10**) is a classic non-selective 5HT2 agonist. A new series of 5HT2C agonists based on the *m*-CPP scaffold was synthesized by fusing the piperazine and aryl rings using ethylene as bridge. It was reported that compound **11** reduced food intake in Wistar rats (Rover et al., 2005).

Other compounds structurally related to *m*-CPP that recently emerged from a high-throughput screening study include CP-809,901 (**12**). CP-809,901 is a potent 5HT2C full agonist (Siuciak et al., 2007). CP-809,901 is active in an animal model of cognitive function, but is inactive in two animal models of antidepressant-like activity. In addition to 5HT2C receptors, CP-809,901 also activates 5HT2A and 5H2B receptors. Thus hallucination and valvular heart disease side effects are predicted to occur with *in vivo* administration in humans—accordingly, drug development of CP-809,901 was discontinued (Liu et al., 2010).

Another *m*-CPP derivative, WAY161503 (**13**)**,** was reported in 2006 (Rosenzweig et al). The tricyclic core structure could be viewed as an amide bridge fusing the aryl and piperazine groups. WAY161503 is an agonist both at 5HT2A and 5HT2B receptors. The affinity of WAY161503 for 5HT2A, 5HT2B, and 5HT2C receptors (Ki ~20, 60, and 30 nM) in comparison to (–)-*trans*-PAT (Ki ~400, 1,000, and 40 nM) indicates the WAY compound has much higher affinity at 5HT2A and 5HT2B receptors, and about equivalent affinity at 5HT2C receptors. The *S*-enantiomer, WAY-161504, is about 100-

fold less potent at activating 5HT2C receptors, with no improvement in receptor subtype selectivity.

Significant overlap can be seen in alignment of (–)-*trans*-PAT and WAY161503 (**Fig. 1-9**; Wilczynski and Booth, unpublished data, 2009), especially, with regard to the PAT tetrahydronaphthyldimethylamine and WAY dichlorotetrahydropyrazinoquinoxalinone moieties. Molecular modeling indicates the NH-moiety of WAY-161503 superimposes closely with $N(CH_3)_2$ group of (–)-*trans*-PAT, so they might occupy similar 3D space in the 5HT2C active site. The most significant difference between WAY-161503 and (–)-*trans*-PAT is the absence of a pendant phenyl moiety in the WAY molecule. It is proposed that the PAT pendant phenyl ring provides for its selective 5HT2C agonism and 5HT2A/5HT2B antagonism (Booth et al., 2009).

Benzodiazepinoindole Analogues

WAY629 (**14**) was identified as a 5HT2C agonist structure in high throughput screening studies (Sabb et al 2004). WAY629 contains an *N*-ethylamine substituted indole motif. WAY629 has 45-fold selectivity regarding binding at the 5HT2C versus 5HT2A receptors. In functional assays, WAY629 is an agonist at 5HT2A and 5HT2C receptors, however, it is 610-fold more potent at the 5HT2C receptor. Unfortunately, affinity and function data for WAY629 at the 5HT2B receptors were not reported. The di-hydrogenated compound WAY162545 (**15**) (racemate) and the (*R,R*)-enantiomer WAY 163909 (**16**) were reported as 5HT2C agonists (Dunlop et al., 2005). These compounds do not activate 5HT2A receptors, however they are 5HT2B partial agonists. WAY 163909 reduces food intake in normal and obese rats and this effect is blocked by 5HT2C antagonist. In rodent models, WAY-163909 has antidepressant activity and reduces impulsivity (Rosenzwig-Lipson et al., 2007; Navarra et al., 2008). WAY-163909

also activates 5HT2B receptors suggesting that it may cause cardiotoxicity, thus, it is not suitable for development as a human therapeutic.

There is not a high degree of structural similarity between (–)-*trans*-PAT and WAY-163909 (RMS=0.52±0.35 Å) (**Fig**. **1-11**; Wilczynski and Booth, unpublished data, 2009). The pendantcyclopentyl group of WAY-163909, held in a nearly co-planar fixed conformation relative to the octahydrocyclopenta-diazepinoindole nucleus, shares no structural counterpart in the (–)-*trans*-PAT molecule. Importantly, the cyclopentyl group, unlike the phenyl moiety of (–)-*trans*-PAT, is not capable of forming π-π stacking binding interactions with protein aromatic amino acids. Thus, the WAY-163909 pendant cyclopentyl group likely provides only steric bulk in the binding pocket of 5HT2 receptors, perhaps accounting for the compound's low 5HT2 receptor affinity and selectivity. Mutational analysis and molecular modeling studies of the 5HT2A receptor indicate important π–π stacking binding interactions occur between phenyl moieties of ligands and receptor amino acids in TMDs 5 & 6 (Choudhary et al., 1993; Shapiro et al., 2000).

Benzazepines

Benzazepines derivatives were first reported in 2005 (Smith et al., 2005). The (*S*)-enantiomer of 8,9-dichloro-1-methyl-2,3,4,5-tetrahydro-1H-benzo[d]azepine (CMTB) (**17**) and lorcaserin [(1*R*-(+)-8-chloro-2,3,4,5-tetrahydro-1-methyl-1H-3 benzazepine] (**18**) are underwent development as 5HT2C agonists.

(*S*)-CMTB is a partial agonist at 5HT2A receptors and nearly a full agonist at 5HT2C receptors. (*S*)-CMTB has low potency partial agonism at 5HT2B receptors. After oral administration to rats, (*S*)-CMTB reduces food intake over a 6-hour period with an EC_{50} value reported as 40 mg/kg.

The benzazepine lorcaserin is a nonselective 5HT2C agonist with significant activation of 5HT2A receptors (75% efficacy) and 5HT2B receptors (100% efficacy) (Jensen, 2006; Smith et al., 2006; Thomsen et al., 2008). Affinity of lorcaserin for 5HT2C receptors (Ki~15 nM) is only about 7.5-times higher than at 5HT2A receptors (Ki~112 nM), thus, activation of both receptors is likely *in vivo*, with possible 5HT2A receptor-mediated psychiatric and cardiovascular effects. Affinity of lorcaserin for human 5HT2C over 5HT2B receptors (Ki~174 nM) is a modest 12-times, suggesting, cardiopulmonary problems could occur as a result of *in vivo* 5HT2B receptor activation. Nevertheless, lorcaserin underwent a large 2-year phase-3 clinical trial (Olmos, 2009). Except for headache/dizziness (18% for lorcaserin, 11% for placebo), incidence of other central nervous system or psychiatric side-effects (e.g., 5HT2A-mediated) has not been disclosed. Echocardiograms performed at baseline and at the end of the 2-year trial, however, suggested no drug effect on heart valves or pulmonary artery pressure. The main problem with the lorcaserin clinical trial is efficacy—placebo adjusted weight-loss was just 3.6% and this was judged to be not impressive (Goldstein, 2009). Increasing the dose of lorcaserin to boost anorexia/weight-loss efficacy likely will result in 5HT2A-mediated psychiatric and cardiovascular side effects, as well as, 5HT2B-mediated cardiopulmonary toxicity.

Recently, another series of benzazepine analogs was reported as selective 5HT2C agonists (Shimadaet al., 2008). These compounds have the same benzazepine ring as locarserin without the1-methyl group. Compound **19** was regarded as the most promising one with a 10-fold of selectivity to 5HT2C over 5HT2A. Compound **19** was a 5HT2A partial agonist, its 5HT2B functional data has not been reported yet.

Design of Selective 5HT2C Agonists: (-)-*Trans*-PAT as a Lead Molecule

As suggested by information summarized in the preceding section, with the exception of (–)-*trans*-PAT **30** (Booth et al., 2009), there are no compounds reported in the literature that activate 5HT2C receptors without also activating 5HT2A and/or 5HT2B receptors. Thus, a marketable 5HT2C agonist drug has not come forth due to liability associated with activation of 5HT2A receptors that can lead to hallucinations and frank psychosis (Nichols, 2004) and/or activation of 5HT2B receptors that can lead to cardio-pulmonary toxicity (Fitzgerald et al., 2000; Launay et al., 2002; Setola et al., 2005).

(-)-*Trans*-PAT, **30** is a stereoselective, high affinity (Ki=40nM), high potency (EC_{50}=20nM) full efficacy agonist at the human 5HT2C receptor. At 5HT2A and 5HT2B receptors, (-)-*trans*-PAT is an inverse agonist (IC_{50}=490 and 1000 nM, respectively) and competitive antagonist (K_B=460 and 1400 nM, respectively) of serotonin (Booth et al., 2009).Thus, drug discovery using (-)-*trans*-PAT as a lead molecular chemical scaffold may provide high potency, truly selective 5HT2C agonists

Table 1-1. List of *in vitro* biological data of published compounds (1)

Section name	5HT2A	5HT2B	5HT2C
5HT **1**	pEC_{50}=7.51	pEC_{50}=8.68	pEC_{50}=8.24
DOI **2**	pEC_{50}=9.05 E_{max}=61%	pEC_{50}=8.85 E_{max}=65%	pEC_{50}=8.10 E_{max}=57%
Nor-*d*-fenfluramine **3**	pEC_{50}=5.98 E_{max}=54%	pEC_{50}=8.06 E_{max}=66%	pEC_{50}=6.77 E_{max}=77%
Tryptamine **4**	pEC_{50}=6.59 E_{max}=71%	pEC_{50}=7.53 E_{max}=92%	pEC_{50}=7.34 E_{max}=71%
BW723C86 **5**	pEC_{50}=6.66 E_{max}=43%	pEC_{50}=8.97 E_{max}=83%	pEC_{50}=7.03 E_{max}=51%
1-Methylpsilocin **6**	E_{max}=31% EC_{50}=633 nM		E_{max}=12% EC_{50}=12 nM
RO600175 **7**	pEC_{50}=6.35 E_{max}=69%	pEC_{50}=9.05 E_{max}=79%	pEC_{50}=7.49 E_{max}=84%
Ver 2692 (PIP) **8**	*K*i=31nM (Displace [^{125}I]DOI) EC_{50}=32 nM E_{max}=88%	*K*i=12nM (Displace [^{3}H]5HT) EC_{50}=1.1 nM E_{max}=65%	*K*i=1.6nM (Displace [^{3}H]5HT) EC_{50}=2.9 nM E_{max}=99%
YM 348 **9**	EC_{50}=93 nM E_{max}=97%	EC_{50}=3.2 nM E_{max}=110%	EC_{50}=1 nM E_{max}=76%
m-CPP **10**	pEC_{50}=6.65 E_{max}=22%	pEC_{50}=7.2 E_{max}=24%	pEC_{50}=7.09 E_{max}=65%
(4R,10aS)-7-Chloro-4,6-dimethyl-1,2,3,4,10,10a-hexahydropyrazino[1,2-a]indole **11**	*K*i=40nM (Displace [^{125}I]DOI)	*K*i=19nM (Displace [^{3}H]5HT)	*K*i=1.9nM (Displace [^{3}H]5HT) E_{max}=97%
CP-809,101 **12**	*K*i=6nM (Displace [^{125}I]DOI) EC_{50}=153 nM E_{max}=67%	*K*i=64nM (Displace [^{3}H]5HT) EC_{50}=65.3 nM E_{max}=57%	*K*i=1.6nM (Displace [^{3}H]5HT) EC_{50}=0.11nM E_{max}=93%

Table 1-2. List of *in vitro* biological data of published compounds (2)

Section name	5HT2A	5HT2B	5HT2C
WAY 161503 **13**	*K*i=18 nM (Displace [^{125}I]DOI) EC_{50}=501 nM Partial agonist	*K*i=60 nM (Displace [^{3}H]5HT) EC_{50}=19.5 nM full agonist	*K*i=32 nM Displace [^{3}H]mesulergine EC_{50}=39.8 nM full agonist
WAY629 **14**	*K*i=2530nM (Displace [^{125}I]DOI) EC_{50}=260,000nM E_{max}=60%		*K*i=56nM (Displace [^{125}I]DOI) EC_{50}=426nM E_{max}=90%
WAY162545 **15**	*K*i=136 nM (Displace [^{125}I]DOI) No activity	*K*i=2101 nM (Displace [[^{125}I]DOI) EC_{50}=563 nM E_{max}=40%	*K*i=385 nM Displace [^{3}H]mesulergine EC_{50}=39.nM E_{max}=85%
WAY163909 **16**	*K*i=212 nM (Displace [^{125}I]DOI) No activity	*K*i=485 nM (Displace [[^{125}I]DOI) EC_{50}=185 nM E_{max}=40%	*K*i=221 nM Displace [^{3}H]mesulergine EC_{50}=8 nM E_{max}=90%
(***S***)-CMTB **17**	EC_{50}=135 nM E_{max}=35%	EC_{50}=10 μM E_{max}=25%	EC_{50}=3 nM E_{max}=90%
Lorcaserin **18**	*K*i=112 nM (Displace [^{125}I]DOI) EC_{50}=168 nM E_{max}=75%	*K*i=174 nM (Displace [^{125}I]DOI) EC_{50}=943 nM E_{max}=100%	*K*i=15 nM (Displace [^{125}I]DOI) EC_{50}=9 nM E_{max}=100%
6,7-dichloro-2,3,4,5-tetrahydro-1***H***-3-benzazepine **19**	*K*i=93 nM (Displace [^{3}H]5HT) E_{max}=27%	*K*i=100 nM (Displace [^{3}H]5HT)	*K*i=8.8 nM (Displace [^{3}H]5HT) E_{max}=87%

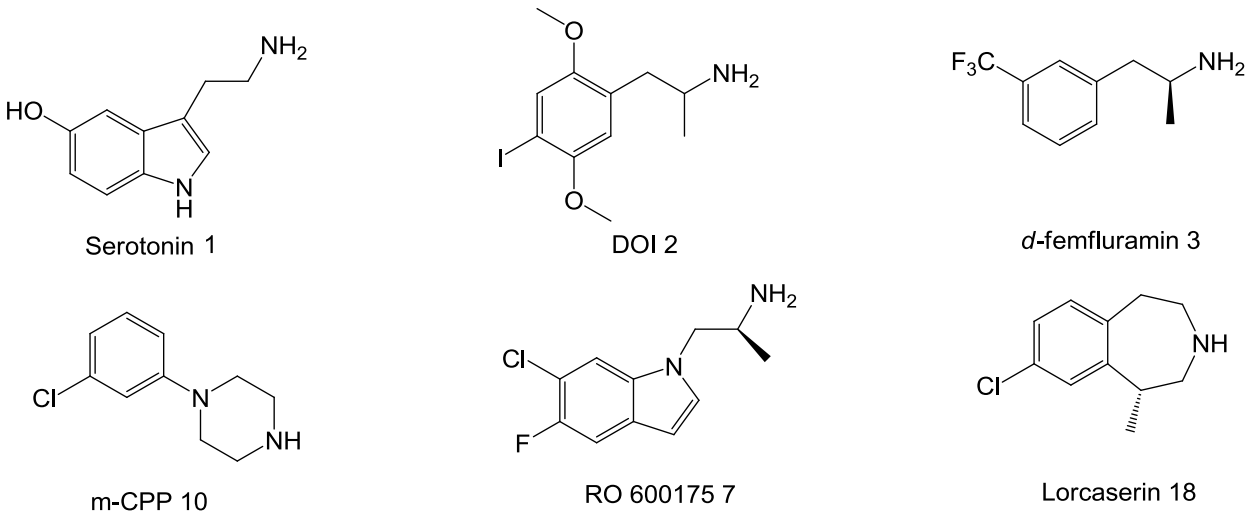

Figure 1-1. Structures of some published 5HT2 agonists

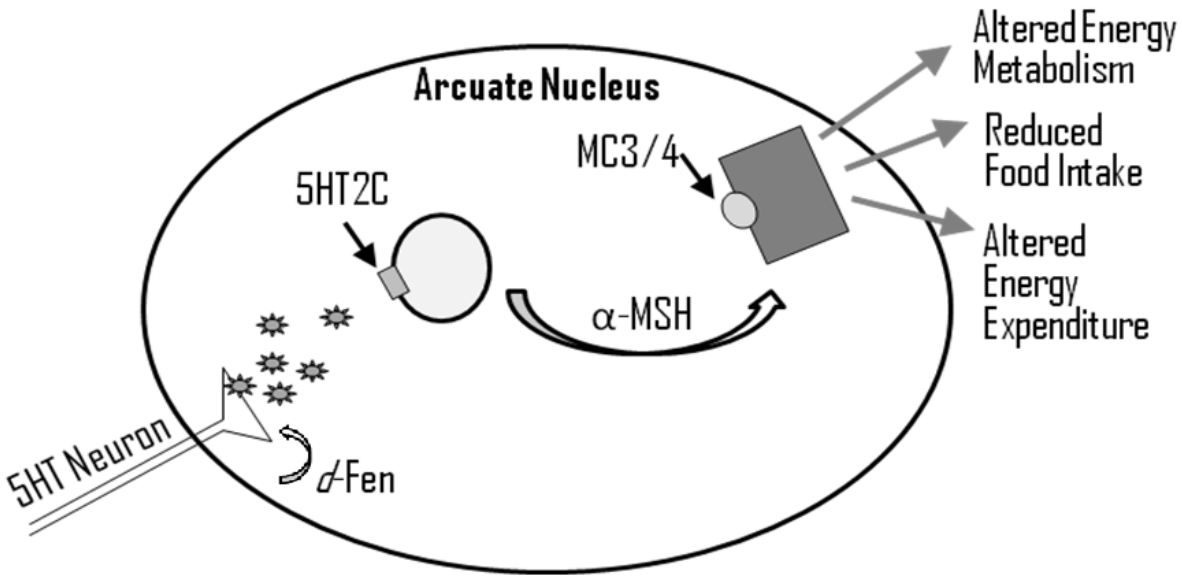

Figure 1-2. S-(+)-Fenfluramine triggers 5HT release, leads to 5HT2C receptors activation in arcuate hypothalamic nucleus, regulates downstream melanocortinergic signaling

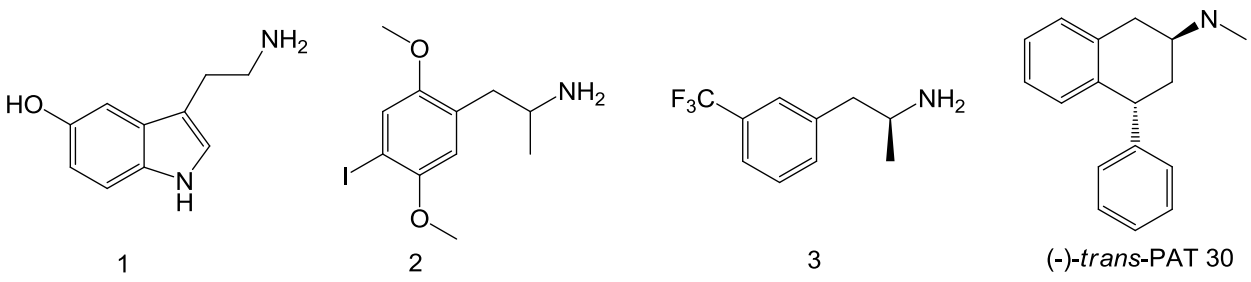

1 2 3

Figure 1-3. Classic nonselective 5HT2 agonists

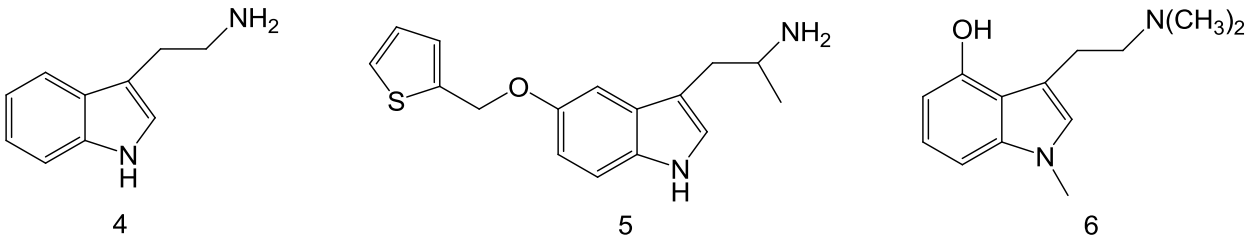

4 5 6

Figure 1-4. 3-Substituted indole analogues

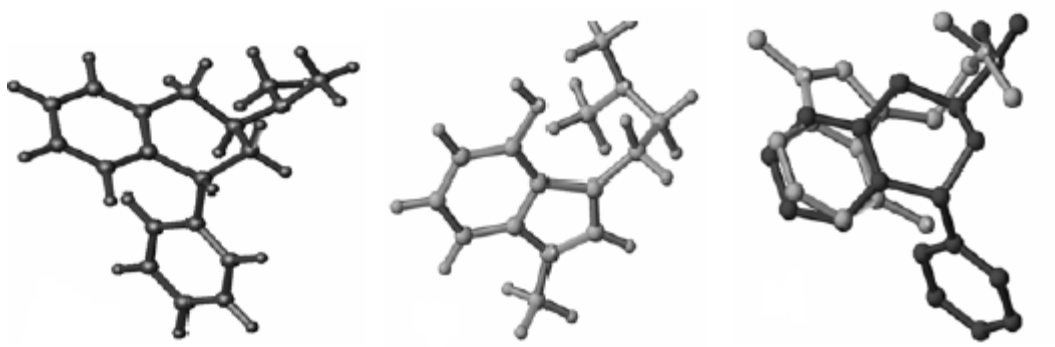

(-)-trans-PAT 1-methylpsilocin Superimposition

Figure 1-5. Molecular modeling comparing structural similarities between (-)-*trans*-PAT and 1-methylpsilocin

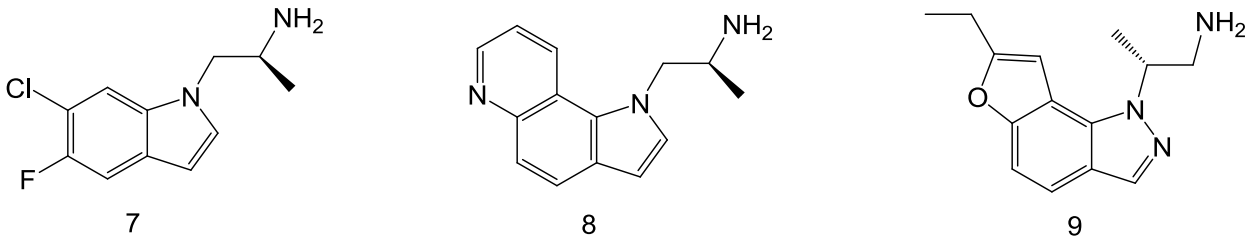

Figure 1-6. *N*-substituted indole analogues

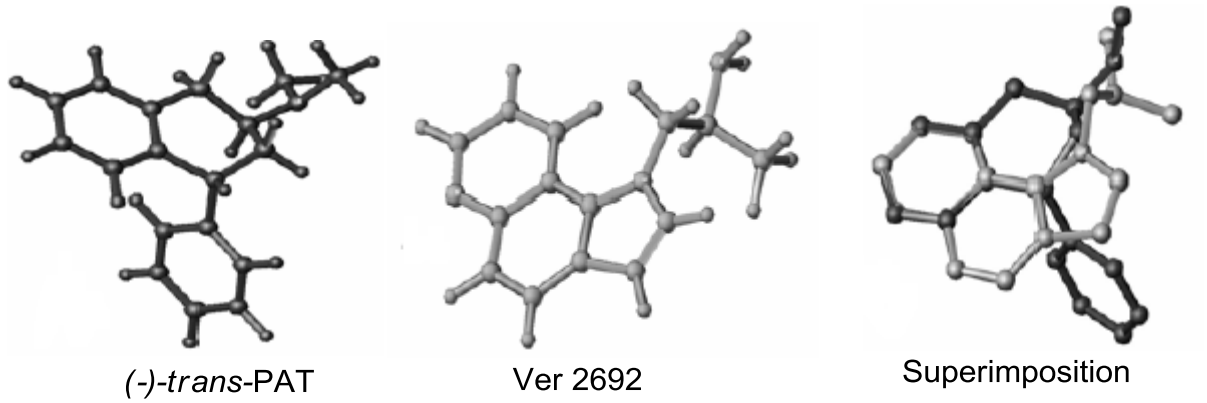

Figure 1-7. Molecular modeling comparing structural similarities between (-)-*trans*-PAT, and Ver 2692

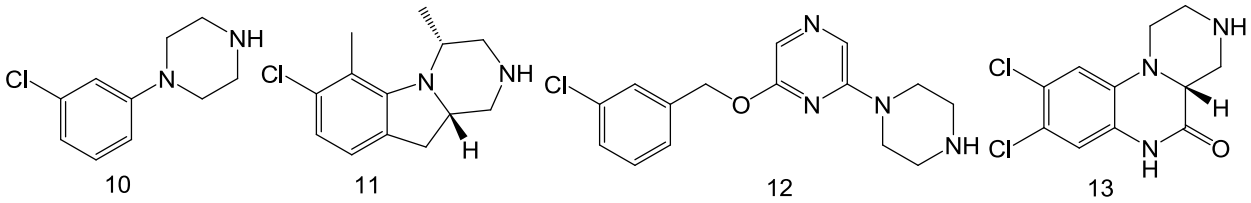

Figure 1-8. *M*-CPP and piperazine analogues

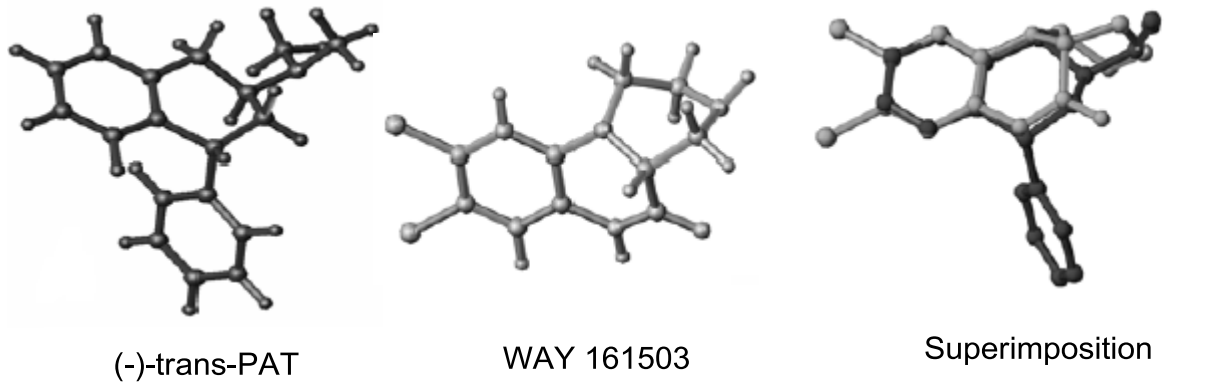

Figure 1-9. Molecular modeling comparing structural similarities between (-)-*trans*-PAT and WAY 161503

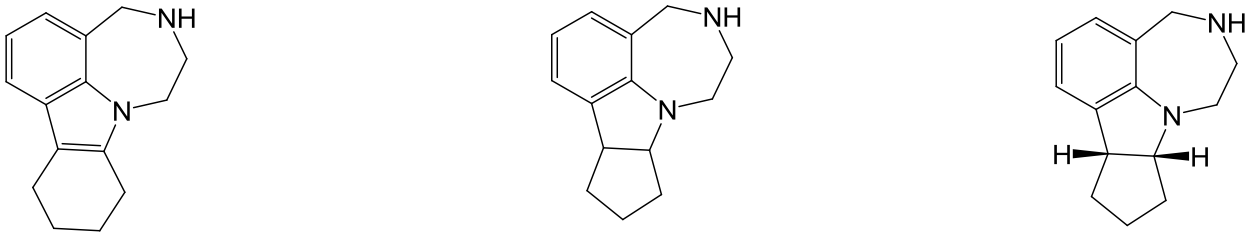

Figure 1-10. Benzodiazepinoindole analogues

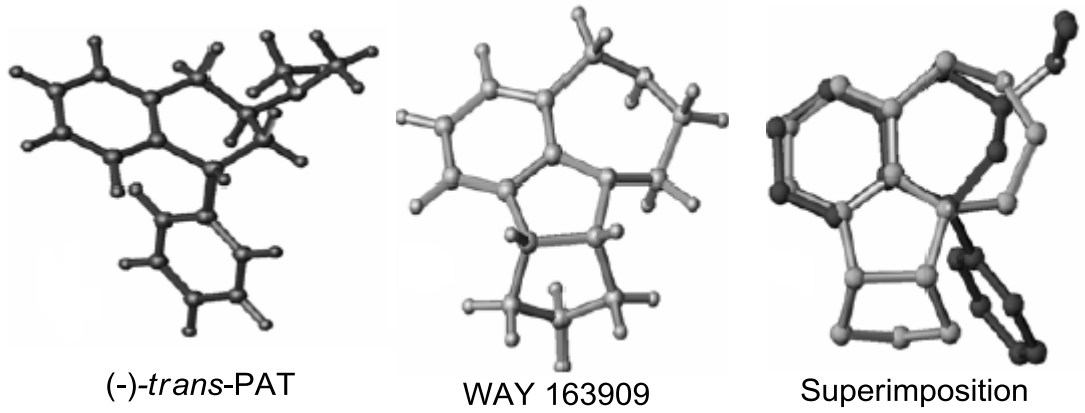

Figure 1-11. molecular modeling comparing structural similarities between (-)-*trans*-PAT and WAY 163909

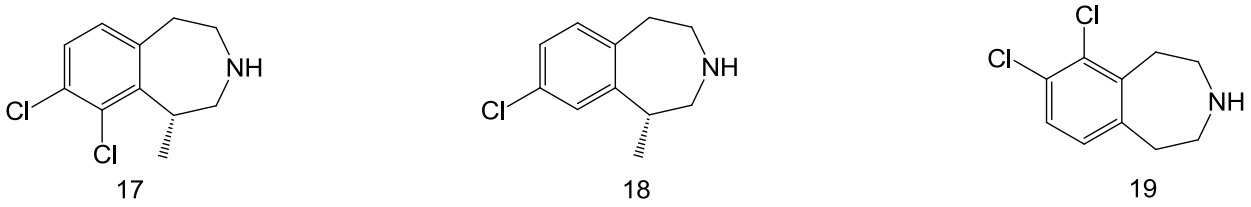

Figure 1-12. Benzazepines

CHAPTER 2
SYNTHESIS OF (-)-*TRANS*-N,N-DIMETHYL-4-PHENYL-1,2,3,4-TETRAHYDRO-2-NAPHTHALENAMINE 30

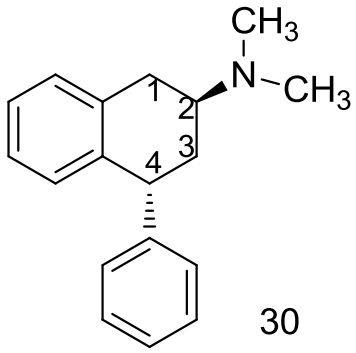

30

Rationale

As indicated above, (–)-*trans*-PAT **30** is a 5HT2C agonist with 5HT2A and 5HT2B inverse agonist activity. This type of multi-functional activity at 5HT2 receptors is consistent with literature that suggests 5HT2C agonists and/or 5HT2A inverse agonists may be beneficial in treating neuropsychiatric disorders such as psychoses and psychostimulant (cocaine, amphetamines) abuse. Moreover, a compound that demonstrates truly selective activation of 5HT2C receptors (i.e., no activation of 5HT2A and 5HT2B receptors) is predicted to show clinical activity for obesity (5HT2C) without troubling psychiatric (5HT2A) and/or cardiopulmonary (5HT2B) side effects. To evaluate the *in vivo* pharmacotherapeutic efficacy of (-)-*trans*-PAT in psychoses, psychostimulant drug addiction, and obesity psychosis, preclinical study in several rodent models was planned. Thus, a large enough quantity (500 mg) of (–)-*trans*-PAT was needed. Scale-up synthesis of (-)-*trans*-PAT was accomplished through modification and optimization of a published synthesis route.

Synthesis Results and Discussion

The scale-up preparation of (-)-*trans*-PAT was based on a published diastereomer recrystallization strategy (Wyrick et al., 1992, 1993, 1995). Meanwhile, several other synthetic routes (**Fig. 2-1**) were proposed and tested. This chapter includes a detailed discussion of the formal synthesis of (-)-*trans*-PAT in multi-gram scale through diastereomer recrystallization and summarizations of other investigated routes.

Retrosynthetic analysis (**Fig. 2-2**) indicates (-)-*trans*-PAT **30** is derived from 2-tetralol **24**, which is prepared by reduction of 2-tetralone **23**. Compound **23** can be prepared straightforwardly through cyclizing α,β-unsatuated ketone **22**.

The synthesis schemes are shown in **Fig. 2-3 – 2-9**.The synthesis started with oxidation of 1-phenyl-2-propanol **20** with pyridinium chlorochromate (PCC) and Al_2O_3 for 5 h to provide product 1-phenyl-2-propanone **21** in 75% yields (maximum loading amount should not exceed 20 g). The next step is a kinetic controlled aldol condensation of compound **21** and benzaldehyde. The original method (Wyrick et al 1993, 1995, 1999) indicated the condensation was complete under aqueous KOH environment at 55°C over a period of 16 h. The pre-cyclizing intermediate **22** could be obtained in 60% yield. However, we found over-condensation occured given this long reaction time. Large amount of side products made recrystallization much less productive. It was found that the optimal reaction period is 6.5 hours. After acidic workup and consequent recrystallization from methanol, the majority of pure product was colleceted. To achieve the highest yield, all the leftover mother solutions were combined and impurities were removed as much as possible by chromatography. The enriched leftover crude product was allowed to recrytallizing for the second time in hexane-methanol (2:1) solvent system. The combined yield was ~62% on a 15 g scale.

Other procedures e.g., using lithium diisopropyamide (LDA) as base, THF as aprotic solvent, conducting the reaction at -78°C, were not used due to facility limitation and workup complexity.

The next step was a polyphosphoric acid (PPA) mediated Frediel-Craft type alkylation to get 2-tetralone **23.** The previous procedure (Wyrick et al 1993, 1995, 1999) employed xylene as solvent. We used toluene instead for cleaner workup. The yield was reported as 80% (Wyrick et al 1993), in contrast to all the other reported yields (all below 50%) for similar ring closure (Vincek & Booth, 2009). The highest yield we achieved was around 40%. The discrepancy might be explained in **Fig. 2-4**. Compound **22** exists as *(Z)*- and *(E)*-isomers. *(E)*-isomer would undergo intra-molecule cyclization, however, steric effect could impede the ring closure for the *(Z)*-isomer. The yield would be in agreement with Wyrick's data (80%) only by assuming all the reactant **22** was the *(E)*-isomer.

By monitoring the reaction conditions, we discovered the reaction was significantly impacted by stirring condition and stoichiometry between the reactants and solvent: (1) Vigorously stirring by a mechanic stirrer would afford the product **23** in 40% yield in 10 g scale over a period of 3.5 h, while magnetic-bar stirring would afford product in 300 mg scale after 12 h reaction period, with total yield around 20%. (2) The stoichiometry between toluene and reactant **22** should be no less than 14 L: 1 mol. Diluted solution enviroment favors intra-molecule cyclization over inter-molecule condensation. In fact, the ratio of toluene vs. reactant **22** as 2.2 L: 1 mol reduced the yield to 30%. The major side product was un-characterizable, ^{1}H NMR indicated it might be polymers resulting from *(Z)*-**22** inter-molecule condensation.

Several other Lewis acids e.g. $AlCl_3$, $AlBr_3$ etc, were tested as cyclization catalysts in this stage of synthesis. However, none of them proved to be productive.

In the next step 2-tetralone **23** was converted to 2-tetralol **24** by $NaBH_4$ reduction. In this way 2-tetralol **24** was synthesized in 10 g scale. Product **24** contains four stereoisomers (**Fig. 2-5**) with a ratio of approximately 75% *cis* vs. 25% *trans*. The result is in agreement with the previous publication (Wyrick et al., 1993).

In the original paper (Wyrick et al., 1993), the reaction period and the conditions to separate racemic *cis*-2-tetralol **24** were not reported. After a detailed investigation for the optimal reaction conditions, we concluded; (1)10 h was the optimal reaction period, (2) silica column method alone was inefficient in completely separating racemic *cis*-2-tetralol **24** on a 10 g scale, as was indicated by the fact that the difference of the retention time (R_f) of *cis*-**24** and *trans*-**24** was minimal in all of the TLC developing systems we tested. Instead, a robust recrystallization method was developed. In short, after workup, in 10 gram scale, a medium-sized silica gel chromatography removed most of impurities in the crude product **24**. Subsequently, the product was allowed to recrytallize in a solvent system (1% ethyl acetate in 99% hexane) following the stoichiometry of 1 g compound: 700 ml solvent. After the crude product **24** was dissolved by rotation in 85°C water bath, the solution was allowed to cool smoothly. The recrystallization was completed after the mixture was kept in -20°C freezer for 2 days. During this period the desired product *cis*-**25** slowly solidified and attached to the wall of the flask. Repeated recrystllizing (up to 4 times) afforded pure *cis*-tetralols **25** (>97%) in 7g scale.

It was found that the leftover solution contained approximately 30%~40% *trans*-**24**, ~40% *cis*-**24** and impurities. Purification and recrystallization of the combined mother solution provided the final batch of desired *cis*-**24**. The combined yield of reduction and separation was 62%.

The *cis*-**24** and *trans*-**24** are diastereomers, thus their ^{1}H-NMR spectrums are different. The percentage of *trans*-**24** was monitored by ^{1}H-NMR peak integration of characteristic ^{1}H-NMR signals (*cis*-**24**: C4 proton δ=4.14,dd vs. *trans*-**24** C4 proton δ=4.25,t) (Wyrick et al., 1993; Gatti et al., 2003).

In the next step, pure racemic *cis*-**24** (also shown as *cis*-**25** in **Fig. 2-3**) was tosylated by *p*-toluenesulfonyl chloride in pyridine on a 5 g scale over a period of 2 days. The pure product (±)-*cis*-**26** was obtained as a solid (yield 81%). The S_N2 type transformation of (±)-*cis*-**26** into azide (±)-*trans*-**27** was achieved by using N_3^- anion as nucleophilic attacking group. The yield was around 75% when DMF-H_2O was used as solvent and the reaction mixture was refuxed for 4 h (Wyrick et al., 1993, 1999). It was found higher yield (~90%) was achieved when DMF alone was used as solvent and the mixture was stirred at R.T. for 3 days. No *cis*-azide ^{1}H-NMR signals was detected in product (±)-*trans*-**27**, indicating the chiral-convension was complete.

The azide (±)-*trans*-**27** was reduced by H_2 using Pd/charcoal as catalyst (yield 95%) following the previous procedure (Wyrick et al., 1993). Starting with more than 350 g of 1-phenyl-2-propanol **20**, we obtained 11g racemic free base (±)-*trans*-**28** after the above process.

The key diastereomeric recrystallization of (±)-*trans*-**28** is shown in **Fig. 2-6**. A previous publication employed (*1R*)-(-)-camphor-10-sulfonic acid, but a poor yield (4%)

was reported (Wyrick et al., 1993). Recrystallization using (-)-dibenzenyl-L-tartaric acid was tested but no crystals formed. We decided to proceed following the aforementioned camphorsulfonic acid strategy with modifications. In the solvent system of acetonitrile and methanol (2:1), (±)-*trans*-**28** was treated with1.3 eq. (*1R*)-(-)-camphor-10-sulfonic acid. The mixture was first vigorously refluxed for 1.5 h, then cooled and stirred at R.T. overnight. Subsequent workup removed dark red impurities from the crude product. Recrystallization was carried out in a modified solvent system (acetonitrile:methanol = 4:1). The saltt was first dissolved (1g compound : 650 ml solvent) by rotating in 75°C water bath, then cooled smoothly, finally kept at 0°C for up to 2 days. During the first several rounds of recrystallization we noticed it was the undesired isomer (+)-*trans*-amine that formed the needle-shaped crystals (optically dextrorotatory) with camphorsulfonic acid. However, by separating the undesired salts the desired (-)-*trans*-**28** was enriched in the mother solution. Subsequent rounds of recrystallization afforded crystals **29** as prisms containing the single enantiomer (-)-*trans*-**28** in the end.

To ensure the purity of the final products, the percentage of (+)-*trans*-**28** (**Fig. 2-6**, component I) vs. (-)-*trans*-**28** (**Fig. 2-6**, component II) was monitored carefully. To this purpose, optical rotation measurement and Mosher reagent [(*R*)-(-)-α-methoxy-α-[(trifluoromethyl)phenyl]acetamide] derivatization assays were performed in each round of recrystallization.

The optical rotation test gave levorotory value of salts **29** (10 mg) in 1 ml absolute methanol. High levorotory values indicate high percentages of component I in the salts. The end point (possible 100% component I) is in the range of $[\alpha]^{25}_{D}$ -68.5º~-70°. However, the optical rotation results were significantly influenced by experimental

errors. Thus, Mosher's reagent assay was conducted by converting recrystallized salts into (*R*)-(-)-α-methoxy-α-[(trifluoromethyl)phenyl]acetamide diastereomers (**Fig. 2-7**; Dale et al., 1969, 1972).

Recrystallized salts **29** (3~5 mg) was converted to free amine **28**. The free amine was transformed to the diastereomeric salts with (*R*)-Mosher acid chloride (**Fig. 2-7**). The sample was directly analysed by ^{1}H-NMR in $CDCl_3$ without purification. The percentage of **31** vs. ***32*** was monitored by ^{1}H-NMR peak integration of the characteristic ^{1}H-NMR signals (**31**: C2 proton δ=4.1,t vs. **32** C2 proton δ=4.23,t) (Wyrick et al., 1993; Gatti et al., 2003).

Several batches of pure 2*S*,4*R*,1'*R*-salt **29** (also shown as compound **33** in **Fig. 2-8**) were collected. Compound **33** was first converted to free base **34**, then *N,N'*-dimethylated by being refluxed with formaldehyde and formic acid. The products were converted to final HCl salt **30** (**Fig. 2-8**, Wyrick et al.,1993). Collectively 500 mg of enantiometically pure final compound **30** was obtained through the resolution of 4 g racemic (±)-*trans*-amine **28**.

The diastereomer recrystallization (yield 10%) proved to be very labor-intensive and time-consuming. To achieve better overall yield, several alternative approaches were investigated along with the scale-up. As shown in **Fig. 2-9**, chiral organoboron reagent (+)-DIP-chloride was proposed to asymmetrically reduce tetralone **23** to (2*R,*4*R*)-tetralol **35**. DIP-chloride has been sucessfully used for the reduction of many acyclic substrates. However, it did not afford the desired (2*R,*4*R*)-*cis*-tetralol **35**.

Another proposed asymmetric synthesis route (**Fig. 2-10**) started with conversion of 2-tetralone **36** to (2*R*)-2-tetralol **37** (88% *ee*) using benzene ruthenium (II) chloride

dimer and (*R*,*R*)-*N*-(2-amino-1,2-diphenylethyl)-*p*-toluenesulfonamide (NAPT). Subsequently the hydroxyl group in compound **37** was protected by tert-butyldimethylsilyl chloride (TBDMS). A strategy included (1) N-bromosuccinimide (NBS) mediated bromination at the benzylic position, (2) nickle (Ni) catalzyed Suzuki coupling a phenyl group at this position, was tested. It was revealed the product from the bromination reaction was unstable even in neutral CS_2 environment, let alone sustaining the strong basic environment that is necessary for Suzuki coupling.

An alternative synthetic strategy based on Jacobsen asymmetric epoxidation on 4-phenyl- 3,4-dihydronaphthalene **41** was proposed (**Fig. 2-11**; Palucki, et al., 1994. Boger et al.,1997). This process began with conversion of α-naphthol **39** to 4-phenyl-1-tetralone **40** using aluminum chloride as the Lewis acid and benzene as the solvent. After (1) $NaBH_4$ reduction, (2) azotropic distillation (3) epoxidation catalysed by Jacobsen's reagent and using either bleach (NaOCl) or 3-chloroperoxybenzoic acid (*m*-CPBA) as oxydant, product **40** was syntehsized. The epoxide **40** was verified by high-definition MS and was reduced to tetralols **41** either by H_2/Pd or by diisobutylaluminum hydride (DIBAL-H). Unfortunately, ^{1}H-NMR revealed the major tetralols obtained was undesired *trans*-configuration product (Most likely *2R,4S*-enantiomer, the absolute stereochemistry assignment was not conducted) with trace amount of desired *cis*-tetralol. The 4-phenyl group might block the bulky catalyst, resulting in the oxidative reagent complex approaching the olefin from the same side (**Fig. 2-12**), thus most of the epoxdation occurred on the opposite side of the 4-phenyl group and formed *trans*-product (Martinelli et al., 1994; Lucero et al., 1994; Maeda et al., 2002).

These alternative synthetic projects, although being unsuccessful, did advance our synthetic knowledge of the PAT structure, as well as, providing valuable procedures for PAT analog preparation that are described in the following chapters.

In vitro Pharmacological Characterization Results

The detailed *in vitro* characterization of (-)-*trans*-PAT and its stereoisomers was published (Booth et al., 2009). In **Table 2-1** *in vitro* competitive binding assay data (measuring displacement of [^{3}H]-radioligands from human 5HT2 receptors) are summarized. In **Table 2-2** *In vitro* functional activity assay data (measuring activation of PLC/ [^{3}H]-IP formation in clonal cells expressing human 5HT2C receptors) are summarized. **Fig. 2-13**, **2-14**, **2-15** shows representative curves for (-)-*trans*-PAT activity in functional assays. (-)-*Trans*-PAT is a full-efficacy agonist, comparable to the endogenous agonist serotonin, at human 5HT2C receptors, (-)-*trans*-PAT is an inverse agonist at human 5HT2A and 5HT2B receptors.

In vivo Pharmacological Characterization Results

Results of an *in vivo* study evaluating anti-obesity efficacy of (-)-*trans*-PAT in mice were published (Rowland NE, Zhuming Sun, et al., 2008). In summary, (-)-*trans*-PAT produces a dose-dependent inhibition of food intake with a 50% inhibitory dose (ID_{50}) of 4.2 mg/kg in C57BL/6 mice that are not food-deprived. The dose–effect curve was similar to that obtained using a published 5HT2 non-selective agonist WAY-161503 (**Fig. 2-16**). After 4-days consequently administration, the anorectic effect of (-)-*trans*-PAT is maintained (**Fig. 2-17**).

In another study the ability of (-)-*trans*-PAT to counteract the effects of the psychostimulant amphetamine were measured in rats (data from Dr. Drake Morgan, UF Department of Psychiatry). As shown in **Fig. 2-18**, (-)-*trans*-PAT fully blocks the

amphetamine-induced locomotor activating effects in rats (ED_{50} ~ 5mg/kg). This effect is not simply due to a generalized sedative effect as a dose of 10 mg/kg (-)-*trans*-PAT failed to decrease locomotor activity when given alone. In addition to the overt anti-amphetamine behavioral effects of (-)-*trans*-PAT demonstrated here, it is noted that amphetamine-induced locomotion is a widely-used model to mimic psychosis (schizophrenia) in rodents (Powell et al., 2006). Thus, the current results suggest antipsychotic activity of (-)-*trans*-PAT.

Discussion: (–)-*Trans*-PAT is a 5HT2C Full Agonist with 5HT2A/2B Inverse Agonism that Shows Promise for Treating Obesity, Drug Abuse and Psychoses

The scale-up synthesis based on the diastereomeric recrystallization strategy afforded 500mg enantiomerically pure (-)-*trans*-PAT. In researching an alternative high-efficient route, new synthetic reactions were investigated. Some of the new reactions were applied in preparation PAT analogs described in the following chapters.2 and 3.

(–)-*Trans*-PAT is the first reported 5HT2C full agonist with 5HT2A/2B inverse agonism. *In vitro* characterization data of (-)-*trans*-PAT and its stereoisomers, and, results of molecular modeling studies were published (Booth et al., 2009). Subsequent mutagenesis studies in our lab (Fang et al., 2010; unpublished data) confirmed (-)-*trans*-PAT protonated amine can form an ionic bond with D3.32 of 5HT2A and 5HT2C receptors, but, not with 5-HT2B receptor. Analogs synthesis and characterization focusing on the substitution on the fused phenyl of tetrahydronaphthalene ring and the pending phenyl of PAT are discussed in the following chapters. A new molecular model based on crystallographic structure of β2-adrenergic receptor has been developed and advanced SAR study is initiated.

Precilnical *in vivo* studies in rodents suggest (-)-*trans*-PAT is a suitable lead compound for development as a drug to treat obesity, psychostimulant addiction, and psychoses. Notably, no overt toxicity was observed in any of the dozens of animals that received peripheral (intraperitoneal) injections of (-)-*trans*-PAT. Moreover, the *in vivo* neurobehavioral studies showing (-)-*trans*-PAT efficacy to modulate amphetamine-induced locomotion in rats confirms that (-)-*trans*-PAT enters the brain after peripheral administration, where is presumably acts as a 5HT2C agonist with 5HT2A/5HT2B inverse activity.

Table 2-1. (-)-*Trans*-PAT and isomers 5HT2 receptors affinity. All the data are presented as Ki ± SEM (nM)

	5HT2A Ki (nM)	5HT2B Ki (nM)	5HT2C Ki (nM)	H1 Ki (nM)
(-)-*trans*-PAT	410 ± 38	1200 ± 6.8	37.6 ± 3	1.95 ± 0.5
(+)-*trans*-PAT	520 ± 3	~ 2500	1300 ± 80	29.8 ± 3.5
(-)-*cis*-PAT	780 ± 2	~ 5000	980 ± 7.8	13.7 ± 2
(+)-*cis*-PAT	1500 ± 2	~ 10000	430 ± 4.8	177.2 ± 9.4

Table 2-2. Functional activities of (-)-*trans*-PAT at 5HT2 receptors. E_{max} was expressed as % 5HT, I_{max} was expressed as % basal inhibition

Section name	5HT2A	5HT2B	5HT2C
(-)-*trans*-PAT	IC_{50}=490 ± 96 nM	IC_{50}=1000 ± 5 nM	EC_{50}=20 ± 2.2 nM
	I_{max}=60 ± 5%	I_{max}=35 ± 2.0%	E_{max}=100 ± 2%

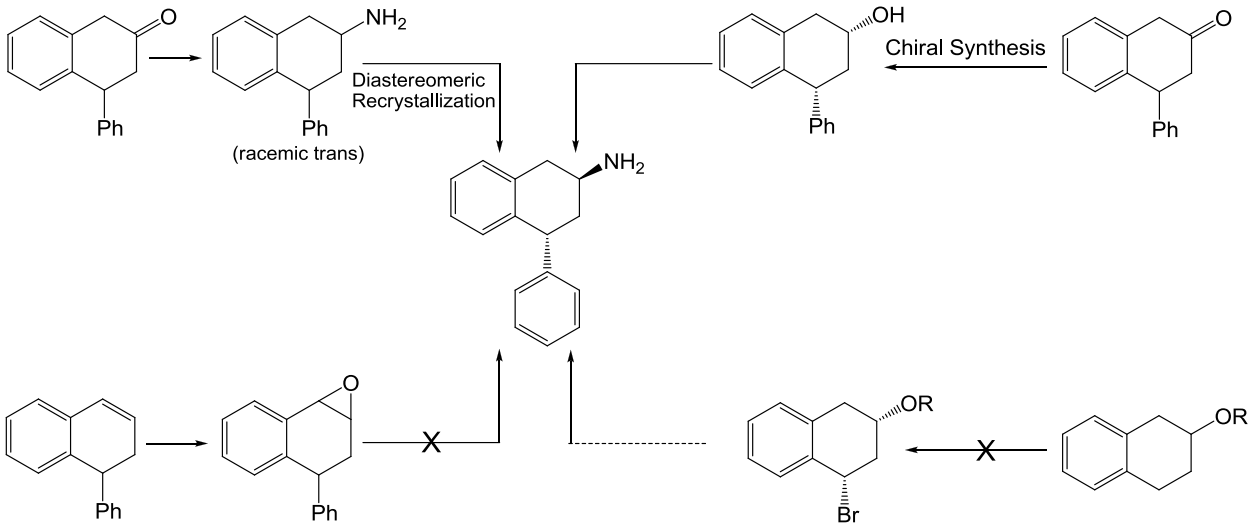

Figure 2-1. Summary of (-)-*trans*-PAT synthetic routes

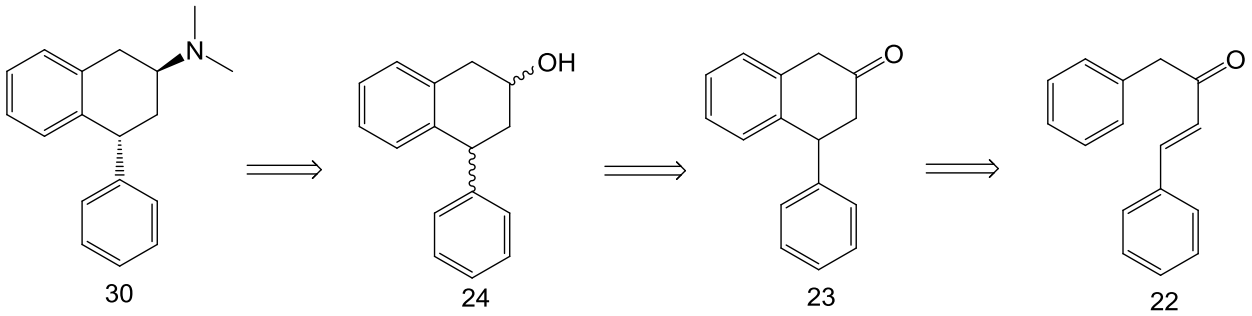

Figure 2-2. Retrosynthetic analysis of diastereomer recrystallization strategy

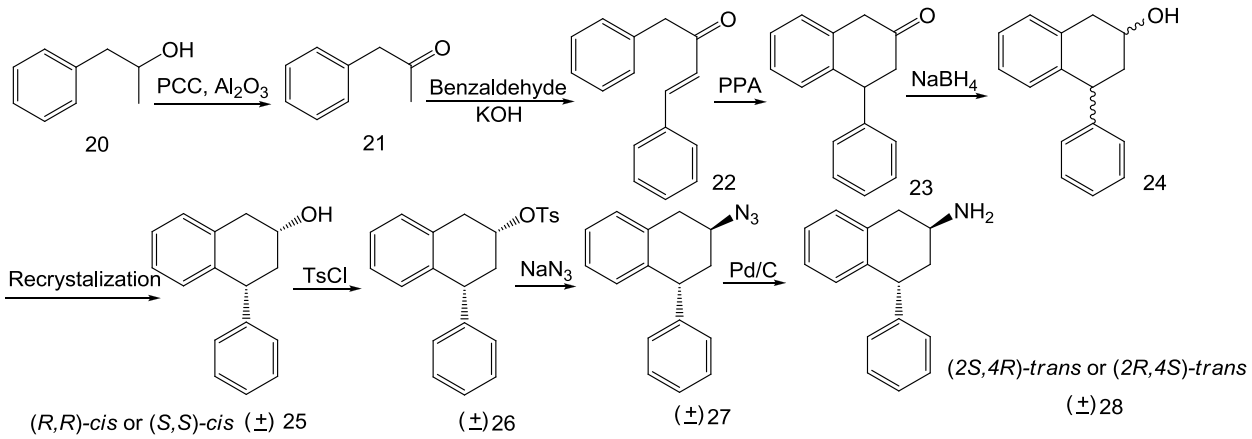

Figure 2-3. Synthesis of (±)-*trans*-2-amino-4-phenyl-1,2,3,4-tetrahydronaphthalene 28

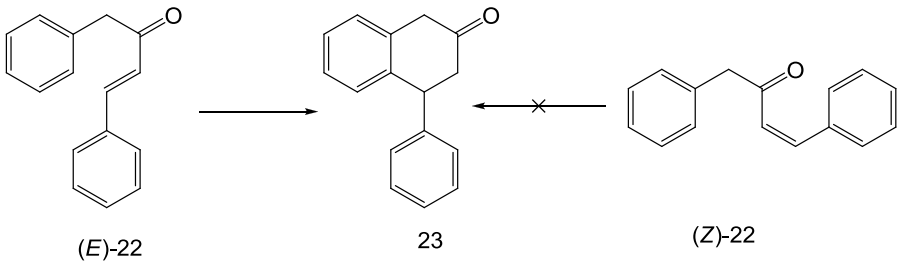

Figure 2-4. Formation of 2-tetralone 23

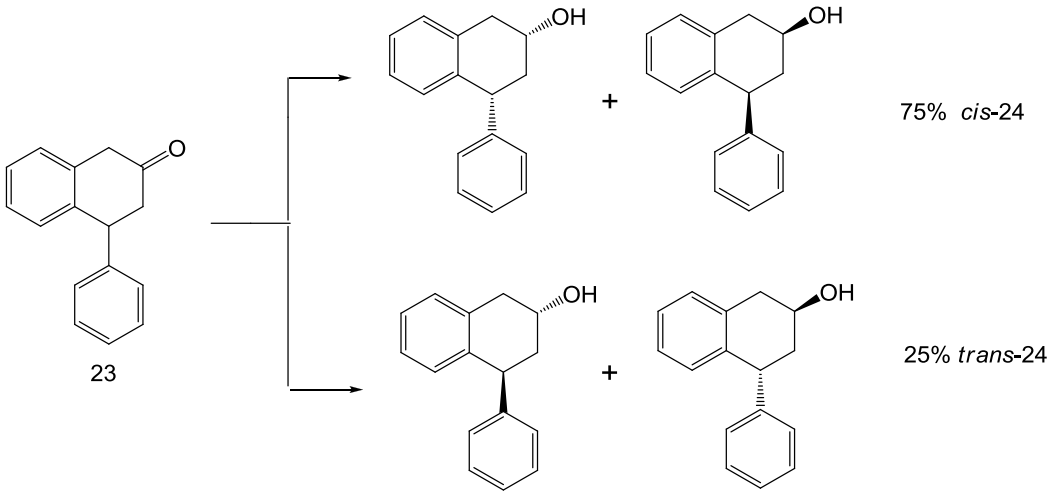

Figure 2-5. $NaBH_4$ reduction to prepare 2-tetralol 24

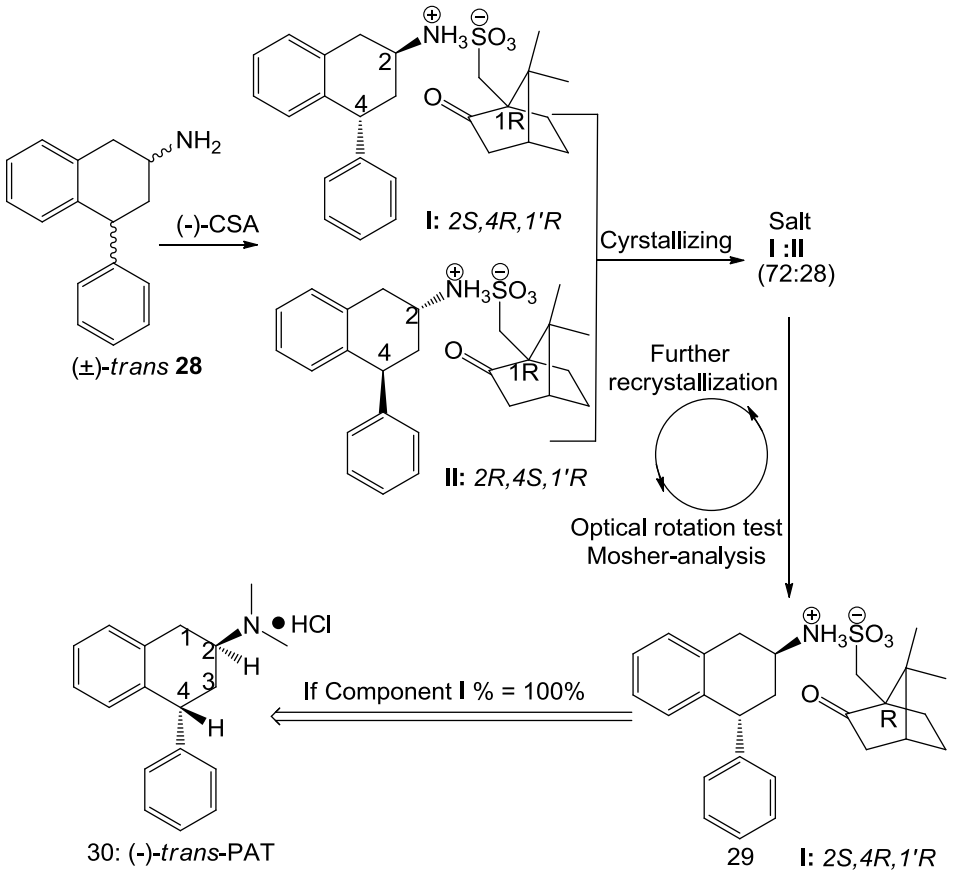

Figure 2-6. Resolution of (±)-*trans* -1-phenyl-3-amino-1,2,3,4-tetrahydronaphthalene 28

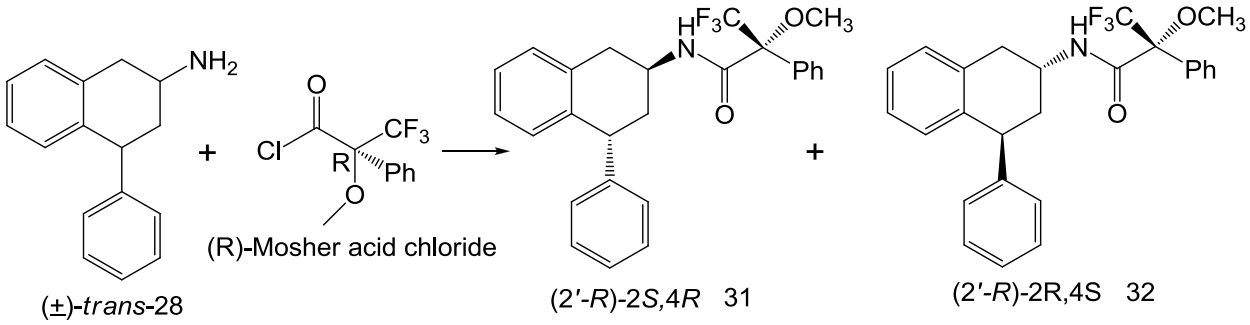

Figure 2-7. Mosher's reagent assay of (-)-*trans*-pat resolution

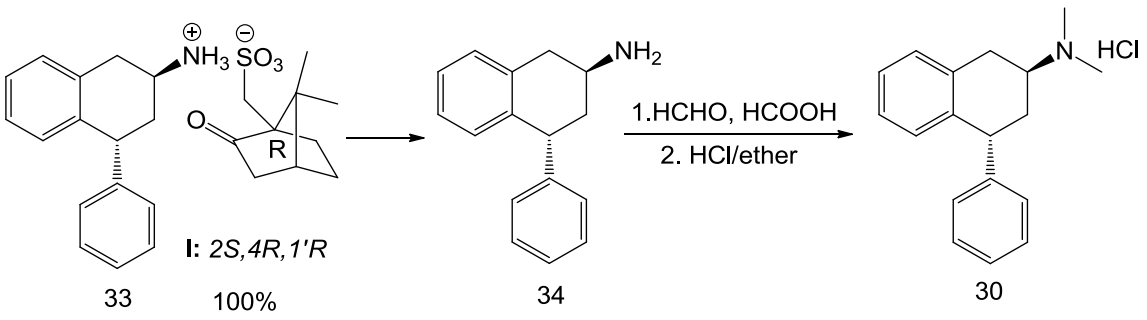

Figure 2-8. Conversion of pure salts to final product 30

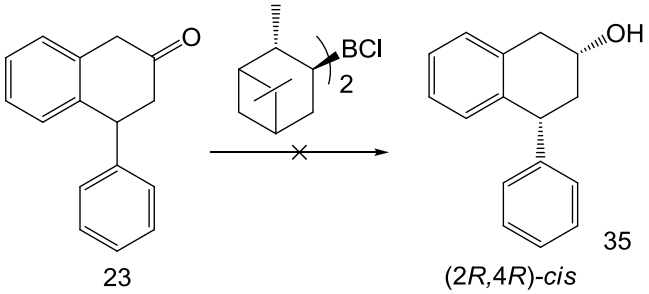

Figure 2-9. (+)-DIP-chloride failed to afford (2*R*,4*R*)-*cis*-tetralol 35

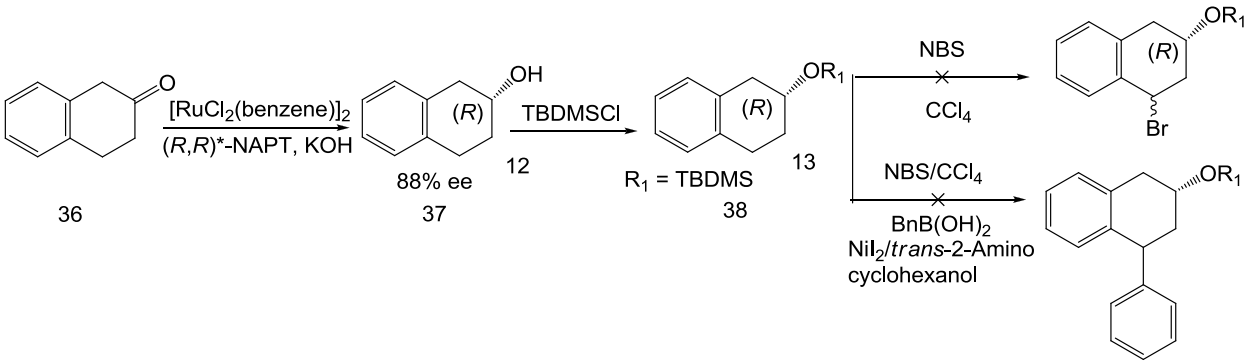

Figure 2-10. Bromination-Suzuki coupling failed to introduce phenyl group to C4 of tetralol 38

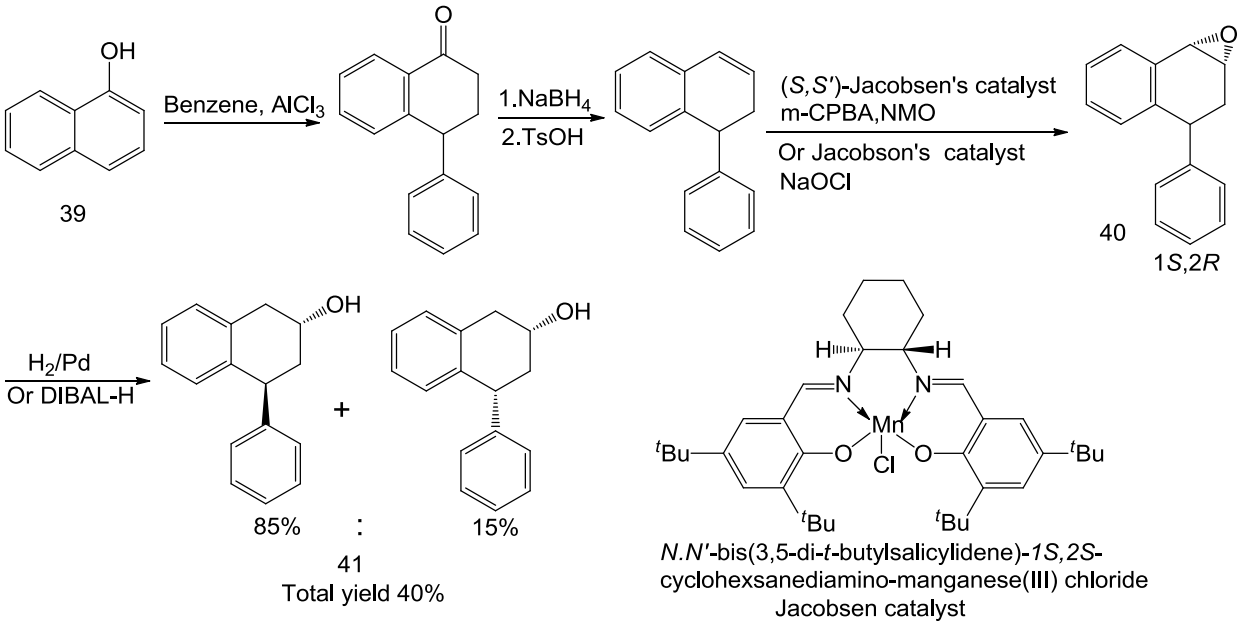

Figure 2-11. Jacobsen epoxidation yielded mainly *trans*-tetralol

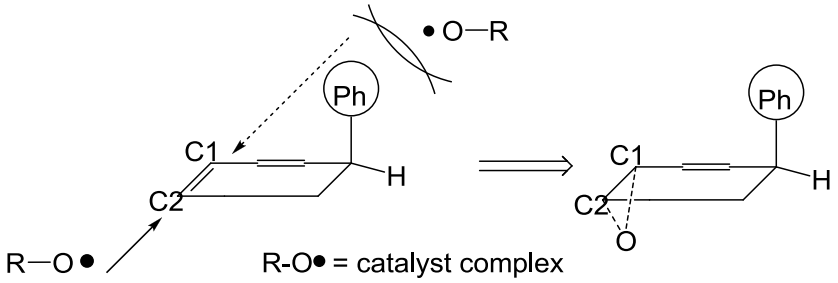

Figure 2-12. Stereochemistry of Jacobsen epoxidation on dihydronaphthalene 41

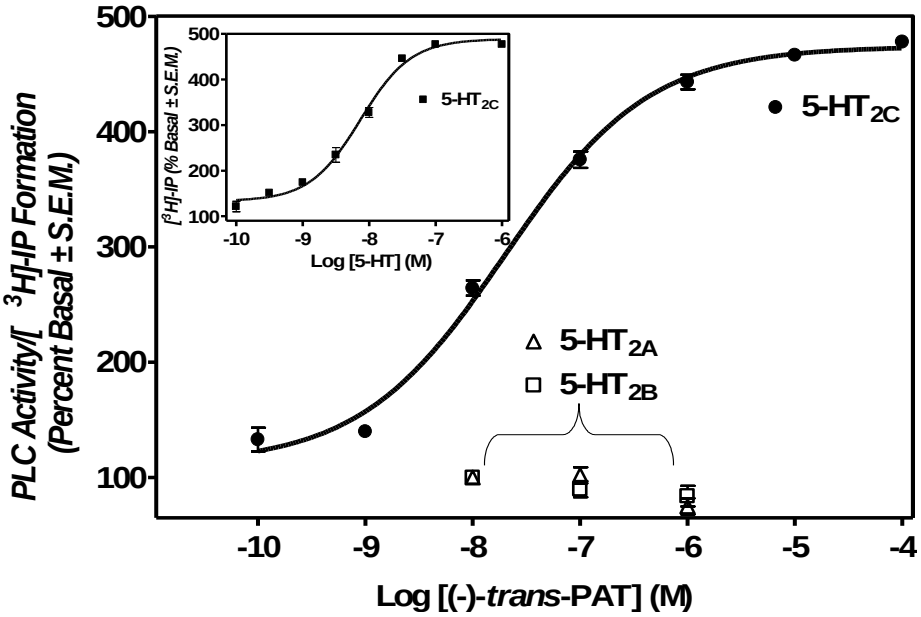

Figure 2-13. Representative concentration-response curve for serotonin (closed squares) and (-)-*trans*-PAT (closed circles) activation of PLC/ [^{3}H]-IP formation in HEK cells expressed cloned human 5HT2C receptors. Single concentration effect of (-)-*trans*-PAT at 5HT2A (open triangles) and 5HT2B (open squares) receptors also is shown (Booth et al., 2009).

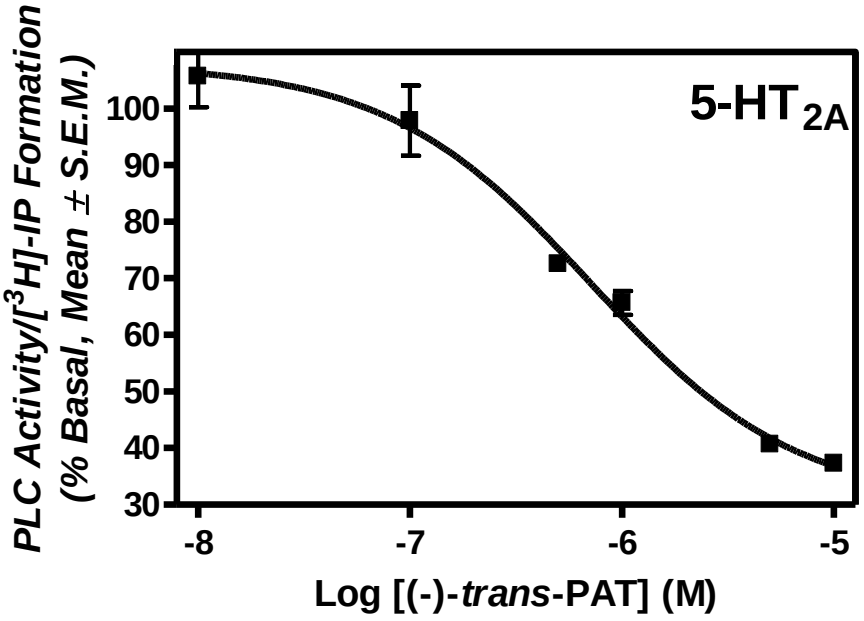

Figure 2-14. Representative data for (-)-*trans*-PAT inverse agonist activity at cloned human 5HT2A receptors (Booth et al., 2009)

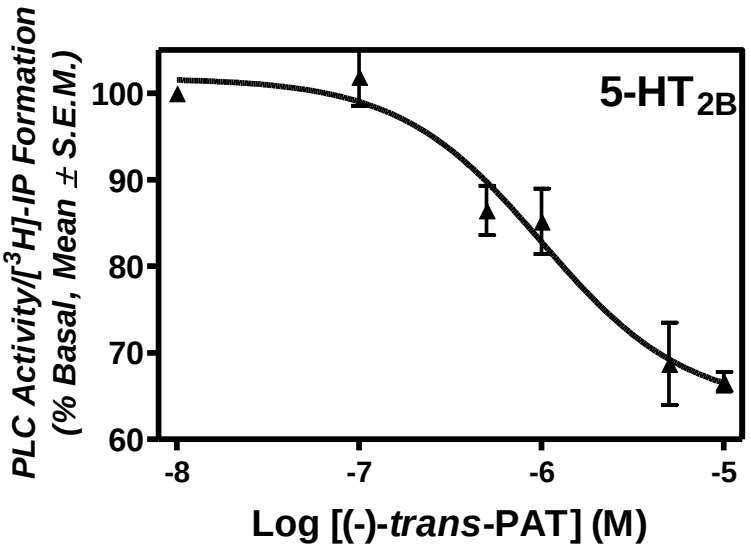

Figure 2-15. Representative data for (-)-*trans*-PAT inverse agonist activity at cloned human 5HT2B receptors (Booth et al., 2009)

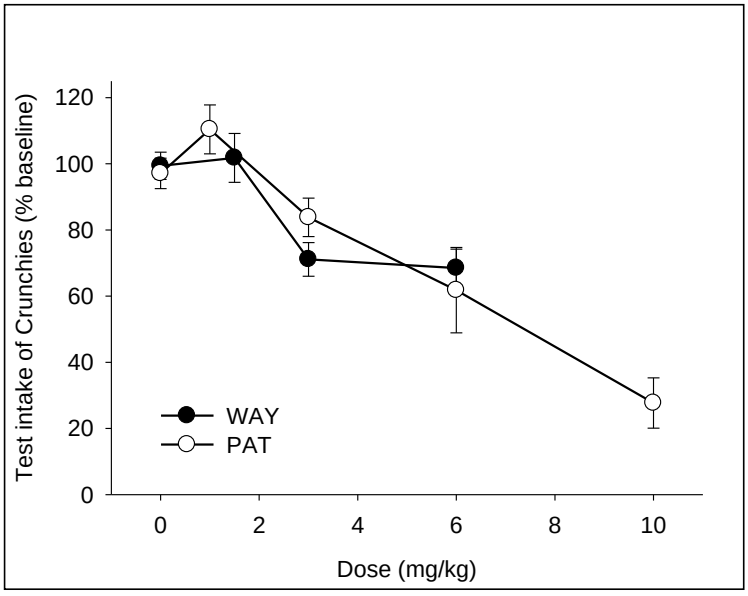

Figure 2-16. Dose-effect curve after i.p. administration of (-)-*trans*-PAT vs. the non-selective 5HT2A/2B/2C agonist WAY161503 on 30 min intake of platatable food by mice. Dose-related inhibition of food intake (DI_{50}): PAT 9.2mg/kg WAY 8.4mg/kg (Rowland, Sun et al., 2008)

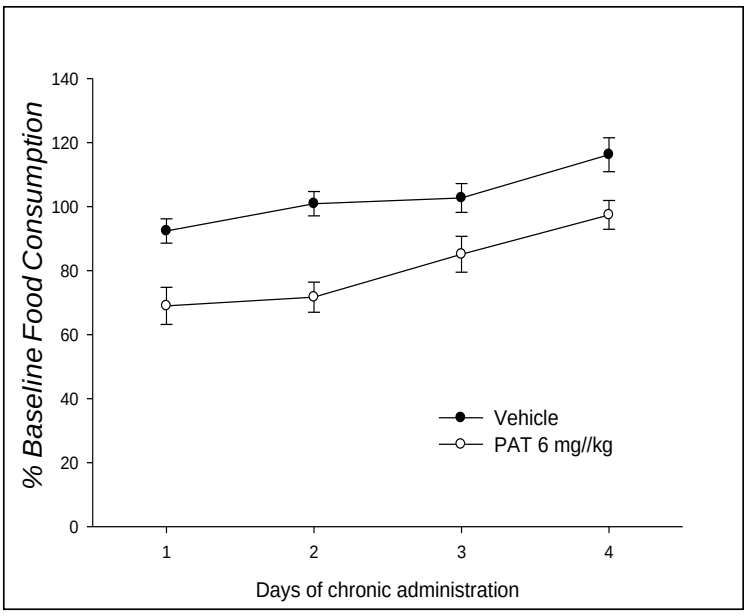

Figure 2-17. No tolerance to (-)-*trans*-PAT anorectic effect with chronic administration. anorectic effect of (-)-*trans*-PAT is maintained after chronic administration (daily i.p. injection for 4-days) (Rowland, Sun et al., 2008)

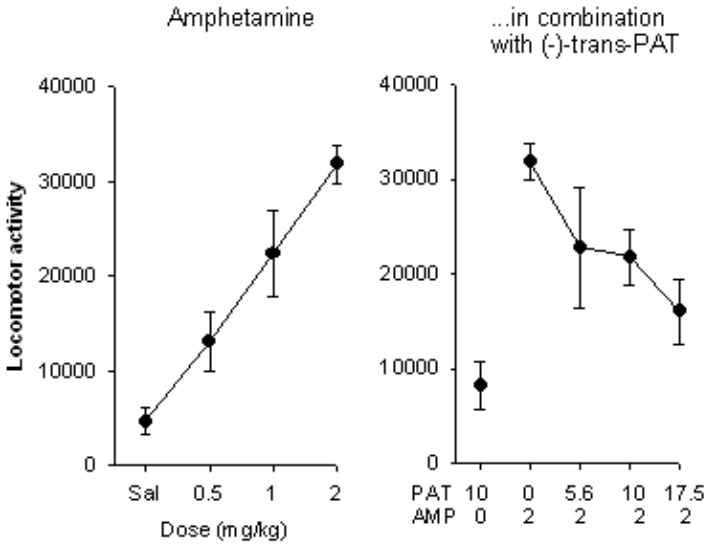

Figure 2-18. (-)-*Trans*-PAT in modulating amphetamine-induced locomotion (data from Dr. Drake Morgan, UF Department of Psychiatry). Left Panel: amphetamine dose-dependently increased locomotor activity. Right Panel: (-)-*trans*-PAT dose-dependently inhibit psycho-locomotor behavioral effect respectively. Agents administered intraperitoneally, alone or in combination immediately before the session.

CHAPTER 3
SYNTHESIS OF N,N-DIMETHYL-4-(4-METHYLPHENYL)-1,2,3,4-TETRAHYDRO-2-NAPHTHALENAMINE ANALOGS OF PAT

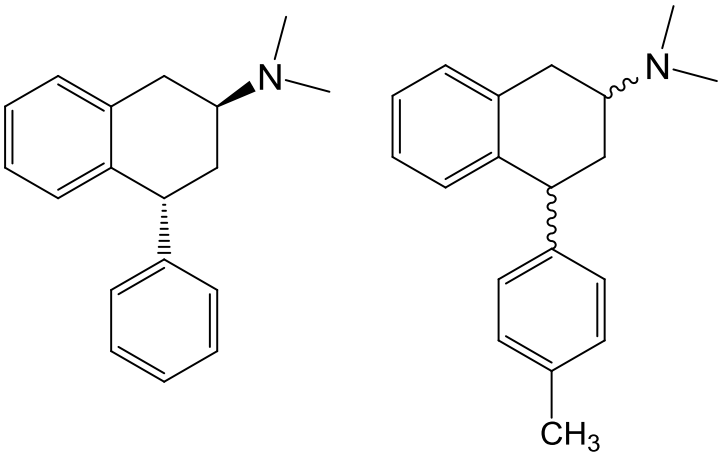

(-)-*trans*-PAT (±)-*trans*-*p*-methyl PAT

Rationale

Often, the addition of an akyl moiety to a lead molecule can enhance lipophilicity to improve penetration into brain tissue. If the alkyl moiety is relatively small with regard to steric bulk, then, affinity for the target receptor may not be adversely affected—in fact, affinity may improve due to enhanced van der Waals interactions between ligand and receptor. Given that the lead molecule (-)-*trans*-PAT **30** demonstrated preclinical efficacy to treat obesity, psychostimulant abuse, and psychoses after peripheral administration in laboratory animals (see **Fig. 2-17**, **2-18**, **2-19**), it was hypothesized that the corresponding 4'- or *para*-methyl analog (*p*-CH_3-PAT**, 48**) might achieve faster and/or great brain penetration after *in vivo* administration and perhaps demonstrate higher potency and efficacy for obesity and neuropsychiatric disorders compared to the parent compound. Implicit in this hypothesis is the assumption that the addition of the 4'-CH_3 moiety to (-)-*trans*-PAT **30** would not adversely impact 5HT2C agonist and 5HT2A/2B inverse agonist activity.For (-)-*trans*-*p*-CH_3-PAT, logP = 4.6, making it nearly

half-log unit more lipophilic compared to (-)-*trans*-PAT (logP = 4.2), suggesting the possibility of improved brain penetration after peripheral administration by intraperitoneal injection to laboratory animal In a preliminary screen, racemic (±)-*trans*-*p*-CH_3-PAT demonstrated higher affinity at 5HT2-type receptors when compared to (-)-*trans*-PAT. Thus, 5 mg of (±)-*trans*-*p*-CH_3-PAT was resolved to the (+)- and (-)-*trans*-*p*-CH_3-PAT enantiomers using a chiral-HPLC system (see Methods). Like the lead (-)-*trans*-PAT, preliminary functional screening indicated that (-)-*trans*-*p*-CH_3-PAT is a 5HT2A and 5HT2B inverse agonist and a 5HT2C agonist. Thus, scale-up synthesis of (-)-*trans*-*p*-CH_3-PAT was undertaken for complete *in vitro* pharmacological characterization, as well as, to obtain enough compound for preclinical *in vivo* studies. Also, the *trans*-*p*-CH_3-PAT analog is a useful initial molecule to probe the role of the PAT (C2) pendant phenyl moiety for binding and function at 5HT2 receptors, and, to characterize the 3-dimensional structure of the binding pocket of 5HT2 receptors. Likewise, synthesis of other *p*-CH_3-PAT isomers, (+)-*trans*, (-)-*cis*, and (+)-*cis*, was undertaken for pharmacological studies, SAR studies, and, to characterize the 3-dimensional structure of 5HT2 receptor subtypes.

Synthesis Results and Discussion

Preparation of (-)-*trans*-*p*-methyl-PAT and stereoisomers (**Fig. 3-1—3-5**) followed methods used to synthesize (-)-*trans*-PAT described in chapter 2. Two major improvements; (1) asymmetric hydrogenation (2) enantiomeric separation by chiral HPLC system (Mongi et al., 2004) afforded the desired *p*-CH_3-PATs (**54, 55, 48,** and **57**, respectively) in good yields and excellent enantiomer excess.

The synthesis (**Fig. 3-1**) started with condensation of 1-phenyl-2-propanone **21** and toluadehyde (reflux at 55°C in aqueous KOH for 14h) to provide product **42**.

Compared to the analogous synthesis in chapter 2, the reaction time was doubled; however, the total yield (25%) was much worse. The reduced electrophillic reactivity of toluadehyde compared to benzaldehyde makes the condensation largely incomplete. Due to limited time we did not explore other alternative methods. Started with 30 g compound **21**, 13.6 g product **42** was synthesized.

In the next step, intermediate **42** was cyclized in toluene using polyphosphoric acid as the catalyst (reflux for 4.5 h, yield 40%) to afford 2-tetralone **43** (4.6 g) as the product. The next step was based on a modified Noyori-type asymmetric hydrogen transferring procedure (Muneto et al., 2004). The intermediate 2-tetralone **43** was converted to (*2R,4R*)-*cis*-tetralol **44** in several batches with good yield and 92% *ee* (**Fig. 3-2**).

In this reaction, 2-propanol served as the solvent and the hydrogen source. Compound **43** was first treated by a catalytic complex (benzene ruthenium (II) chloride and *R,R*-NAPTS solution) and then by KOH solution. The mixture was allowed to react over 1.5h. The workup should be conducted directly after the reaction by thoroughly filtering through silica gel/ celite pad based on our observation that ruthenium-containing impurities might slowly decompose 2-tetralol products.

The percentage of *cis*- vs. *trans*-**44** (**Fig. 3-2**) in the product **44** was monitored by ^{1}H-NMR peak intergation of characteristic ^{1}H-NMR signals (*cis*-**44**: C4 proton δ=4.12,dd vs. *trans*-**44** C4 proton δ=4.24,t; Wyrick et al., 1993; Gatti et al., 2003). The enantiomeric excess (92%) was determined by comparing the percentage of each enantiomer after the final product was separated using chiral HPLC system discussed later.

To separate 2 g racemic *cis*-**44** and *trans*-**44** (similar R_f in most TLC systems) A silica-gel chromatography procedure was developed and used 7%ethyl acetate in hexane as eluent. The separation was monitored by ^{1}H-NMR spectrum. In this way *cis*-**44** (>98%, 1 g), *trans*-**44** (20 mg) and 450 mg mixture were collected.

The conversion from *cis*-**44** (1 g) to final product *N,N'*-dimethylated HCl salt **48** (500 mg) was completed following analogous procedures described in chapter 2. Optical rotation assay indicated compound **48** ($[\alpha]^{25}_D$ -67.5º in absolute methanol) contains mostly the desired (*2S,4R*)-trans-isomer. Mosher's reagent assay indicates the undesired (*2R,4S*)-enantiomer exists in trace amount (<2%, **Fig. 3-3**).

Prior to *in vitro* affinity and functional experiments, a chiral stationary phase HPLC (CSP-HPLC) using a Kromasil® CelluCoat™ column was employed to remove the trace amount of (*2R,4S*)-*trans*-*p*-CH_3-PAT impurity from the product (*2S,4R*)-*trans*-*p*-CH_3-PAT **48**. The HPLC system used a mobile phase system consisting of 15% ethanol in 85% hexane with 0.1% diethyl amine as modifier and the flow rate 1.5ml/min to resolve 1 mg compound dissolved in 200µl mobile phase in a single run. Further purified amine **48** (40 mg) was collected in this manner. Later a more efficient mobile phase system (5% methanol, 5% ethanol, 90% hexane and 0.2% diethyl amine as modifier) was developed and applied to (+)-*cis*, (-)-*cis* and (+)-*trans p*-CH_3-PAT isomers (**54**, **55**, **48** and **57**) separation.

Preparation of the (+)-*cis*, (-)-*cis* and (+)-*trans p*-CH_3-PAT isomers **54** and **55** are summarized in **Fig. 3-4 and 3-5.** The previously synthesized 2-tetralone **43** was reduced by $NaBH_4$ and the resulting (±)-*cis* tetralol **49** was converted to (±)-*trans*-tetralol **50** using a modified Mitsunobu conditions (Wyrick et al., 1993). The *trans*-2-tetralol **50**

was converted to racemic *cis*-*p*-CH_3-PAT **53** following previously described procedures. Chiral HPLC separation afforded enantiomerically pure products (+)-*cis*-**54** and (-)-*cis*-**55**. R_f for (-)-*cis*-**54**: 11.8 min; R_f for (+)-*cis*-**55**: 11.2 min. Assignment of the absolute configuration was based on analogy to the X-ray crystal structure of (-)-*cis*-*N,N*-dimethyl-1,2,3,4-tetrahydro-2-naphthalenamine 1-(*R*)-(–)-camphor-10-sulfonic acid salt (Bucholtz et al., 1998).

To synthesize the (+)-*trans* product **57**, the (±)-*cis* tetralol **49** was converted to (±)-*trans*-*p*-CH3-PAT following the routine synthesis (**Fig. 3-7**). The final product was collected after chiral HPLC separation. R_f for (-)-*trans*-**48**: 11.8 min; R_f for (+)-*trans*-**57**: 11.3 min; Structural elucidation was confirmed by polarimetry.

In vitro Pharmacological Characterization Results

To determine 5HT2 receptor affinity for the *p*-CH_3-PAT isomer, *In vitro* competitive binding assay measured *p*-CH_3-PAT isomers ability to displace of [^{3}H]-radioligands from human 5HT2 receptors expressed in HEK cell membranes (Booth et al., 2009) was conducted. Affinity results are summarized in **Table 3-1** and representative competition displacement are shown in **Fig. 3-6, 3-7** and **3-8**. *In vitro* functional activity was measured as (-)-*trans*-*p*-CH_3-PAT activation of PLC/ [^{3}H]-IP formation in HEK cells expressed human 5HT2C receptors (Booth et al., 2009). Functional activity results are summarized in **Table 3-2**. and representative potency-efficacy curves are listed in **Fig. 3-9–3-11**. Overall, results indicate (–)-*trans*-*p*-CH_3-PAT is a near full-efficacy agonist at human 5HT2C receptors and an inverse agonist at human 5HT2A and 5HT2B receptors. (-)-*Trans*-*p*-CH_3-PAT is 3-times more potent regarding inverse agonism at 5HT2A receptors compared to (-)-*trans*-PAT (2-times more potent at 5HT2B). However, (-)-*trans*-*p*-CH_3-PAT is 10-times less potent regarding agonism at 5HT2C receptors.

In vivo Anti-Stimulant Effects and Discussion of (-)-*Trans*-PAT and (-)-*Trans-p*-CH_3-PAT: Indication for Drug Abuse Pharmacotherapy

Amphetamine-induced locomotion in rodents is a widely-used rodent behavioral model for schizophrenia. In our studies (**Fig. 3-12**), male, Sprague-Dawley rats (n=8) were tested during 1 hour locomotor activity sessions, with saline, PATs, or amphetamine administered intraperitoneally alone or in combination immediately before the session. Amphetamine dose-dependently increased locomotor activity that is taken as psychotomimetic activity. When combined with the highest dose of amphetamine (2 mg/kg), both (-)-*trans*-PATand (-)-*trans-p*-CH_3-PAT dose-dependently inhibit the psycho-locomotor behavioral effects. Time course analyses suggest that the PATs are active within 15 minutes and effects are maintained throughout the 1-hr session. Preliminary studies with methamphetamine suggest that at the dosage of 1.0 mg/kg, (-)-*trans-p*-CH_3-PAT partially blocks the stimulant effects of methamphetamine (**Fig. 3-13**). In all cases, the rats displayed no overt signs of toxicity. According to the results, (-)-*trans*-PAT and (-)-*trans-p*-CH_3-PAT have equal efficacy. However, the *p*-CH_3 analog is 3-times more potent. The results suggest (-)-*trans*-PAT and (-)-*trans-p*-CH_3-PAT may show efficacy for treatment of psychoses, as well as, amphetamine and methamphetamine abuse.

Disscussion

As mentioned above, (-)-*trans-p*-CH_3-PAT, like the leading compound (-)-*trans*-PAT, is a 5HT2C agonist with 5HT2A/2B inverse agonist activity. It is quite surprising that at 5HT2C receptors, (-)-*trans-p*-CH_3-PAT has about 1/9 affinity and agonist functional potency (PLC/IP signaling) compared to (-)-*trans*-PAT. However, at 5HT2A receptors, (-)-*trans-p*-CH_3-PAT is 3-times more potent than (-)-*trans*-PATas an inverse

agonist. It is intriguing that the pending toluyl vs. phenyl make such activity differences. *In vitro* results above indicate (-)-*trans-p*-CH_3-PAT is 3-times more potent regarding 5HT2A inverse agonist activity compared to (-)-*trans*-PAT. In the amphetamine-induced locomotion model, (-)-*trans-p*-CH_3-PAT is 3-times more potent to inhibit the psycho-locomotor behavioral effect. This might due to the fact that 5HT2A inverse agonism activity of PATs may be at least as important as 5HT2C agonist activity regarding PAT-type pharmacotherapeutic potential to treat psychostimulant drug abuse (Fletcher et al., 2002; Bubar and Cunningham, 2006). Also, (-)-*trans-p*-CH_3-PAT (LogP=4.6) is more lipophilic than (-)-*trans*-PAT (LogP=4.2), thus, superior brain penetration may also contribute to higher potency of Me-PAT vs. PAT regarding psychotherapeutic activity. Future studies, especially *in silica* molecule modeling will greatly help the structure-activity relation understanding here.

In vivo Anorexia effect and Disscussion of (-)-*Trans-p*-CH_3-PAT

In vivo study evaluating anti-obesity efficacy of (-)-*trans-p*-CH_3-PAT was conducted (data from Dr. Neil Rowland, UF Department of Psychology) using a published rodent model (Rowland, Zhuming et al., 2008).Preliminary results are summarized below (as % untreated mice food consumption for vehicle-treated and (-)-*trans-p*-CH_3-PAT treated mice).

% untreated mice food consumption	
Vehicle:	112.8 +/- 6.3
Dose of (–)-*trans*-p-methyl-PAT	
1 mg/kg:	89.0 +/- 4.0
3 mg/kg:	98.5 +/- 5.7
9 mg/kg:	83.0 +/- 10.6

Discussion

The above *in vivo* results closely relate to the *In vitro* binding and function activities data. (-)-*trans*-*p*-CH_3-PAT produces no anorexia effects at 10mg/kg, whereas, the ED_{80} for (-)-*trans*-PAT anorexia effect occurs at 10mg/kg and ED_{50} is 5mg/kg. It correlates well with the fact that (-)-*trans*-*p*-CH_3-PAT has about 1/10 affinity and agonist functional potency (PLC/IP signaling) compared to (-)-*trans*-PAT. Overall, It is highly possible that 5HT2C agonism might translate more closely to anorexia activity and 5HT2A inverse agonism might translate more closely to anti-amphetamine effects (anti-addiction for psychostimulants, antipsychotic).

Table 3-1. (-)-*Trans-p*-methyl-PAT isomers 5HT2 receptors affinity

	5HT2A Ki (nM)	5HT2B Ki (nM)	5HT2C Ki (nM)	H1 Ki (nM)
(-)-*trans-p*-methyl-PAT	210 ± 40	250 ± 27	330 ± 50	18 ± 2.0
(+)-*trans-p*-methyl-PAT	70 ± 3.8	52 ± 6.6	381 ± 76.7	12 ± 0.9
(-)-*cis-p*-methyl-PAT	1500 ± 10	9000	3000 ± 10	3000
(+)-*cis-p*-methyl-PAT	520 ± 17	500 ± 20	1500 ± 12	19.6 ± 3.30

Table 3-2. Functional activities of (-)-*trans-p*-methyl-PAT at 5HT2 receptors (in comparison to (-)-*trans*-PAT)

Section name	5HT2A	5HT2B	5HT2C
(-)-*trans*-PAT	IC_{50}=490 ± 96 nM	IC_{50}=1000 ± 5 nM	EC_{50}=20 ± 2.2 nM
	I_{max}=60 ± 5 %	I_{max}=35 ± 2.0 %	E_{max}=100 ± 2%
(-)-*trans-p*-methyl-PAT	IC_{50}=140 ± 15 nM	IC_{50}=420± 12 nM	EC_{50}~200 nM
	I_{max}=50 ± 4 %	I_{max}=50 ± 3 %	E_{max}~100%

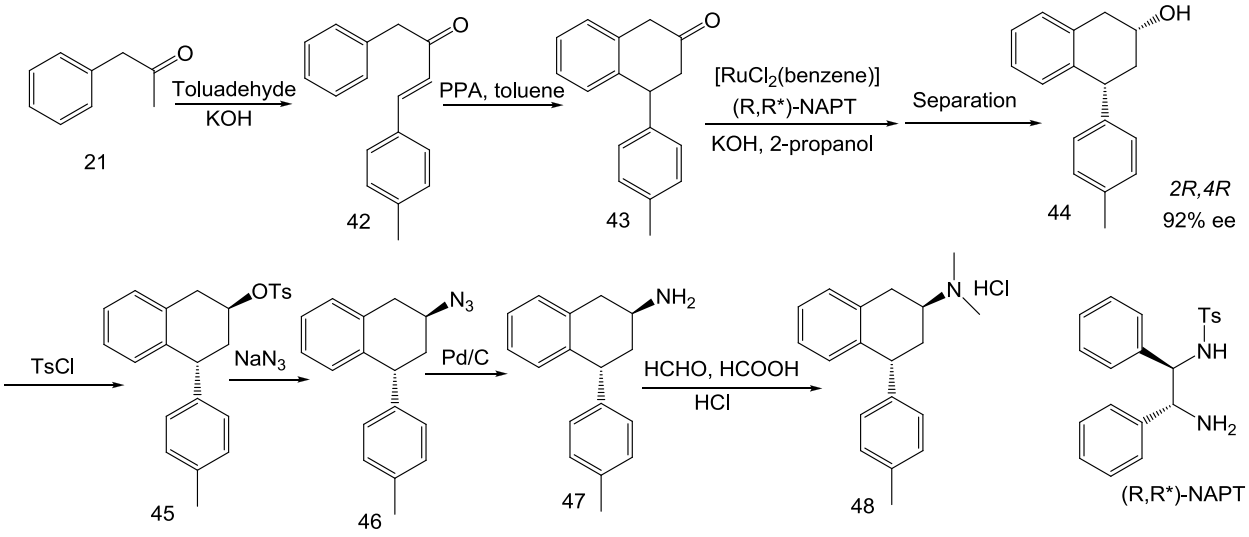

Figure 3-1. Synthesis of (-)-*trans-p*-CH_3-PAT 48

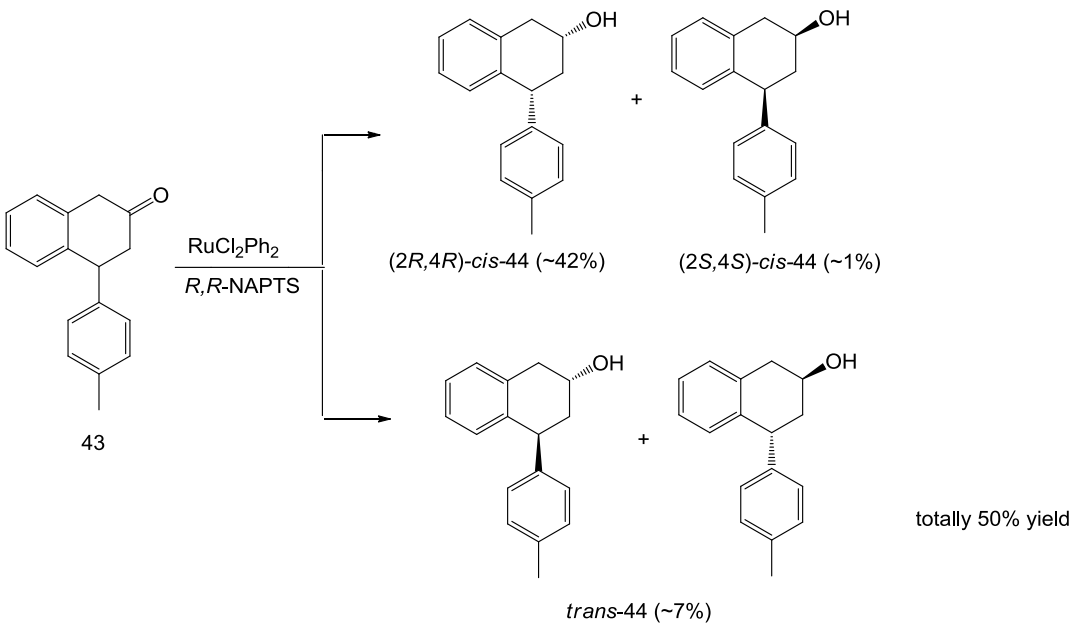

Figure 3-2. Asymmetric reduction with $RuCl_2Ph_2$ and Noyori ligand NAPT to prepare 2-tetralol 44

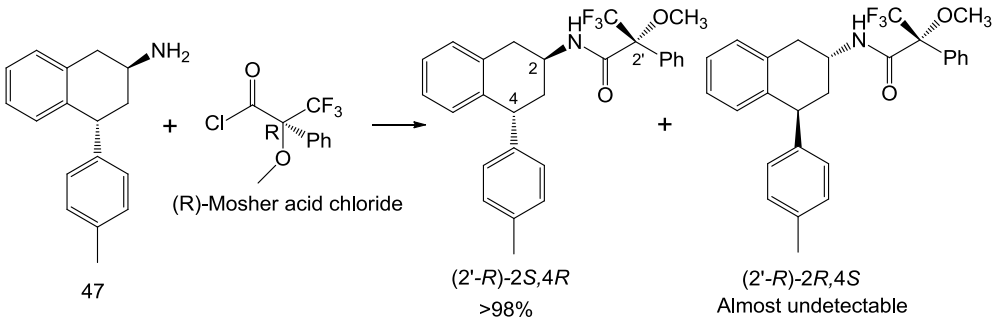

Figure 3-3. Mosher's reagent assay of (-)-*trans*-*p*-CH_3-PAT resolution

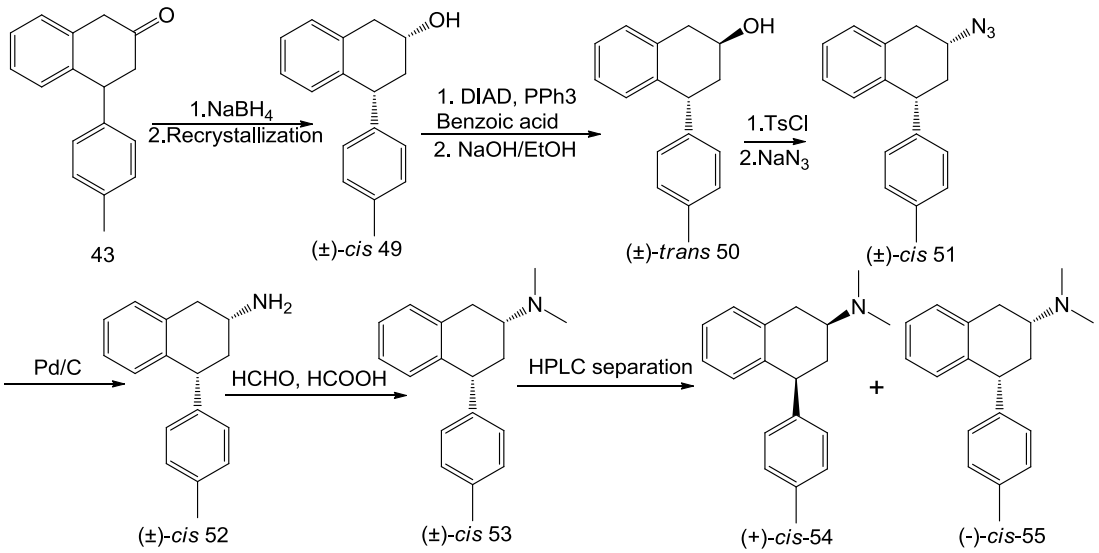

Figure 3-4. Synthesis of (+)-*cis* and (-)-*cis*-*p*-CH_3-PAT(54 and 55)

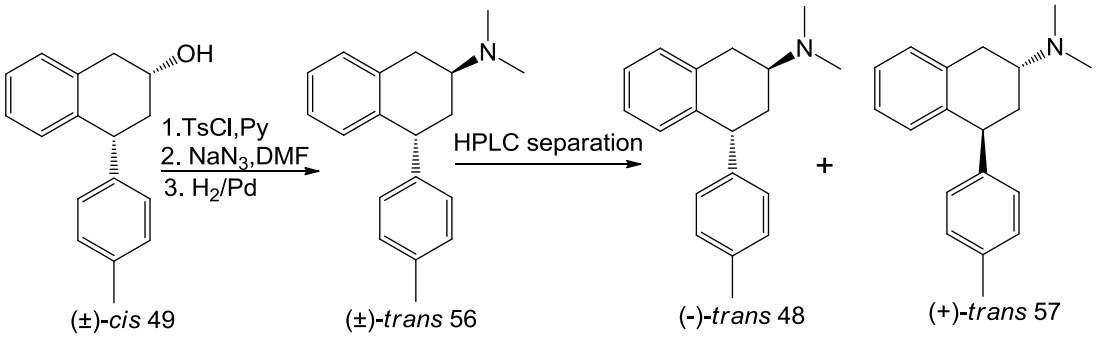

Figure 3-5. Synthesis of (+)-*trans*-*p*-CH_3-PAT 57

5-HT $_{2A}$

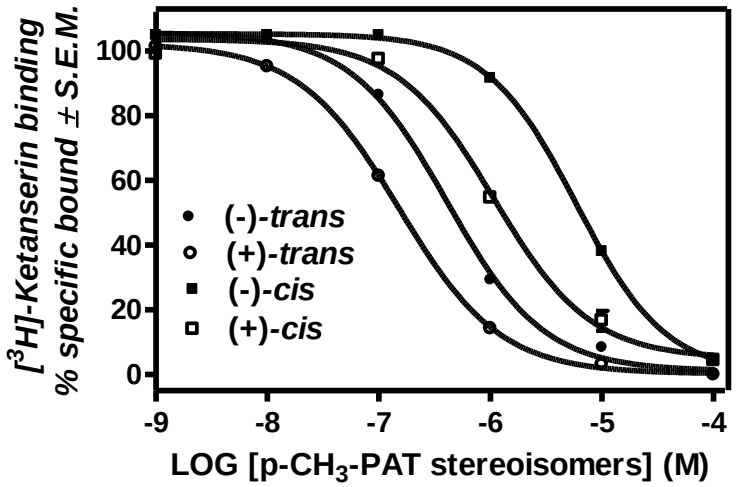

Figure 3-6. Representative concentration-response curves for *p*-CH_3-PAT-isomers displacement of [^{3}H]-ketanserin from 5HT2A receptor. Ki values summarized in Table 3-1

5-HT $_{2B}$

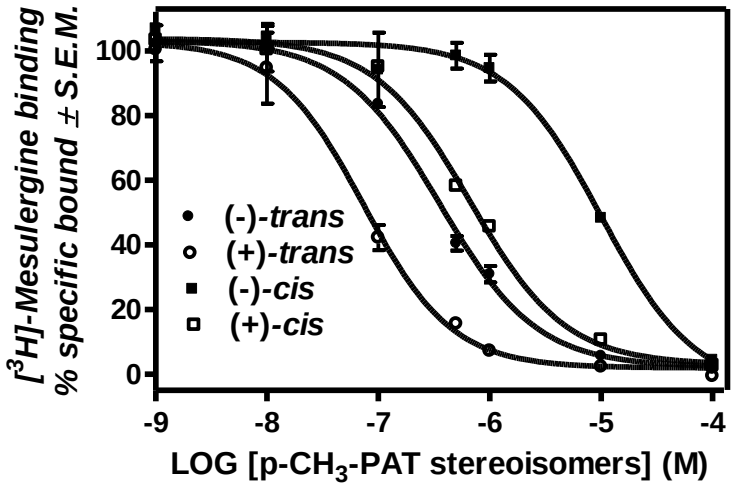

Figure 3-7. Representative concentration-response curves for *p*-CH_3-PAT-isomers displacement of [^{3}H]-mesulergine from 5HT2B receptor. Ki Values summarized in Table 3-1

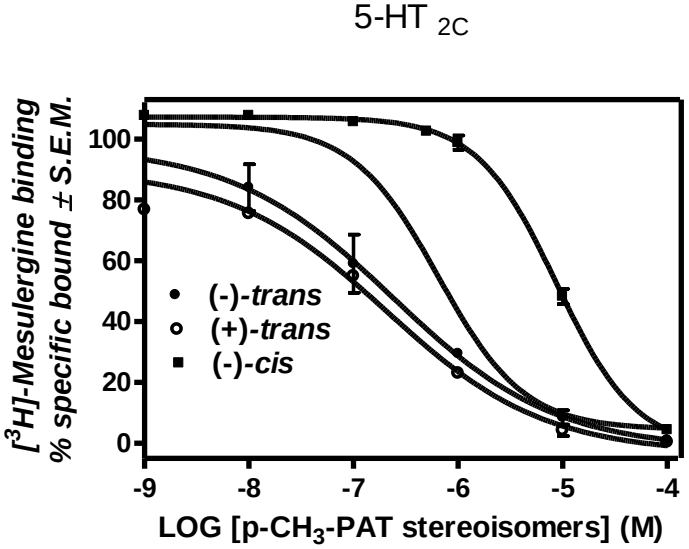

Figure 3-8. Representative concentration-response curves for *p*-CH_3-PAT-isomers displacement of [^{3}H]-mesulergine from 5HT2C receptor. Ki Values summarized in Table 3-1

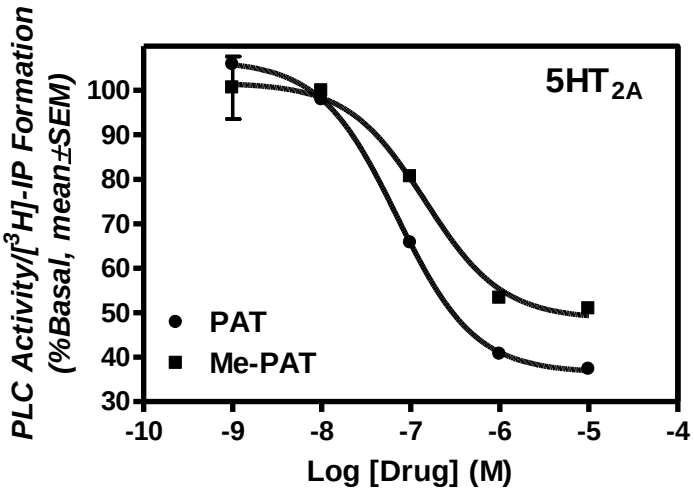

Figure 3-9. Representative data for (-)-*trans*-*p*-CH_3-PAT (closed cubic) compared to (-)-*trans*-PAT (closed circles) inverse agonist activities at cloned human 5HT2A receptors expressed in HEK Cells. IC_{50} Data summarized in Table 3-2 (data from Dr. Lijuan Fang)

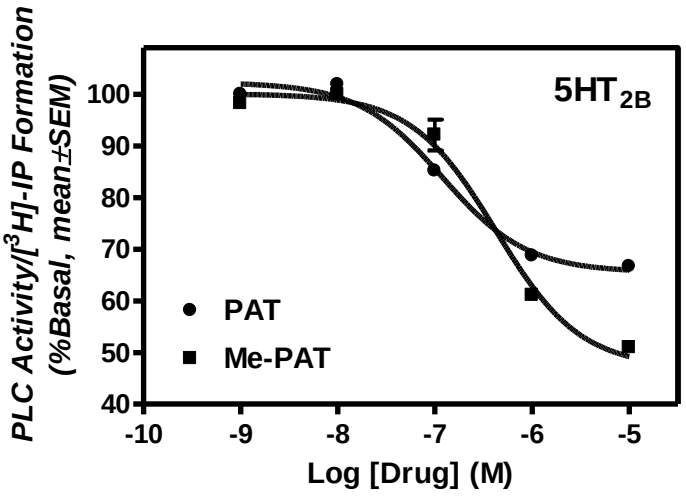

Figure 3-10. Representative data for (-)-*trans*-*p*-CH_3-PAT (closed cubic) compared to (-)-*trans*-PAT (closed circles) inverse agonist activities at cloned human 5HT2B receptors expressed in HEK Cells. IC_{50} data summarized in Table 3-2 (data from Dr. Lijuan Fang)

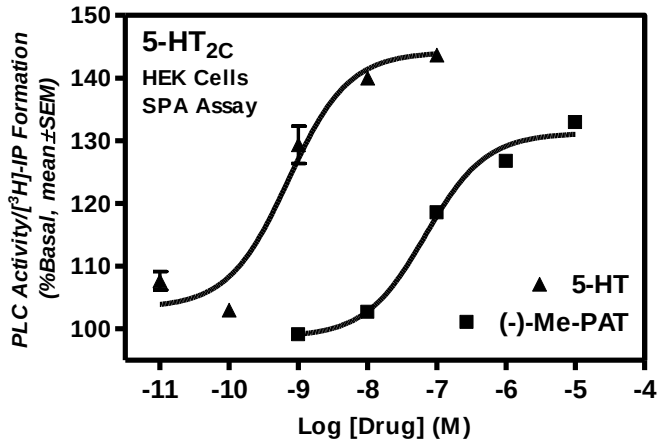

Figure 3-11. Representative data for (-)-*trans*-*p*-CH_3-PAT (closed cubic) compared to (-)-*trans*-PAT (closed circles) agonist activities at cloned human 5HT2C receptors expressed in HEK cells. IC_{50} data summarized in Table 3-2 (data from Dr. Lijuan Fang)

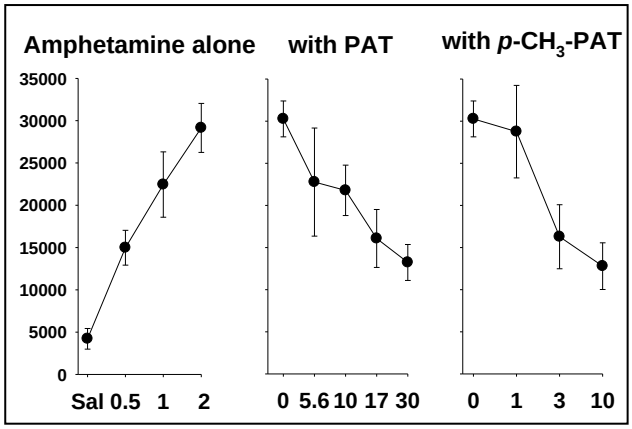

Figure 3-12. (-)-*Trans*-*p*-CH_3-PAT compared to (-)-*trans*-PAT in modulating amphetamine-induced locomotion (data from Dr. Drake Morgan, UF Department of Psychiatry). Left panel: amphetamine dose-dependently increased locomotor activity. Middle and right panels: (-)-*Trans*-PAT and (-)-*trans*-*p*-CH_3-PAT dose-dependently inhibit the psycho-locomotor behavioral effect respectively. PATs, or amphetamine administered intraperitoneally, alone or in combination immediately before the session

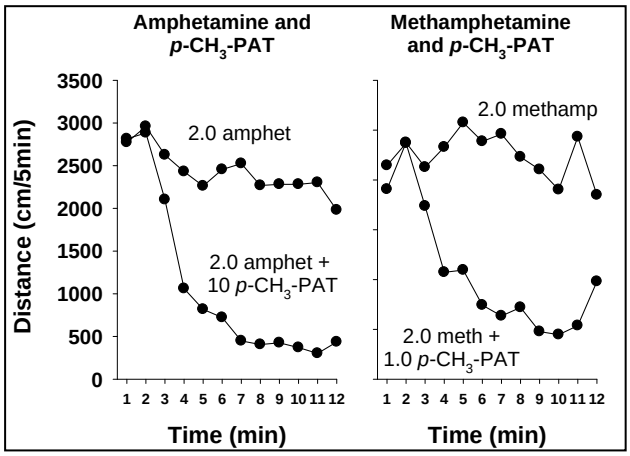

Figure 3-13. Single dosage (-)-*trans*-*p*-CH_3-PAT in modulating amphetamine and methamphetamine-induced locomotion (data from Dr. Drake Morgan, UF Department of Psychiatry). Left panel: (-)-*trans*-*p*-CH_3-PAT blocks the stimulant effects of amphetamine at 10mg/kg. Rght panels: (-)-*trans*-*p*-CH_3-PAT partially block methamphetamine-induced locomotion at 10mg/kg. Agents administered intraperitoneally, in combination immediately before the 12-min experiment sessions

CHARPTER 4
SYNTHESIS OF PAT ANALOGS WITH SUBSTITUTIONS ON THE TETRAHYDRONAPHTHYL AND PENDANT PHENYL.

Rationale

Preliminary results (**Fig. 4-1**) from our lab indicats the racemic-*trans* PAT analog (±)-*trans*-6-OH,7-Cl-PAT has relatively high affinity (Ki~23 nM) for 5HT2C receptors (Fang and Booth, unpublished data, 2008). In comparison to 5HT2C affinity of the lead analog (-)-*trans*-PAT (Ki~40 nM), racemic (±)-*trans*-6-Cl,7-OH-PAT appears to have about 2-times higher affinity. Using a 5HT2C molecular model built by homology to the crystal structure of bovine rhodopsin, ligand docking studies suggested the 7-Cl and/or or 6-OH substituent may form a hydrogen bond with the 5HT2C amino acid residue S3.36 (Wilczynski and Booth, unpublished data, 2009). Likewise, several other residues in 5HT2C TMD helices 3, 6, and 7 may form hydrogen bond interactions with the substituted tetrahydronapthyl moiety of PAT. Interestingly, preliminary functional activity results indicated that (±)-*trans*-6-OH,7-Cl-PAT is a 5HT2C *inverse* agonist with IC_{50}~15 nM. Thus, 6-OH,7-Cl-PAT and related molecules, in comparison to the 5HT2C agonist (-)-*trans*-PAT, may provide useful drug design information regarding the structural requirements for agonist vs. inverse agonist activity at 5HT2C receptors. The preparation of enantiomerically pure (+) and (-)-*trans*-6-OMe,7-Cl-PAT (**58** and **59**), as the precursors to obtain (+) and (-)-*trans*-6-OH,7-Cl-PAT was proposed. It is noteworthy that the 6-OMe,7-Cl-PATs (LogP=4.6) are more lipophilic than 6-OH,7-Cl-PATs (LogP=4.3), suggesting superior brain penetration may be apparent for the *O*-methylated derviatives. To fully characterize the 3-dimensional structure-activity requirements governing agonist vs. inverse agonist activity, the corresponding *cis*-6-OMe,7-Cl PATs (**60** and **61**) also were proposed for synthesis.

In addition to the 6-OMe,7-Cl-PAT compounds, above, PAT analogs **62**, **63**, **64**, **65**, **66**, and **67**, with a chlorine or bromine moiety at the *meta*-position of the (C4) pendant phenyl were proposed, based on results of on-going studies in our lab that indicate halogen substitution at the *meta*-position enhances 5HT2 receptors affinity of PAT-type structures. It is noted, too, that a halogen moiety enhances lipophilicity (LogP>5 for analogs proposed).that may allow for superior brain penetration. To establish the relative contribution of the 7-Cl substituent (analogs **58**-**67**) with regard to binding and function, the novel analogs (+)- and (-)-*trans*-6-OMe,3'-Cl-PAT **68** and **69** that have no hydrogen at position 7 also were proposed.for synthesis.

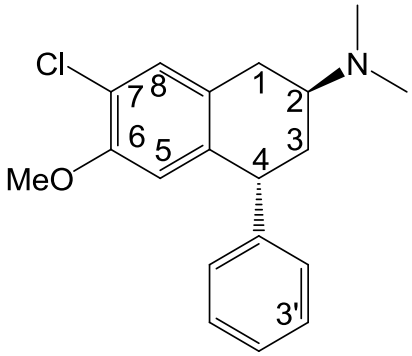

(-)-*trans*-*N,N*-dimethyl-4-phenyl-6-methoxy-7-chloro-1,2,3,4-tetrahydro-2-naphthalen--amine

58

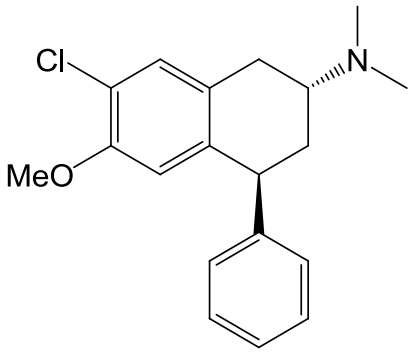

(+)-*trans*-*N,N*-dimethyl-4-phenyl-6-methoxy-7-chloro-1,2,3,4-tetrahydro-2-naphthalen--amine

59

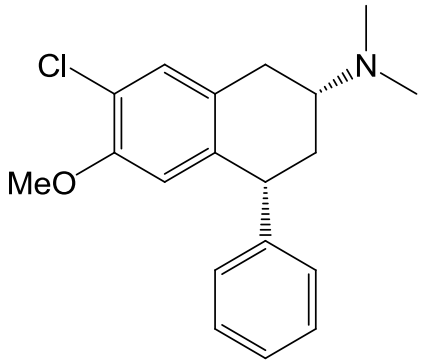

(-)-*cis*-*N,N*-dimethyl-4-phenyl-
6-methoxy-7-chloro-
1,2,3,4-tetrahydro-2-naphthalen--amine

60

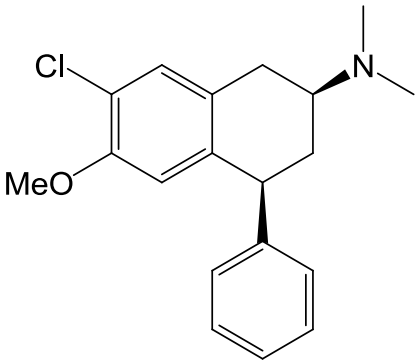

(+)-*cis*-*N,N*-dimethyl-4-phenyl-
6-methoxy-7-chloro-
1,2,3,4-tetrahydro-2-naphthalen--amine

61

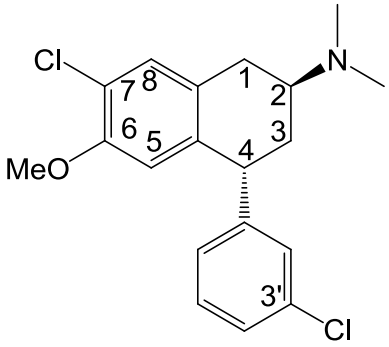

(-)-*trans*-*N,N*-dimethyl-4-(3-chlorophenyl)-
6-methoxy-7-chloro-
1,2,3,4-tetrahydro-2-naphthalen–amine

62

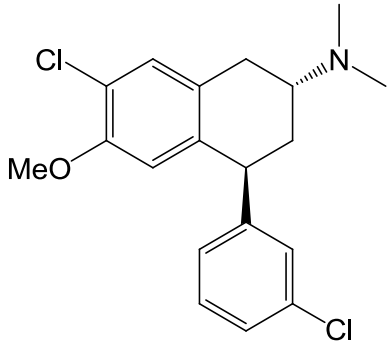

(+)-*trans*-*N,N*-dimethyl-4-(3-chlorophenyl)-
6-methoxy-7-chloro-
1,2,3,4-tetrahydro-2-naphthalen--amine

63

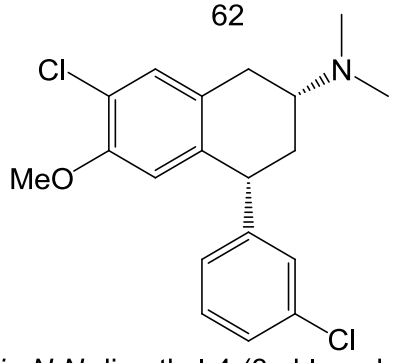

(-)-*cis*-*N,N*-dimethyl-4-(3-chlorophenyl)-
6-methoxy-7-chloro-
1,2,3,4-tetrahydro-2-naphthalen–amine

64

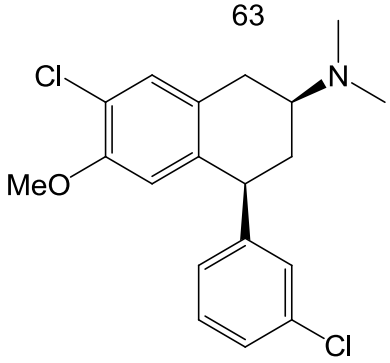

(+)-*cis*-*N,N*-dimethyl-4-(3-chlorophenyl)-
6-methoxy-7-chloro-
1,2,3,4-tetrahydro-2-naphthalen--amine

65

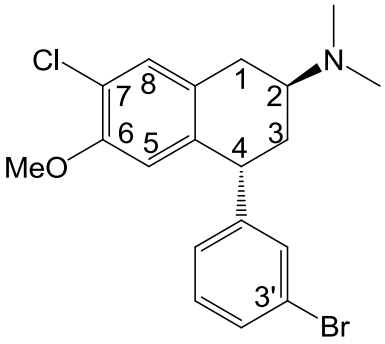

(-)-*trans*-*N,N*-dimethyl-4-(3-bromophenyl)-6-methoxy-7-chloro-1,2,3,4-tetrahydro-2-naphthalen–amine

66

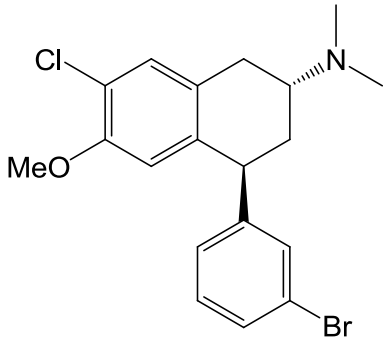

(+)-*trans*-*N,N*-dimethyl-4-(3-bromophenyl)-6-methoxy-7-chloro-1,2,3,4-tetrahydro-2-naphthalen--amine

67

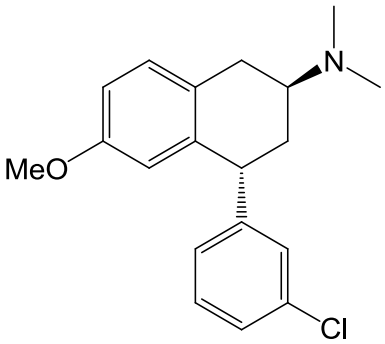

(-)-*trans*-*N,N*-dimethyl-4-(3-chlorophenyl)-6-methoxy-1,2,3,4-tetrahydro-2-naphthalen--amine

68

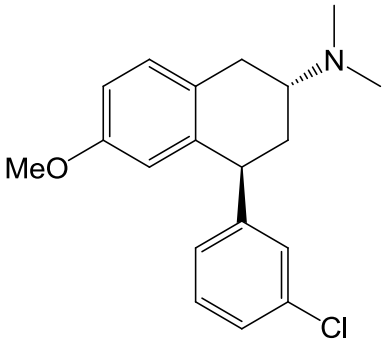

(+)-*trans*-*N,N*-dimethyl-4-(3-chlorophenyl)-6-methoxy-1,2,3,4-tetrahydro-2-naphthalen--amine

69

Synthesis Results and Discussion

To synthesize 6-OMe,7-Cl-PAT analogs **58**, **59**, **60** and **61** (**Fig. 4-2**), commercially available 2-(4-methoxyphenyl) acetic acid was chlorinated (20 g scale) based on a published procedure (Mai et al., 2006). Recrystallization (10% toluene in 90% hexane as solvent) afforded pure product **70** as colorless needle-like crystals (yield 50%).

In the next step, a novel trifluoroacetic acid anhydride (TFAA) mediated Friedel-Craft type condensation reaction developed in our lab (Vincek and Booth, 2009) successfully converted compound **70** to phenyltetralen-2-ol phenylacetate **71** with *meta*-bromostyrene. Briefly, pre-cooled compound **70** was dissolved in TFAA under nitrogen protection. Once the mixture turned an orange-colored liquid, it was transferred (via a double-end needle) to a bottle containing styrene and allowed to sit overnight. Workup involved ethyl acetate extraction followed by multiple washing the organic layer using saturated $NaHCO_3$ in water. After silica-gel chromatography using 5% ethyl acetate in hexane as solvent, product **71** was obtained as thick oil (yield 70% calculated based on starting bromostyrene).

The phenyltetralen-2-ol phenylacetate **71** was reduced by $NaBH_4$ (yield 50%) using the procedure in the analogous synthesis described in chaptor 2. Racemic (±) *cis*-hydroxy intermediate **72** was obtained. It was found that ~2% of *trans*-**75** co-exists based on ^{1}H-NMR peak integration of the characteristic ^{1}H-NMR signals (*cis*-**72**: C4 proton δ=4.1,m Vs. *trans*-**75** C4 proton δ=4.3,t; Wyrick et al., 1993; Gatti et al., 2003). The product collected was used in the next synthetic step without further separation.

To synthesize *cis*-product **60** and **61**, the racemic *trans*-ol **75** was prepared from racemic *cis*-**72** based on a modified Mitsunobu reaction procedure (Wyrick et al., 1993).

In the next step, both intermediate **72** and **75** were treated with platinum/charcoal and triethyl amine (TEA) in MeOH solution under a H_2 baloon (Monguchi et al., 2006). In this way the *m*-bromo on the pendant phenyl was de-coupled. This mild reaction condition proved selective i.e., no de-coupling of the 7-chloro was observed. The products (**73** and **76**) were quantitatively collected through simple filtration and concentration.

In the next step, compound **73** or **76** was tosylated by TsCl and pyridine respectively. Compared to the analogous reaction in chapter 2 and 3, the reaction time in this case was adjusted to 8 hours The crude tosylated product was directly used in the amination step to avoid possible decomposing.

A facile amination procedure was developed to obtain intermediates **74** and **77**. Brieftly, the tosylated versions of **73** and **76** were transferred to a thick-wall flask containing dimethyl amine (40% in H_2O). The bottle was sealed and the mixture was stirred at 80°C overnight. After workup and silica gel chromatography racemic dimethylated product **74** or **77** was collected. This procedure replaced the NaN_3-mediated azide formation and Pd/charcoal catalysed hydrogenation used previously (Wyrick et al., 1993), wherein Pd/C mediated hydrogenation at 45psi could result in de-coupling of the 7-chlorine. It should be noted the yields for the tosylation, Mitsunobu reaction and amination reactions were low (around 30-40%). however, quantities of products obtained were suitable to immediately undertake *in vitro* pharmacological experiments.

In the final step, a chiral stationary phase HPLC (CSP-HPLC) using a Kromasil® CelluCoat™ column was employed to enantiomerically separate the racemic *N,N*-dimethyl PAT analogs **74** and **77** .The HPLC system used a mobile phase system

consisting of 8% ethanol in 92% hexane with 0.1% diethyl amine and 0.1% trifluoroacetic acid added in as modifiers and the flow rate 4ml/min to resolve 1 mg compound dissolved in 200 µl mobile phase in a single run. The collected eluents were partitioned between CH_2Cl_2 and water (adding H_2O in first), extracted by CH_2Cl_2 and dried by Na_2SO_4 to completely remove the salt formed by diethyl amine and trifluoroacetic acid in the HPLC mobile phase. Repeated separation and purification using the CSP-HPLC system described above afforded each enantiomerically pure final product in 10 mg scale as white highly hydroscopic solids. R_f for (-)-*trans*-**58**: 15.5 min; R_f for (+)-*trans*-**59**: 12.0 min; R_f for (-)-*cis*-**60**: 14.7 min; R_f for (+)-*cis*-**61**: 12.8 min. Assignment of absolute configuration was based on analogy to the X-ray crystal structures of (–)-*trans*-*N,N*-dimethyl-1,2,3,4-tetrahydro-2-naphthalenamine 1-(*R*)-(–)-camphor-10-sulfonic acid salt (Wyrick et al., 1993) and (-)-*cis*-*N,N*-dimethyl-1,2,3,4-tetrahydro-2-naphthalenamine 1-(*R*)-(–)-camphor-10-sulfonic acid salt (Bucholtz et al., 1998).

To synthesize 6-OMe,7-Cl,3'-Cl-PAT analogs **62**, **63**, **64** and **65** (**Fig. 4-3**), compound **70** and commercially available *meta*-chlorostyrene yielded substituted phenyltetralen-2-ol phenylacetates **78** using TFAA procedure described above (Vincek & Booth, 2009). Compound **78** was reduced by $NaBH_4$ to afford racemic *cis*-ol **79**. *Trans*-ol **81** was prepared from compound **79** using Mitsunobu conditions. Both *cis*-**79** and *trans*-**81** were converted to final enantiomers **62**, **63**, **64** and **65** using analogous methods described above. CSP-HPLC separation results: R_f for (-)-*trans*-**62**:14.8 min. R_f for (+)-*trans*-**63**: 12.2 min; R_f for (-)-*cis*-**64**: 12.7 min, R_f for (+)-*cis*-**65**: 19.4 min.

To synthesize *trans*-6-OMe,7-Cl,3'-Br-PAT analogs **66** and **67**, (**Fig. 4-4**), the phenyltetralen-2-ol phenylacetate intermediate **71** was reduced by $NaBH_4$, followed by tosylation and amination to give (±)-*trans* **83.** The CSP-HPLC system described above was used to separate the entantiomers of (±)-*trans* **83**. R_f for (-)-*trans*-**66**: 14.6 min; R_f for (+)-*trans*-**67**: 13.1 min.

To synthesize *trans*-6-OMe, 3'-Cl-PAT analogs **68** and **69** (**Fig. 4-5**), commercially available 2-(4-methoxyphenyl) acetic acid and and *meta*-chlorostyrene yielded intermediate **84** using TFAA procedure described above (Vincek & Booth, 2009). After $NaBH_4$ reduction, product *cis* -**85** was subjected to tosylation and amination. The racemic (±)-*trans*-**86** was separated by CSP- HPLC. R_f for (-)-*trans*-**68**: 14.5 min; R_f for (+)-*trans*-**69**: 12.7 min.

In vitro Pharmacological Characterization Results

Preliminary *in vitro* competitive binding assay measured the ability of PAT analog **66**, **67**, **68**, and **69** to displace [^{3}H]-radioligands from human 5HT2C receptors expressed in HEK cell membranes (Booth et al., 2009). Affinity values (Ki) are summarized in **Table 4-1** and representative radioligand competition displacement curves are shown in **Fig. 4-6**.and **4-7**.

In addition, functional activity of PAT analog **68** was measured as activation of PLC/ IP signaling in HEK cells expressing human 5HT2C receptors (Booth et al., 2009). Preliminary results are that compound **68** is a potent partial agonist at 5HT2C receptors compared to the endogenous agonist 5HT. Representative potency-efficacy curves are shown in **Fig. 4-8** (Canal and Booth, unpublished data, 2010). Comprehensive *in vitro* characterization of all the novel PAT analogs described in this chapter has been

initiated by pharmacologists in the medicinal chemistry laboratories of Dr. Booth at University of Florida.

Disscussion and Future Studies

Novel Friedel-Craft type cycli-acylalkylation and enolized *O*-acylation reaction (Vincet, Booth 2009) facilitated preparation of stable phenylacetate intermediates **71**, **78**, and **84**, avoided the need of low yielding claisen condensation and polyphosphoric acid (PPA)-mediated cyclization that used in previous PAT analogs synthesis. All the novel analogs were obtained in 10-40mg scale; enantiomeric purity is 100% as measured by the sensitive CSP-HPLC methods described above.

In vitro 5HT2C radioligand competitive displacement assay results for analogs **66**, **67**, **68**, and **69** revealed (-)-*trans*-6-OMe-7-Cl-3'-Br-PAT **66** (Ki=~10nM) has 5-fold higher binding affinity than its (+)-*trans*-isomer **67** (Ki=~50 nM) whilst (-)-*trans*-6-OMe-3'-Cl-PAT **68** (Ki=~10nM) has 10-fold higher binding affinity than its (+)-*trans*-isomer **69** (Ki=~100 nM). In both cases, (-)-*trans*-enantiomers demonstrate higher binding affinity on 5HT2C receptors, consistent with our observation that most (-)-*trans*-configuration PAT analogs show higher binding affinity and functional potency than their corresponding (+)-*trans*-enantiomers (Booth et al., unpublished data, 2010)—*para*-substituted analogs are exceptions (e.g., see Chapter 3, *in vitro* affinity results). And computer-aided 5HT2C molecular modeling and ligand docking studies have been initiated by Dr. Cordova in the Booth lab to probe binding modes of PATs.

Preliminary results support the hypothesis tested that (-)-*trans*-PAT analogs with halogen substituted on the *meta*-position of the pending phenyl have high binding affinity at 5HT2C receptors than (+)-*trans*-isomers. In fact, analogs **66** and **68** are among the highest affinity of PAT analogs (n=80) that the Booth labs have synthesized.

The shallow Hill slopes (n_H=0.6) of the radioligand competitive displacement curves for analogs **66**, **67**, **68** and **69** are characteristic of ligands with agonist functional activity at aminergic GPCRs (Knight et al., 2004). Encouragingly, analog **68** showed potent partial agonism (EC_{50}=20 nM) in comparison to the endogenous agonist 5HT in preliminary study, suggesting, one or more of the other analogs 58 – 69 may also be potent 5HT2C agonists.

The results mentioned above indicate novel PAT analogs described in this chapter significantly expand the biochemical space probed in the putative orthosteric binding pocket of 5HT2-type receptors. The analogs synthesized and pharmacotherapeutical information that has/ will be obtained greatly contribute to our research for high potency, high selectivity 5HT2C agonists.

Previous 5HT2C molecular modeling studies based on bovine rhodopsin (Booth et al., 2009) indicated the (-)-*trans*-PAT protonated amine can form an ionic bond with D3.32 of 5HT2A and 5HT2C receptors (distance 1.7Å), but, not with 5HT2B receptors. Experimental result from mutagenesis studies confirmed PAT ligand interaction with 5HT2C residue D3.32 (Li and Booth; unpublished data, 2010). The bovine –rhodopsin-based model also suggested 5HT2C amino acid residue S3.36 might form hydrogen bonds with the 7-Cl and/or or 6-OH substituent. Recently, however, a new 5HT2C molecular model based on crystallographic structure of the human β2-adrenergic receptor (ADRB2, which is closer to 5HT2 receptors concerning sequence similarity than bovine rhodopsin) revealed the PAT tetrahydronaphthalene moiety does not bind in close proximity to 5HT2C S3.36 (Cordova and Booth, unpublished results, 2010) — this was experimentally confirmed by mutagenesis studies results that indicate (-)-*trans*-

PAT binds to the S3.36A 5HT2C point-mutated receptor with affinity similar to the wild type receptor (Canal and Booth, unpublished data, 2010). New molecular modeling results (Cordova and Booth, unpublished data, 2010) suggest PAT tetrahydronaphthyl ring substituents (6 and/or 7 positions) might be capable of hydrogen bonding with 5HT2C residues in TMD 5 (e.g., S5.43) similar to the putative 5HT2C interaction with the 5-OH moiety of 5HT (Kroeze et al., 2002). In addition to mutagenesis studies, the analogs synthesized here (**58** – **69**) will help determine the 3-dimensional interactions between the 5HT2C receptor and the PAT tetrahydronaphthyl and (C4) pendant phenyl moieties.

To further investigate these new 6,7-substituted PAT analogs as neurobiochemical probes and drug discovery leads, more than one gram of versatile intermediate **72** was synthesized and purified, providing sufficient agent to get *trans*-6-OMe,7-Cl PAT analogs, as well as *trans*-6-OH,7-Cl analogs in the near future. It is intriguing to verify the previous notion that *trans*-6-OH,7-Cl-PAT is an inverse agonist on 5HT2C receptor, and, if it is the case, to probe the possible mechanisms of the functional activity switch i.e. *trans*-6-OMe,7-Cl-PAT agonism vs. *trans*-6-OH,7-Cl-PAT inverse agonism.

With regard to drug discovery, analogs with highest 5HT2C agonist activity and 2A/2B inverse agonism will be assessed as pharmacotherapeutic candidates in rodent models of obesity, psychostimulant abuse and psychotic disorders, e.g., see Rowland et al., 2008.

Table 4-1. Preliminary binding affinities of PAT analogs 66,67,68,69 at 5HT2C receptors

	5HT2C binding affinity (nM)
(-)-*trans*-6-OMe-7-Cl-3'-Br-PAT **66**	~ 10
(+)-*trans*-6-OMe-7-Cl-3'-Br-PAT **67**	~ 50
(-)-*trans*-6-OMe-3'-Cl-PAT **68**	~ 10
(+)-*trans*-6-OMe-3'-Cl-PAT **69**	~ 100

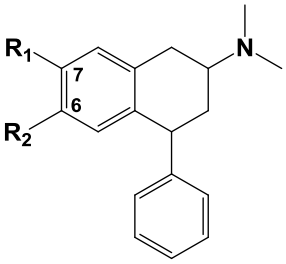

	5HT2A Ki (nM)	5HT2B Ki (nM)	5HT2C Ki (nM)	5HT2C IC_{50} (nM) Imax (%) basal
R_1=Cl, R_2=OH				
(±)-*trans*-6-OH,7-Cl-PAT	28.5 ± 2.10	500 ± 4	23.2 ± 1.95	IC_{50}=15 ± 1.2 I_{max}=50% ± 2
(±)-*cis*-6-OH,7-Cl-PAT	>1000	>1000	>1000	Not determined
R_1=OH, R_2=OH				
(±)-*trans*-6-OH,7-OH-PAT	~500	>1000	~300	Not determined
(±)-*cis*-6-OH,7-OH-PAT	>1000	>1000	>1000	Not determined

Figure 4-1. Preliminary *in vitro* characterization results of 6-OH,7-Cl-PATs and 6-OH, 7-OH-PATs

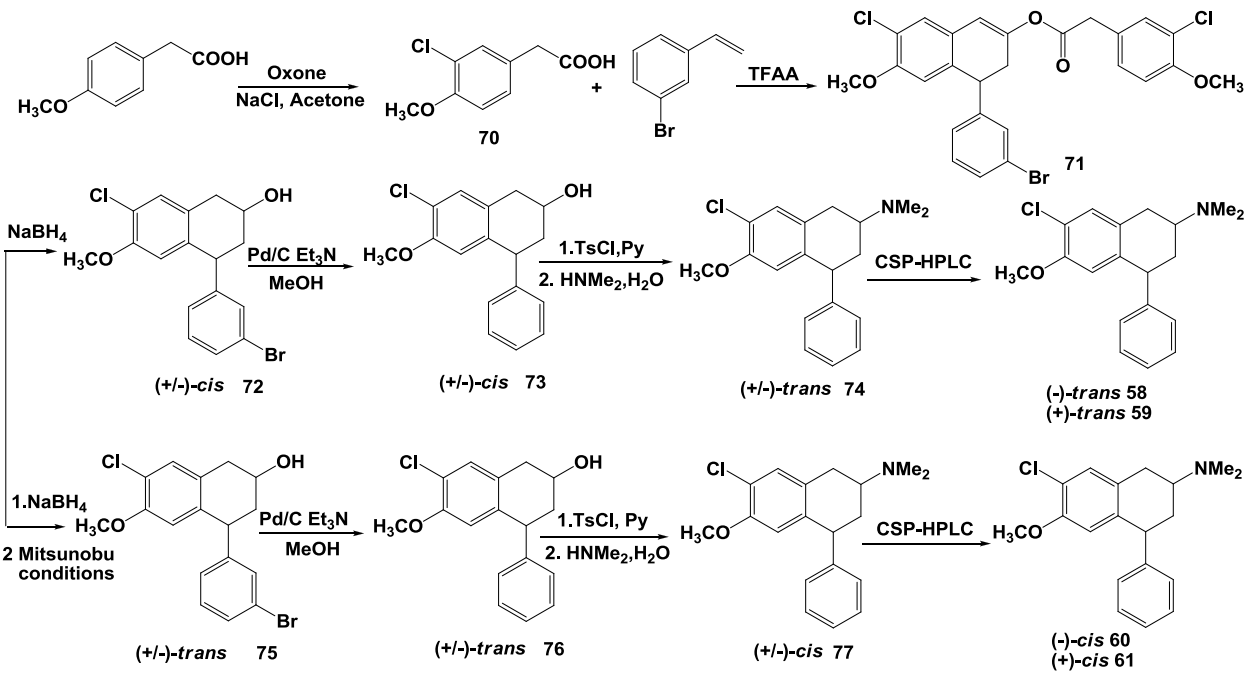

Figure 4-2. Synthesis of *N,N*-dimethyl-4-phenyl-6-methoxy-7-chloro-1,2,3,4-tetrahydro-2-naphthalene-amine 58,59,60,61

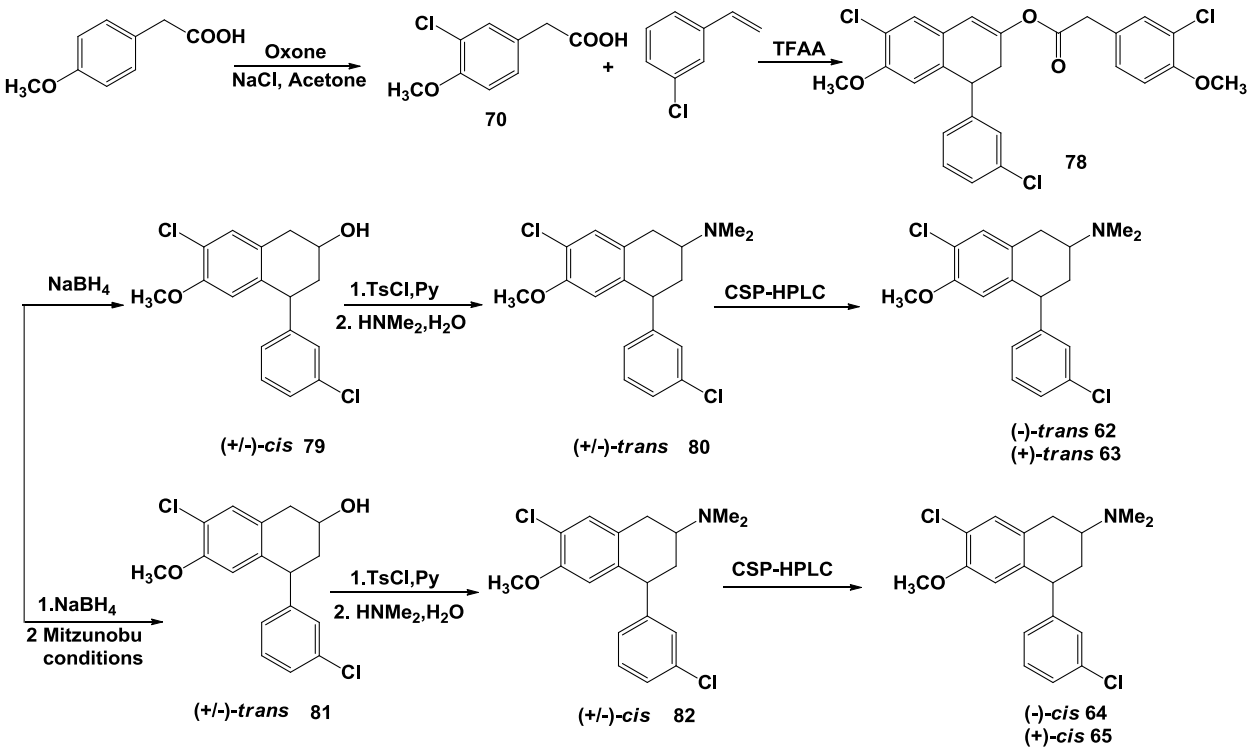

Figure 4-3. Synthesis of *N,N*-dimethyl-4-(3-chlorophenyl)-6-methoxy-7-chloro-1,2,3,4-tetrahydro-2-naphthalene-amine 62,63,64,65

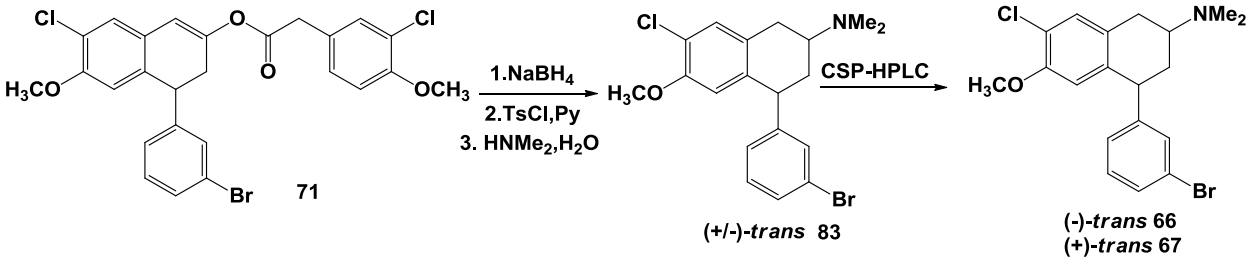

Figure 4-4. Synthesis of *trans-N,N*-dimethyl-4-(3-bromophenyl)-6-methoxy-7-chloro-1,2,3,4-tetrahydro-2-naphthalene-amine 66,67

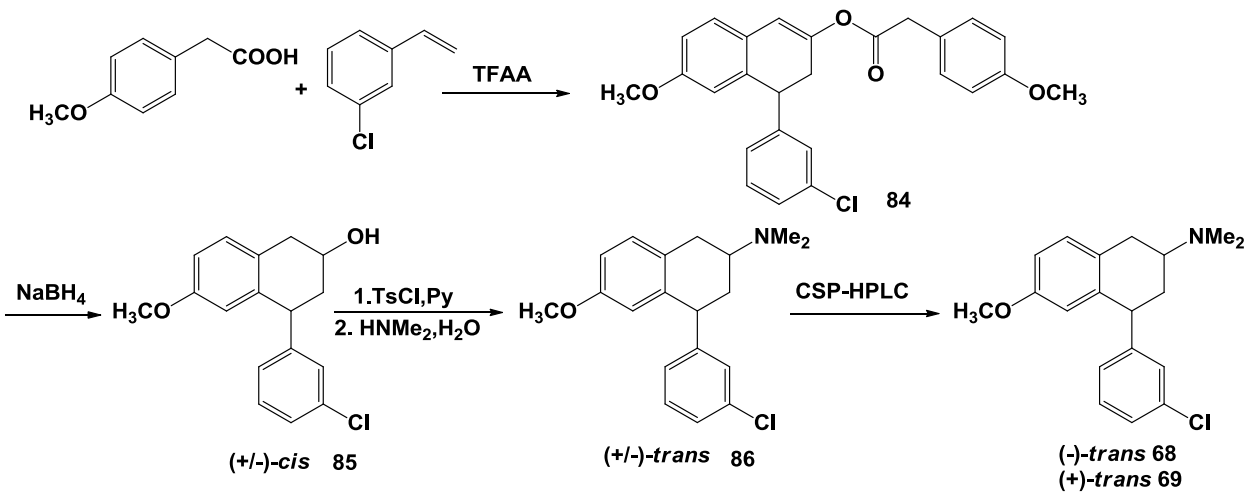

Figure 4-5. Synthesis of *Trans-N,N*-dimethyl-4-(3-chlorophenyl)-6-methoxy-1,2,3,4-tetrahydro-2-naphthalene-amine 68,69

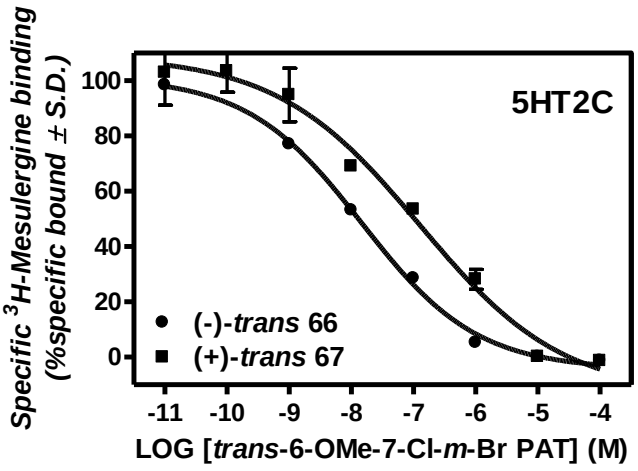

Figure 4-6. Representative concentration-response curves for *trans*-6-OMe-7-Cl-3'-Br-PAT isomer (66, 67) displacement of [^{3}H]-mesulergine from 5HT2C receptors. Ki values summarized in Table 4-1

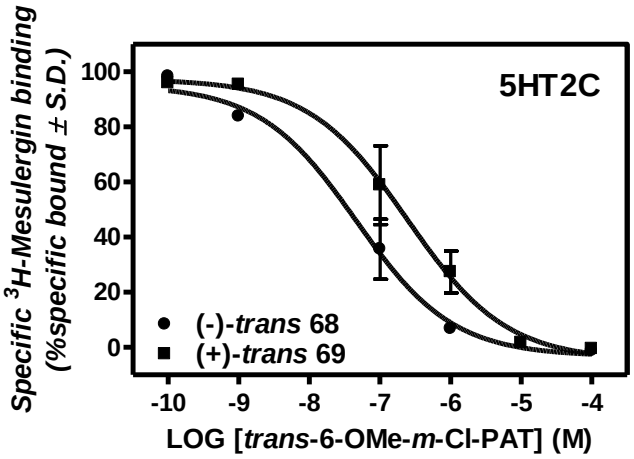

Figure 4-7. Representative concentration-response curves for *trans*-6-OMe-3'-Cl-PAT isomer (68, 69) displacement of [^{3}H]-mesulergine from 5HT2C receptors. Ki values summarized in Table 4-1

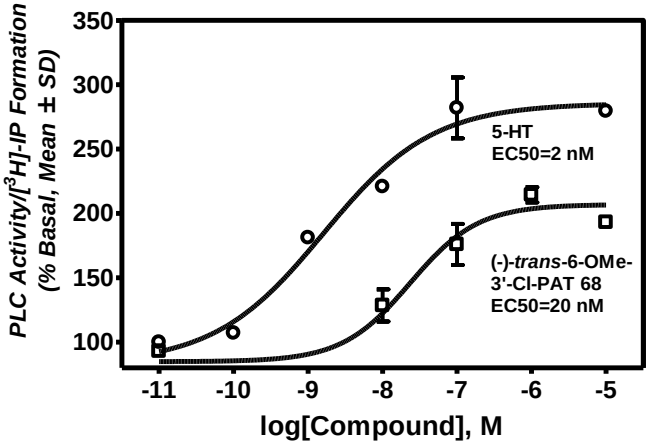

Figgure 4-8. Representative concentration-response curve for serotonin (circles) and (-)-*trans*-6-OMe-3'-Cl-PAT 68 (squares) activation of PLC/ [^{3}H]-IP Formation in clonal cells expressed cloned Human 5HT2C receptors

APPENDIX : EXPERIMENTAL PROCEDURES

All chemicals were used as received from the manufacturers. Proton NMR spectra were obtained on an Oxford NMR AS400 spectrometer using $CDCl_3$ as solvent (TMS). Melting points were determined on a Meltemp apparatus and are corrected. Thin-layer chromatography was performed using Silica gel 60 precoated plates (EMD Chemicals Inc.). Column chromatography was performed using silica gel (230-400 mesh, Fisher Scientific). [^{3}H]-Ketanserin (specific activity 72.2 Ci/mmol) and myo-[2-^{3}H(N)]-inositol (specific activity 18.5 Ci/mmol) were purchased from Perkin-Elmer Life Science (Boston, MA) and [N^6-methyl-^{3}H]-mesulergine (specific activity 72.0 Ci/mmol) was purchased from Amersham Biosciences (GE healthcare, Piscataway, NJ). Unless otherwise noted, all other compounds were obtained in highest purity from Sigma-Aldrich (St. Louis, MO).

A: SYNTHETIC CHEMISTRY

1,-Phenyl-2-propanone (21). Pyridinium chlorochromate (40.2g, 0.186mol) and Al_2O_3 (45g, 0.44mol) were dissolved in CH_2Cl_2 200ml in a 500ml flask. The flask was connected with a mechanic stirrer, then was put into ice/salt bath and stirred for 20min. To this cooled solution, 1-phenyl-2-propanol **20** (21ml, 0.156mol) was added dropwise. The mixture was stirred at 0~4°C for 30 min, then was allowed to recover to R.T. and proceeded for another 8 hours. TLC showed no starting material 21 could be detected. For the workup, diethyl ether was added (150mlx4) to extract the product, the ether solution was filtered through a thick pad of celite/florisil. The solvent was concentrate to afford dark-green liquid as crude product. After silica column (3.5 % ethyl acetate in hexane as eluent), 15.6g pure product 21 was obtained as colorless liquid with the yield of 75%.

^{1}H-NMR:δ 7.4-7.08 (m, 5H), 3.65 (s, 2H), 2.08 (s, 3H) .

1,4-Dipheny-3-buten-2-one (22) and 4-(4-methylphenyl)-1-phenyl-3-buten-2-one (42). Benzaldehyde (23.85g, 0.225mol) was mixed with 850ml water containing KOH (3.5g, 85%), Compound **21** (15.1g,0.113mol) was added into this mixture. The batch was stirred and refluxed at 55 ºC for 6.5 hours. For the workup, hydrochloric acid (37%) was added to monitor the PH of the mixture turn to 4, CH_2Cl_2 was used (200mlx3) to extract the product. The organic layer was washed with water, dried with anhydrous Na_2SO_4. The crude product was concentrated and recrystalized by adding 20ml methanol and put in -20°C freezer overnight. The light-yellow solid formed over this period was filtered out for the next step. After several rounds of the same process, all the leftover mother solutions were combined and concentrated. The mixture was silica-chromatographed using 2.5% ethyl acetate in hexane as eluent. The crude product was concentrated and recrystallized time in hexane-methanol (2:1) solvent system to afford the last batch.

MP 66-69 ºC ; ^{1}H-NMR:δ 7.63 (d, *J*=12 Hz, 1H), 7.52-7.25 (m, 10H), 6.78 (dd, *J*=12, 1.8Hz, 1H), 3.95 (s, 2H).

In preparation of compound **42**, the reaction time was adjusted to13 h.

^{1}H-NMR:δ 7.61 (d, *J*=12 Hz, 1H), 7.43-7.17 (m, 10H), 6.74 (d, *J*=12 Hz, 1H), 3.97 (s, 2H), 2.37 (s,3H).

4-Phenyl-2-tetralone (23) and 3,4-dihydro-4-(4-methylphenyl)-2(1H)-naphthalenone (43). In a 1L multi-neck flask contained 470ml toluene and 36g polyphosphoric (110%), Compound **3** (7.5g, 0.0339mol) was added. The mixture was allowed to be agitated vigorously by a mechanic stirrer and refluxed at 110-120 ºC for 3 h with nitrogen protection. After TLC showed no starting material existed in the reaction

mixture, the batch was cooled to R.T. CH_2Cl_2 was added for extraction (200mlx5). The organic layer was partitioned with water, washed with brine. The solution was concentrated off half the solvent, and then dried with anhydrous Na_2SO_4. After being evaporated *in vacuo*, the crude product was collected as thick dark orange oil. Silica column was performed using 3% ethyl acetate in hexane to get the pure compound **23** as orange-yellow oil. The yield was 41%.

^{1}H-NMR:δ 7.37-7.14 (m,8H), 7.15 (d, *J*=5.1 Hz, 1H), 4.48 (t, *J*=4.2 Hz, 1H), 3.62 (dd, *J*=24.8, 15Hz, 2H), 2.9 (m, 2H).

For the preparation of compound **43**, the reaction time was elongated to 4.5h. The purified product was solidified slowly in 4°C environment.

^{1}H-NMR:δ 7.35-6.99 (m, 8H), 4.43(t, *J*=4.8 Hz, 1H), 3.70-3.56 (dd, *J*=25.5, 15.6Hz, 2H), 2.90 (m, 2H), 2.36 (s, 3H).

1,2,3,4-Tetrahydro-4-pheynl-2-naphthol (24). Compound 23 (10.5g, 0.047mol) was dissolved in 345ml MeOH. The solution was cooled to 0 ºC by ice/salt bath. $NaBH_4$ (6.23g, 0.16mol) was added in portion over a period of 5min. The mixture was stirred at 0 ºC for 30min, then was slowly recovered to R.T. Till no more H_2 bubble was detectible, The mixture was allowed to reflux at 55 ºC for 10 hrs. For the workup, 65ml water was added. The mixture was evaporated to nearly dryness, the gem was extracted by CH_2Cl_2, the solution was partitioned with water, dried with anhydrous Na_2SO_4. After evaporation *in vacuo*, crude product 11.2g was obtained as orange-yellow solid. A mediun size silica gel column (80ml) was performed to remove the majority of impurities using 6.5% ethyl acetate in hexane as eluent. The purified crude product **24** 9.1g was afforded as yellow solid. ^{1}H-NMR showd *cis:trans* = 75%:25%.

(±)-*Cis*-1,2,3,4-tetrahydro-4-pheynl-2-naphthol (25) and (±)-*cis*-1,2,3,4-tetrahydro-4-(4-methylphenyl)-2-naphthol (49). The purified crude product **24** was treated with 650ml solvent (1% ethyl acetate in hexane). The mixture was heated and rotated in 85°C water bath till the compound was totally dissolved. The solution was allowed to cool down smoothly. The recrystallization was completed after the mixture was kept in -20°C freezer for 2 days. During this period the desired product *cis*-**24** was slowly solidified and attached to the wall of the flask. Up to 4 times of repeatedly recrystllizing would afford pure *cis*-tetralols **25**(>97%) in 6g scale. After several rounds of the same process, all the remaining mother solvent was combined and concentrated. The obtained compound was purified and recrystallized follow the same procedure again to afford the final batch of desired product **25.** The total yield of this reduction and separation step was 62%.

MP 110-112 ºC; ^{1}H-NMR: δ 7.34-7.02 (m, 8H) 6.76 (d, *J*=6, 1H), 4.21-4.13 (m, 2H), 3.2 (dd, *J*=11.7, 2.7 Hz, 1H), 2.92 (dd, *J*=11.1, 7.8 Hz, 1H), 2.39 (m, 1H). 1.89 (dd, *J*=17.7, 9Hz, 1H).

Compound **49** was prepared through the same process (70% yield).

^{1}H-NMR:δ 7.3-7.0 (m, 7H), 6.77 (d, *J*=5.7 Hz,1H), 4.42 (m, 1H), 4.40 (dd, *J* =9, 4.2 Hz, 1H), 3.22-3.17 (dd, *J* =11.6, 2.6Hz, 1H), 2.95-2.88 (dd, *J* =11.7, 7.2Hz, 1H), 2.38 (m, 1H), 2.36 (s,3H), 1.9 (dd, *J* =17.7, 9 Hz, 1H).

(*2R,4R)-cis*-1,2,3,4-tetrahydro-4-(4-methylpheynl)-2-naphthalenol (44). A mixture of benzene ruthenium (II) chloride dimer (86mg, 0.17mmol) and (*R*,*R*)-*N*-(2-amino-1,2-diphenylethyl)-*p*-toluenesulfonamide (125mg, 0.34mmol) in 2-propanol 60ml was stirred at 80°C for 30 mim under argon. In a separate flask, a solution of KOH (96

mg 1.7mmol) in 2-propanol 45ml was stirred and pre-heated to 50°C. The starting material **43** (2.0g, 8.47mmol) in 2-propanol 150ml was pre-heated to 50°C, and was added the catalyst mixture followed by KOH solution and stirred at 50°C for 1.5h. After the reaction, the mixture was immediately filtered through a thick pad of silica gel/ celite using ethanol as solvent. The solution was concentrated. The crude product existed as dark-green solid. Medium size silica gel column was performed using 7% ethyl acetate in hexane as eluent. The separation was monitored by TLC and ^{1}H-NMR. Up to 3 times of column chromatography afforded 500 mg pure (*2R,4R)-cis*-**44** (yield 25%).

^{1}H-NMR:δ 7.32-7.0 (m, 7H), 6.77 (d, *J*=5.7 Hz,1H), 4.42 (m, 1H), 4.40 (dd, *J* =9, 4.2 Hz, 1H), 3.22-3.17 (dd, *J* =11.6, 2.6Hz, 1H), 2.95-2.88 (dd, *J* =11.7, 7.2Hz, 1H), 2.38 (m, 1H), 2.36 (s,3H), 1.9 (dd, *J* =17.7, 9 Hz, 1H). $[\alpha]^{25}_{D}$ -18º (MeOH, c=1).

(±)-*Trans*-1,2,3,4-tetrahydro-4-(4-methylpheynl)-2-naphthol (50). Tetralol 49 (100mg, 0.42mmol) was dissolved in 5.5ml THF. Triphenylphosphine (216mg, 0.82mmol) and benzoic acid (103mg, 0.83mmol) was added into this solution. Diisopropyl azodicarboxylate (163µl, 0.83mmol) was added dropwise. The mixture was stirred at R.T. overnight. The solvent was evaporated *in vacuo*. The remaining gum was silica-gel purified using toluene as eluent. The intermediate was dissolved in ethanol. 800µl 1N NaOH in methanol was added. The mixture was stirred at R.T. overnight.

The mixture was then evaporated *in vacuo*. The final product was obtained as colorless thick oil through silica gel column using 10% ethyl acetate in hexane as eluent. Total yield was 52%.

^{1}H-NMR:δ 7.4-7.0 (m, 8H, ArH), 4.42 (t, *J*=5.1 Hz, 1H), 4.40 (m, 1H), 3.37 (dd, *J*=12.5, 3.8Hz, 1H), 2.96 (dd, *J*=12.5, 5.3Hz, 1H), 2.42 (s, 3H), 2.35(m, 1H), 2.18 (m, 1H).

(±)-*Cis*-2-tosyl-1,2,3,4-tetrahydro-4-phenyl-naphthalene (26) and *(2R,4R)*-2-tosyl-1,2,3,4-tetrahydro-4-(4-metylphenyl)-naphthalene (45). Compound **25** (5g, 22.3mmol) was dissolved in pyridine 120ml. To this solution *p*-toluenesulfonyl chloride (8.5g, 44.5mmol) was added in portion. The mixture was stirred at R.T. for 2 days. The reaction was quenched by adding ice/water. The crude compound was extracted with ethyl acetate and dried with anhydrous Na_2SO_4. It was further purified by silica column using first 4% ethyl acetate in hexane 500ml then 10% ethyl acetate in hexane to the end as eluent. Pure compound **26** was collected as light yellow solid (81% yield)

^{1}H-NMR:δ 7.81(d, *J*=6.3 Hz, 2H), 7.32-7.01 (m, 10H), 6.72 (d, *J*=6 Hz, 1H), 4.9 (m, 1H), 4.1(dd, *J*=8.7, 3.6 Hz, 1H), 3.14(d, *J*=6.3 Hz, 2H), 2.45 (m, 1H), 2.43 (s, 3H), 2.1(dd, *J*=18, 9 Hz, 1H).

Compound **45** was prepared from **44** through the same process as a white solid (81% yield).

^{1}H-NMR:δ 7.81 (d, *J*=6.2 Hz, 2H), 7.35-7.0 (m, 9H), 6.73 (d, *J*=5.7 Hz, 1H), 4.90 (m, 1H), 4.1 (m, 1H), 3.13 (d, *J*=6 Hz, 2H), 2.45 (s, 3H), 2.37 (m, 1H), 2.33 (s, 3H), 2.05 (dd, *J*=18, 9Hz, 1H).

(±)-*Trans*-2-azido-1,2,3,4-tetrahydro-4-phenyl-naphthalene (27) and (2*R,4R*)-2-azido-1,2,3,4-tetrahydro-4-(4-metylphenyl)-naphthalene (46) and (±)-*cis*-2-azido-1,2,3,4-tetrahydro-4-(4-methylphenyl)-naphthalene (51). Compound **26** (4.5g, 11.3mmol) was dissolved in DMF 41ml. The solution was treated with NaN_3 (1.85g,

28.5mmol). The mixture was stirred at R.T. for up to 3 days. The reaction was quenched by adding ice/water. The product was extracted by CH_2Cl_2. The organic layer was washed by water, dried with anhydrous Na_2SO_4. The concentrated crude product was purified by silica gel column using hexane as eluent first, then swiched to 10% ethyl acetate in hexane. The pure product 27 was collected as thick colorless oil (yield 89%).

^{1}H-NMR:δ 7.33-7.04 (m, 8H), 6.91 (d, *J*= 5.7Hz, 1H), 4,36 (t, *J*=4.5 Hz, 1H), 3.98 (m, 1H), 3.24 (dd, *J*=12.3, 3.6 Hz, 1H), 2.93 (dd, *J*=12.6, 5.7 Hz, 1H), 2.29-2.12 (m, 2H).

Compound **46** was prepared from **45** through the same process as thick colorless oil

^{1}H-NMR:δ 7.29-6.90 (m, 8H), 4,32 (t, *J*=4.7 Hz, 1H), 3.98 (m, 1H), 3.16 (dd, *J*=12.8, 3.7Hz, 1H), 2.91 (dd, *J*=12.6, 5.4Hz, 1H), 2.35 (s, 3H), 2.32-2.1 (m, 2H).

Compound **51** was prepared from **50** through the same process as thick colorless oil which solidified at 4°C overnight.

^{1}H-NMR:δ 7.26-7.0 (m, 7H), 6.78 (d, *J*=6 Hz, 1H), 4.01 (m, 1H), 3.86 (m, 1H), 3.17 (m, 1H), 2.97 (m, 1H), 2.43 (m, 1H), 2.35 (s, 3H), 1.91 (dd, *J*=18, 9Hz, 1H).

(±)-*Trans*-2-amino-1,2,3,4-tetrahydro-4-phenyl-naphthalene (28) and (*2R,4S*)-2-amino-1,2,3,4-tetrahydro-4-(4-metylphenyl)-naphthalene (47) and (±)-*cis*-2-amino-1,2,3,4-tetrahydro-4-(4-metylphenyl)-naphthalene (52). Compound **27** (2.4g, 9.6mmol) was dissolved in 2-propanol 110ml and CH_2Cl_2 10ml. The mixture was treated with 10% Pd on carbon (0.1g) and shaken on a Parr hydrogenation apparatus (45 psi) overnight. The catalyst was filtered off and the filtrate was evaporated *in vacuo* to afford the crude amine as a solid. For further purification, the crude amine was column-chromatographed on silica gel using CH_2Cl_2 as the eluent first , then switched to 10%

methanol in CH_2Cl_2. The purified (±)-*trans*-**28** was obtained as slight green solid (yield 93%).

MP 62-63 ºC ^{1}H-NMR:δ 7.29-7.01 (m, 8H), 6.94 (d, *J*=12, 6.3Hz, 1H), 4,35 (t, *J*=3.9 Hz 1H), 3.28 (m, 1H), 3.14 (dd, *J*=6.2, 3.9Hz, 1H), 2.63 (dd, *J*=12.3, 6.3Hz, 1H), 2.03 (m, 2H).

Compound **47** was prepared from **46** through the same process as dark-green thick oil

^{1}H-NMR:δ 7.17-6.91 (m, 8H), 4.32 (t, *J*=3.9 Hz, 1H), 3.3 (m, 1H), 3.16 (dd, *J*=12.3, 3.6Hz, 1H), 2.62 (dd, *J*=12, 6.3Hz, 1H), 2.32 (s, 3H), 2.02 (m, 2H).

Compound **52** was prepared from **51** through the same process as thick green oil

^{1}H-NMR:δ 7.26-7.0 (m, 7H), 6.77 (d, *J*=5.7 Hz 1H), 4.07 (m, 1H), 3.27 (m, 1H), 3.06(m, 1H), 2.73 (m, 1H), 2.34 (s, 3H), 2.27 (m, 1H), 1.70 (dd, *J*=18, 9Hz 1H).

Resolution of (±)-*trans*-2-amino-1,2,3,4-tetrahydro-4-phenyl-naphthalene (28). Compound **28** (4.3g, 19.2mmol) and *(1R)-(-)*-camphorsulfonic acid (5.81g, 25mmol) were dissolved in 160ml of acetonitrile/methanol 2:1. The solution was stirred and heated to 110°C and kept under reflux for 1.5hrs, then was cooled smoothly to R.T. and stirred overnight. The solvent were evaporated *in vacuo* to afford the crude salt as dark-orange solid. The crude salt was washed by hexane and small amount of methanol. The remaining solid was treated with acetonitrile/methanol 4:1at the approximate ratio of 1g: 650ml. The mixture was rotated in 75°C water bath till the compound was dissolved completely. The solution was cooled down smoothly and kept at 0°C for up to 2 days. In the first several rounds of processing the crystals falling off were needle-shaped and optically dextrorotatory. Mosher reagent derivatization assay

revealed it contains more of the undesired (+)-*trans*-amine than (-)-*trans*-isomer. The needle-like crystals were separated and the mother solution was concentrated. Several subsequent recrystallizations using the same solvent system afforded pure (-)-*trans*-**28** camphorsulfonic salt as colorless prisms ~650mg in 5 batches. MP 218-220 ºC, $[\alpha]^{25}_{D}$ -68.5º (MeOH).

Each batch of the pure crystals was recovered to free amine (-)-*trans*-**28** by stirring in a mixture of 10ml CH_2Cl_2 and 10ml of saturated aqueous $NaHCO_3$ 10ml overnight. The organic layer was separated and dried with anhydrous Na_2SO_4. The solvent was evaporated *in vacue*. The pure amine was a slight –green solid. (Total resolution yield 10%)

Procedures for Mosher reagent assay. 3~5mg previously obtained crystals was first converted back to free amine **28** by being partitioned between dichloromethane and aqueous $NaHCO_3$. The amine was then dissolved in 200µl dichloromethane, treated by 50µl pyridine and 5µl (R)-Mosher acid chloride. The mixture was stirred at R.T. for 2 h, After evaporation *in vacue*, the mixture was directly tested to get ^{1}H-NMR spectrum in $CDCl_3$ without purification.

(–)-*Trans*-*N,N*-dimethyl-4-pheynl-1,2,3,4-tetrahydro-2-naphthalenamine (30); (–)-*trans*-*N,N*-dimethyl-4-(4-methylpheynl)-1,2,3,4-tetrahydro-2-naphthalenamine (48) and (±)-*cis*-*N,N*-dimethyl-4-(4-methylpheynl)-1,2,3,4-tetrahydro-2-naphthalenamine (53). Free amine (-)-*trans*-**28** (280mg, 1.26mmol) of amine was added in 5.1ml of 95% formic acid and 3.4ml of 38% formaldehyde. The mixture was stirred at 100 ºC for 7 hrs. The volatileswas evaporated *in vacuo* and the residue was dissolved in CH_2Cl_2 and partitioned with saturated aqueous $NaHCO_3$. The organic layer

was dried with anhydrous Na_2SO_4. After evaporation the crude product was collected as a light yellow gum, which solidified upon standing. The amine was dissolved in ethyl acetate. 3ml of 1N HCl in ether was added dropwise. The solvent was evaporated *in vacue*. The salt was washed by ethyl acetate and hexane, dried *in vacue*.

30 free base $[\alpha]^{25}_D$ -57.1º (MeOH) ^{1}H-NMR:δ 7.28-7.0 (m, 8H), 6.95 (d, *J*=5.4 Hz, 1H), 4.36 (d, *J*=3.3 Hz, 1H), 3.03 (dd, *J*=12, 3Hz, 1H), 2.85 (dd, *J*=12.2, 7.3Hz, 1H), 2.64 (m, 1H), 2.23 (s, 6H), 2.13 (m, 2H).

30 HCl salt MP 208-210ºC. $[\alpha]^{25}_D$ -66.5º (MeOH) ^{1}H-NMR (CD_3OD) 7.36-6.98 (m, 8H), 4.58 (m,1H), 3.47 (m, 1H), 3.1-2.92 (m, 2H), 2.9 (s, 6H), 2.21(m, 2H)

Compound **48** was prepared from **47** through the same process as yellow thick oil

48 free base $[\alpha]^{25}_D$ -64.2º (MeOH). ^{1}H-NMR 7.26-6.89 (m, 8H), 4.32 (t, *J*=3.7 Hz, 1H), 3.02 (dd, *J*=12.2, 3.8Hz, 1H), 2.85 (dd, *J*=12.2, 7.4Hz, 1H), 2.64 (m, 1H), 2.3 (s, 3H), 2.25 (s, 6H), 2.1(m, 2H).

48 HCl salt MP 220-222ºC. $[\alpha]^{25}_D$ -67º (MeOH). ^{1}H-NMR (CD_3OD) 7.35-6.91 (m, 8H), 4.55 (m,1H), 3.57 (m,1H), 3.16-2.91 (m, 2H), 2.88(s, 6H), 2.4(m, 2H). 2.34 (s, 3H)

Compound **53** was prepared from **52** through the same process as yellow thick oil

^{1}H-NMR 7.39 (s,1H), 7.28-7.2 (m,5H), 7.14 (t, *J*=5.4Hz,1H), 6.90 (d, *J*=5.7Hz,1H), 4.2 (dd, *J*=9, 3.9Hz,1H), 3.18-3.03 (m,2H), 2.96 (m,1H), 2.51 (s,6H), 2.48 (s,3H), 2.46 (m,1H), 1.87 (dd, *J*=18.2, 9.2Hz 1H).

^{1}H-NMR spectra of **54** are the same as **53**

(+)-*Cis*-N,N-dimethyl-4-(4-methylpheynl)-1,2,3,4-tetrahydro-2-naphthalenamine ((+)-*cis*-54). Free amine $[\alpha]^{25}_D$ + 28.6º. HCl salt $[\alpha]^{25}_D$ + 17.0º

(-)-*Cis*-N,N-dimethyl-4-(4-methylpheynl)-1,2,3,4-tetrahydro-2-naphthalenamine ((-)-*cis*-55). Free amine $[\alpha]^{25}_{D}$ -28.9º. HCl salt $[\alpha]^{25}_{D}$ -18.2º

(+)-*Trans*-N,N-dimethyl-4-pheynl-1,2,3,4-tetrahydro-2-naphthalenamine ((+)-*trans*-57). (±)-*Trans*-**57** was prepared from **49** through tosylation, azidition, reduction and dimethylation. The process and intermediates' 1H-NMR are the same as preparation and spectra of **45-48.** (±)-*Trans*-**57** was collected from HPLC separation

Free amine $[\alpha]^{25}_{D}$ + 65.4º. HCl salt $[\alpha]^{25}_{D}$ + 61.3º

2-(3-chloro-4-methoxyphenyl)acetic acid (70). 2-(4-methoxyphenyl)acetic acid (1g, 6.0mmol) was dissolved in 10ml acetone, Oxone (3.7g, 6.0mmol) was added in, the suspension was stirred at R.T. for 15min, NaCl aqueous solution (1.4g in 10ml H_2O) was added, the mixture was stirred for 6hrs. For the workup, the mixture was evaporated in vacuo, the residue was diluted with water and extracted with ethyl acetate, the organic layer was washed with brine, dryed by Na_2SO_4, concentrated *in vacuo*. The crude product was recrystalized using 10% toluene in hexane as solvent. The final product was collected as white needle-like solid (yield 50%).

^{1}H-NMR (CD_3OD) 7.3 (m, 1H), 7.1 (m,1H) 6.9 (m, 1H) 3.9 (s,3H) 3.6 (S,2H)

4-(3-bromophenyl)-6-methoxy-7-chloro-3,4-dihydronaphthalen-2-yl 2-(3-chloro-4-methoxyphenyl)acetate (71), 4-(3-chlorophenyl)-6-methoxy-7-chloro-3,4-dihydronaphthalen-2-yl 2-(3-chloro-4-methoxyphenyl)acetate (78), and 4-(3-chlorophenyl)-6-methoxy-3,4-dihydronaphthalen-2-yl 2-(4-methoxyphenyl)acetate (84). A flask containing *meta*-chlorostyrene(0.4ml, 3mmol) was pre-cooled in ice/water. In a separated flask, under nitrogen protection, Compound **70**(1.8g, 9mmol) was dissolved in trifluoroacetic acid anhydride (1.3ml, 9.5mmol). Once the mixture turned to

an orange color liquid, a double-end needle was used to transfer the liquid into the bottle contains styrene. The mixture was stirred overnight. For the workup, ethyl acetate was used for extraction for three times. Large amount of saturated $NaHCO_3$ water solvent was used washing the crude product for four times. The organic layer was combined and dried by Na_2SO_4. After medium silica gel column using 5% ethyl acetate in hexane as solvent, crude product **78** was obtained as colorless thick oil. 70% yield calculated based on *meta*-chlorostyrene consumption.

78 ^{1}H-NMR ($CDCl_3$) δ 7.4-6.2 (m,9H), 6.20 (s, 1H), 4.21 (t, J = 3.7 Hz, 1H), 3.9 (s,3H), 3.8 (s,3H), 3.69 (s, 2H), 2.05 (m, 2H)

Compound **71** was prepared using *meta*-bromostyrene following the same procedure.

71 ^{1}H-NMR ($CDCl_3$) δ 7.4-6.2 (m,9H), 6.20 (s, 1H), 4.21 (t, J= 3.6 Hz, 1H), 3.8 (s,3H), 3.7 (s,3H), 3.65 (s, 2H), 2.05 (m, 2H)

Compound **84** was prepared using 2-(4-methoxyphenyl)acetic acid and *meta*-chlorostyrene following the same procedure.

84 ^{1}H-NMR ($CDCl_3$) δ 7.30-6.34 (m,11H), 6.25 (s, 1H), 4.24 (t, J = 3.7 Hz, 1H), 3.8 (s,3H), 3.72 (s,3H), 3.69 (s, 2H), 2.05 (m,2H)

(±)-*Cis* -4-(3-bromophenyl)-6-methoxy-7-chloro-1,2,3,4-tetrahydronaphthalen-2-ol (72) , (±)-*cis* 4-(3-chlorophenyl)-6-methoxy-7-chloro-1,2,3,4-tetrahydronaphthalen-2-ol (79), and (±)-*cis* 4-(3-chlorophenyl)-6-methoxy-1,2,3,4-tetrahydronaphthalen-2-ol (85). $NaBH_4$ (240mg,6.34mmol) was dissolved in 17ml MeOH. The solution was cooled to 0 ºC by ice/salt bath. Compound **78** (1.1g, 2.17mmol) was dissolved in 4ml toluene/methanol (1:1). The solution was injected into

the flask containing $NaBH_4$ solution. The mixture was stirred at 0 ºC for 15min, then was slowly recovered to R.T. Till no more H_2 bubble was detectible, The mixture was allowed to reflux at 55 ºC overnight. For the workup, 10ml water was added. The mixture was evaporated to nearly dryness, the gem was extracted by CH_2Cl_2, the solution was partitioned with water, dried with anhydrous Na_2SO_4. After evaporation *in vacuo*, crude product was obtained as orange-yellow solid. A mediun size silica gel column (80ml) was performed first using pure CH_2Cl_2 as eluent, then switched to 3% MeOH in CH_2Cl_2. The purified crude product **79** was afforded as yellow thick oil (yield75%).

79 ^{1}H-NMR ($CDCl_3$) δ 7.28-7.01(m, 5H), 6.27 (s,1H), 4.16-4.07 (m,2H), 3.62 (s,3H) 3.08 (dd, *J* = 10.8, 3.9Hz, 1H), 2.79 (dd, *J* = 11.1, 6Hz, 1H), 2.38 (m, 1H), 1.8 (dd, *J* = 19, 9Hz, 1H).

72 was prepared through reduction of **71** following the dame procedure.

72 ^{1}H-NMR ($CDCl_3$) δ 7.29-7.0(m, 5H), 6.24 (s,1H), 4.13-4.08 (m,2H), 3.6 (s,3H) 3.1 (dd, *J* = 11.3, 3.5Hz, 1H), 2.81 (dd, *J* = 12.3, 6Hz, 1H), 2.41(m, 1H), 1.78 (dd, *J* = 18.5, 8.7Hz, 1H).

85 was prepared through reduction of **84** following the dame procedure.

85 ^{1}H-NMR ($CDCl_3$) δ 7.3-7.1 (m, 4H), 6.73 (m,1H), 6.26 (s,1H), 4.14-4.07 (m,2H), 3.67 (s,3H) , 3.13 (dd, *J* = 11.6, 3.6Hz, 1H), 2.82(dd, *J* = 11.3, 7.8Hz, 1H), 2.37(m, 1H), 1.83 (dd, *J* = 18.2, 8.7 Hz, 1H).

(±)-*Trans* 4-(3-bromophenyl)-6-methoxy-7-chloro-1,2,3,4-tetrahydronaphthalen-2-ol (75) , (±)-*trans* 4-(3-chlorophenyl)- -6-methoxy-7-chloro-1,2,3,4-tetrahydronaphthalen-2-ol (81). Compound **79** (616mg, 1.9mmol) was

dissolved in 25ml THF. Triphenylphosphine (998mg, 3.8mmol) and benzoic acid (465mg, 3.8mmol) was added into this solution. Diisopropyl azodicarboxylate (749µl, 3.8mmol) was added drop-wise. The mixture was stirred at R.T. overnight. The solvent was evaporated *in vacuo*. The remaining gum was silica-gel purified using toluene as eluent. The intermediate was dissolved in ethanol 45ml. 1N NaOH in methanol (3.6ml) was added. The mixture was stirred at R.T. overnight. The mixture was then evaporated *in vacuo*. The final product was obtained as colorless thick oil through silica gel column using 3% MeOH in CH_2Cl_2 as eluent. Total yield was 35%.

81 ^{1}H-NMR ($CDCl_3$) δ 7.4-7.0 (m, 5H), 6.41 (s,1H), 4.3 (m, 1H), 4.21 (m,1H), 3.6 (s,3H), 3.14 (dd, *J* = 12.2, 3.6Hz, 1H), 2.79 (*J* = 12.4, 4.5Hz, 1H), 2.21-2.17 (m, 1H), 2.04-1.98 (m, 1H).

Compound **75** was prepared from **72** following the same procedure

75 ^{1}H-NMR ($CDCl_3$) δ 7.37-6.98 (m, 5H), 6.40 (s,1H), 4.2 (m,2H), 3.7(s,3H) , 3.14 (dd, *J* = 12.3, 3.6Hz, 1H), 2.75 (*J* = 12.2, 4.6Hz, 1H), 2.24-2.17 (m, 1H), 2.05-1.97 (m, 1H).

(±)-*Cis* 4-phenyl-6-methoxy-7-chloro-1,2,3,4-tetrahydronaphthalen-2-ol (73) and (±)-*trans* 4-phenyl-6-methoxy-7-chloro-1,2,3,4-tetrahydronaphthalen-2-ol (76). Hydroxyl intermediates *cis*-**72** (170mg, 0.46mmol) was dissolved in 5ml MeOH, platinum/charcoal (5.1mg), and triethyl amine 80µl were added in consequently. The mixture was stirred at RT under a hydrogen bulb for 2hs. The products were quantitatively obtained through simple filtration and concentration.

73^{1}H-NMR ($CDCl_3$) δ 7.40-6.82 (m, 6H), 6.21 (s,1H), 4.2-4.02 (m,2H), 3.6 (s,3H) , 3.14-3.04 (m, 1H), 2.82-2.77 (m,1H), 2.39 (m, 1H), 1.8 (q, *J* = 12.1 Hz, 1H).

76 ^{1}H-NMR ($CDCl_3$) δ 7.35-7.02 (m, 6H), 6.41 (s,1H), 4.3 (t, 1H), 4.21 (m,1H), 3.6 (s,3H), 3.14-3.10 (m, 1H), 2.79-2.72 (m,1H), 2.21-2.17 (m, 1H), 2.04-1.98 (m, 1H).

(-)-*Trans*-*N,N*-dimethyl-4-(3-chlorophenyl)-6-methoxy-7-chloro-1,2,3,4-tetrahydro-2-naphthalene-amine (62), (+)-*trans*-*N,N*-dimethyl-4-(3-chlorophenyl)-6-methoxy-7-chloro-1,2,3,4-tetrahydro-2-naphthalene-amine (63), (-)-*Cis*-*N,N*-dimethyl-4-(3-chlorophenyl)-6-methoxy-7-chloro-1,2,3,4-tetrahydro-2-naphthalene-amine (64), and (+)-*Cis*-*N,N*-dimethyl-4-(3-chlorophenyl)-6-methoxy-7-chloro-1,2,3,4-tetrahydro-2-naphthalene-amine (65). Compound **80** (or **82** for *cis* analogs preparation) (337mg, 1.04mmol) was dissolved in pyridine 7ml. To this solution *p*-toluenesulfonyl chloride (397mg, 2.08mmol) was added in by portion. The mixture was stirred at R.T. overnight. The reaction was quenched by adding ice/water. The crude compound was extracted with ethyl acetate and dried with anhydrous Na_2SO_4. It was further purified by silica column using 10% ethyl acetate in hexane to get the crude product.Without further purification, the crude product was transferred into a thick-wall flask, dimethyl amine 4ml(40% in H_2O) was added. The bottle was sealed and the mixture was stirred at 80°C overnight. After extraction using CH_2Cl_2, the crude product was washed by water, dried by Na_2SO_4. Small silica gel column and 5% MeOH in dichloromethane as solvent was used to purify the product.

Shimadzu HPLC system with Kromasil® CelluCoat™ column was used to separate the racemic products. The mobile phase system contained 8% ethanol in 92% hexane with 0.1% diethyl amine and 0.1% trifluoroacetic acid added as modifiers. The flow rate was 4ml/min. loading amount was 1~2mg compound solved in 200µl mobile phase. The eluents containing the desired product were combined and concentrated. The salt from

DEA and TFA made the product a colorless liquid. The product needed to be partitioned between CH_2Cl_2 and water (adding H_2O first), extracted by CH_2Cl_2 and dried by Na_2SO_4 to totally get rid of the salt. Several rounds of HPLC separation and purification afforded us pure final products. The compounds were converted to HCl salts by being dissolved in HCl/ether solution and evaporated *in vacuo*.

62 Highly hygroscopic solid $[\alpha]^{25}_D$ = (-)14º (*c* 1.00, CH_2Cl_2) , R_f of (-)-*trans*-**62**: 14.8min in HPLC separation ^{1}H-NMR ($CDCl_3$) δ 7.38-7.20 (m, 3H), 6.92 (s,1H), 6.85 (m, 1H), 6.54 (s, 1H), 4.42 (m, 1H), 3.79 (s,3H), 3.34-3.21 (m,2H), 3.10-2.98 (m,1H), 2.75 (s,6H), 2.40-2.35 (m,2H), ^{13}C NMR ($CDCl_3$) δ 29.1, 31.8, 42.2, 43.4, 56.2, 57.9, 112.8, 122.1, 125.5, 126.4, 127.4, 128.2, 130.1, 130.7, 134.3, 134.8, 146.0, 154.1. HRMS *m/z* Calcd for $C_{19}H_{22}Cl_2NO$ 350.108, 352.105 $[M+H]^+$, Found 350.1085, 352.1055, $[C_{19}H_{21}Cl_2NO +H]^+$ isotope pattern confirmed.

63 Highly hygroscopic solid $[\alpha]^{25}_D$ = (+)14º(*c* 1.00, CH_2Cl_2), R_f of (+)-*trans*-**63**: 12.2min in HPLC separation. ^{1}H-NMR, ^{13}C NMR and HRMS spectra are the same with **62**.

64 Highly hygroscopic solid $[\alpha]^{25}_D$ = (-)272º(*c* 1.00, CH_2Cl_2) , R_f of (-)-*cis*-**64**: 12.7min in HPLC separation ^{1}H-NMR ($CDCl_3$) δ 7.31-7.05 (m, 5H), 6.26 (s, 1H), 4.15 (dd, *J*=9.15, 3.45 Hz,1H), 3.63 (m,1H), 3.62 (s,3H), 3.17-2.99 (m,2H), 2.85 (s,6H), 2.54-2.50 (m,1H), 1.89 (dd, *J* =18.6, 9 Hz, 1H), ^{13}C NMR ($CDCl_3$) δ 28.7, 29.7, 34.4, 45.7, 56.1, 60.9, 112.4, 121.7, 125.0, 126.8, 127.7, 128.5, 130.3, 130.6, 134.8, 136.7, 146.0, 154.0. HRMS *m/z* Calcd for $C_{19}H_{22}Cl_2NO$ 350.108, 352.105 $[M+H]^+$, Found 350.1086, 352.1057, $[C_{19}H_{21}Cl_2NO +H]^+$ isotope pattern confirmed.

65 Highly hygroscopic solid $[\alpha]^{25}_{D}$ = (+)282º(*c* 1.00, CH_2Cl_2) , R_f of (+)-*cis*-**65**: 19.4min in HPLC separation. ^{1}H-NMR, ^{13}C NMR and HRMS spectra are the same with **64**.

(-)-*Trans*-*N,N*-dimethyl-4-phenyl-6-methoxy-7-chloro-1,2,3,4-tetrahydro-2-naphthalene-amine (58), (+)-*trans*-*N,N*-dimethyl-4-phenyl-6-methoxy-7-chloro-1,2,3,4-tetrahydro-2-naphthalene-amine (59), (-)-*cis*-*N,N*-dimethyl-4-phenyl-6-methoxy-7-chloro-1,2,3,4-tetrahydro-2-naphthalene-amine (60), (+)-*cis*-*N,N*-dimethyl-4-phenyl-6-methoxy-7-chloro-1,2,3,4-tetrahydro-2-naphthalene-amine (61). Compounds were prepared began with intermediate **74** or **77** following the same procedure described above.

58 Highly hygroscopic solid $[\alpha]^{25}_{D}$ = (-)46º(*c* 1.00, CH_2Cl_2), R_f of (-)-*trans*-**58**: 14.6min in HPLC separation. ^{1}H-NMR ($CDCl_3$) δ 7.32-7.14 (m, 4H), 6.93 (d, *J*=6 Hz, 2H), 6.54 (s,1H), 4.49 (m,1H), 3.76(s,3H), 3.27-3.21 (m,1H), 3.08-2.98 (m,2H), 2.72 (s,6H), 2.41-2.30 (m,2H), ^{13}C NMR ($CDCl_3$) δ 29.3, 31.8, 42.2, 43.7, 56.1, 58.0, 112.9, 121.8, 125.6, 127.1, 128.1, 128.5, 128.8, 130.6, 135.2, 143.9, 154.0, 162.6. HRMS *m/z* Calcd for $C_{19}H_{23}ClNO$ 316.147, 318.144 $[M+H]^+$, Found 316.146, 318.145, $[C_{19}H_{21}ClNO+H]^+$ isotope pattern confirmed.

59 Highly hygroscopic solid $[\alpha]^{25}_{D}$ = (+)42º(*c* 1.00, CH_2Cl_2), R_f of (+)-*trans*-**59**: 13.06min in HPLC separation. ^{1}H-NMR, ^{13}C NMR and HRMS spectra are the same with **58.**

60 Highly hygroscopic solid $[\alpha]^{25}_{D}$ = (-)98º(*c* 1.00, CH_2Cl_2), R_f of (-)-*cis*-**66b**: 14.6min in HPLC separation. ^{1}H-NMR ($CDCl_3$) δ 7.36-7.15 (m,6H), 6.28 (s,1H), 4.18-4.14 (dd, *J*=8.7, 3.6 Hz, 1H), 3.59 (s,3H), 3.19-3.07 (m,2H), 2.85 (s,6H), 2.52-2.50 (dd,

J=7, 2 Hz, 1H), 2.34-2.30 (t, *J*= 5.5 Hz, 1H), 1.96-1.87 (dd, *J*= 18.5, 9.1 Hz, 1H).^{13}C NMR ($CDCl_3$) δ 34.3, 39.2, 40.3, 46.0, 56.0, 61.1, 112.6, 121.3, 124.9, 127.4, 128.5, 129.0, 130.4, 137.5, 143.8, 153.8, 162.7. 163.1.HRMS *m/z* Calcd for $C_{19}H_{23}ClNO$ 316.147, 318.144 $[M+H]^+$, Found 316.146, 318.145, $[C_{19}H_{21}ClNO +H]^+$ isotope pattern confirmed.

61 Highly hygroscopic solid $[\alpha]^{25}_D$ = (+)111º(*c* 1.00, CH_2Cl_2), R_f of (+)-*cis*-**67b**: 12.8min in HPLC separation. . ^{1}H-NMR, ^{13}C NMR and HRMS spectra are the same with **60.**

(-)-*Trans*-*N,N*-dimethyl-4-(3-bromophenyl)-6-methoxy-7-chloro-1,2,3,4-tetrahydro-2-naphthalene amine (66) and (+)-*trans*-*N,N*-dimethyl-4-(3-bromophenyl)-6-methoxy-7-chloro-1,2,3,4-tetrahydro-2-naphthalene amine (67),

(-)-t*rans*-*N,N*-dimethyl-4-(3-chlorophenyl)-6-methoxy-1,2,3,4-tetrahydro-2-naphthalene-amine (68), and (-)-*Trans*-*N,N*-dimethyl-4-(3-chlorophenyl)-6-methoxy-1,2,3,4-tetrahydro-2-naphthalene-amine (69). Compounds were prepared began with intermediate **71** or **85** respectively following the same procedure described above.

66 Highly hygroscopic solid $[\alpha]^{25}_D$ = (-)14º(*c* 1.00, CH_2Cl_2), R_f of (-)-*trans*-**66**: 14.6min in HPLC separation. ^{1}H-NMR ($CDCl_3$) δ 7.39 (t, *J*=5.7 Hz, 1H), 7.26 (d, *J*=3.6Hz,1H), 7.19 (t, *J*=5.7 Hz, 1H), 7.09 (s, 1H), 6.87(d, *J*=6 Hz, 1H), 6.50 (s,1H), 4.45 (m,1H), 3.78(s,3H), 3.29-3.23 (m,2H), 3.9-3.02 (m,3H), 2.76 (s,6H), 2.38-2.34 (m,2H), ^{13}C NMR ($CDCl_3$) δ 29.1, 31.8, 42.3, 43.4, 56.2, 57.9, 112.8, 122.2, 123.1, 125.5, 126.9, 130.3, 130.8, 131.1, 134.3, 146.3, 154.2, 162.7. HRMS *m/z* Calcd for $C19H_{22}BrClNO$

394.057, 396.055 $[M+H]^+$, Found 394.058, 396.056, $[C_{19}H_{21}BrClNO +H]^+$ isotope pattern confirmed.

67 Highly hygroscopic solid $[\alpha]^{25}_D$ = (+)14º(*c* 1.00, CH_2Cl_2), R_f of (+)-*trans*-**67**: 13.1min in HPLC separation. ^{1}H-NMR, ^{13}C NMR and HRMS spectra are the same with **66.**

68 Highly hygroscopic solid $[\alpha]^{25}_D$ = (-)10º(*c* 1.00, CH_2Cl_2), R_f of (-)-*trans*-**68**: 14.5min in HPLC separation. ^{1}H-NMR ($CDCl_3$) δ 7.264 (d, *J*=1.2 Hz, 1H), 7.260-7.15 (m,1H), 7.10 (d, *J*=6.3 Hz, 1H), 7.09 (s, 1H), 6.91 (dd, *J*=4.8, 1.5 Hz,1H), 6.78 (dd, *J*=5.4, 1.8 Hz, 1H), 6.44 (d, *J*=1.5 Hz, 1H), 4.32 (t, *J*=3.6 Hz, 1H), 3.69 (s,3H), 3.04-2.99 (dd, *J*= 11.9, 3.8 Hz, 1H), 2.85-2.79 (m,1H), 2.69, (m,1H), 2.34 (s,6H), 2.16-2.11 (m,2H),^{13}C NMR ($CDCl_3$) δ 31.1, 34.4, 41.5, 44.0, 55.2, 56.6, 113.4, 114.3, 126.4, 126.8, 127.8, 128.7, 129.5, 130.3, 134.1, 137.7, 148.4, 157.9. HRMS *m/z* Calcd for $C19H_{23}ClNO$ 316.147, 318.144 $[M+H]^+$, Found 316.417, 318.144, $[C_{19}H_{23}ClNO +H]^+$ isotope pattern confirmed.

69 Highly hygroscopic solid $[\alpha]^{25}_D$ = (+)12º(*c* 1.00, CH_2Cl_2), R_f of (+)-*trans*-**69**: 12.7min in HPLC separation. ^{1}H-NMR, ^{13}C NMR and HRMS spectra are the same with **68.**

B: PHARMACOLOGICAL ASSAYS

Clonal cell culture and transfection (Booth et al., 2009).Chinese hamster ovary K1 cells (CHO, ATCC CCL-61) were maintained in Ham's F-12 medium supplemented with 10% fetal bovine serum and 1% sodium bicarbonate (Mediatech 25-035-CI), 10 IU/ml penicillin and 10 ug/ml streptomycin. Human embryonic kidney 293 cells (HEK, ATCC CRL-1573) were maintained in Eagle minimum essential medium with 10% fetal

bovine serum and 2 mM L-glutamine, 0.1 mM non-essential amino acids, 1.5 g/L sodium bicarbonate, 1.0 mM sodium pyruvate, 10 IU/ml penicillin, and 10 ug/ml streptomycin. Cells were grown in a humidified incubator at 37 °C with 5% carbon dioxide.

The cDNAs encoding the human serotonin 5HT2A, 5HT2B, and 5HT2C (unedited isoform) receptors were obtained from UMR (Rolla, MO). Serotonin 5HT2A and 5HT2B receptors were transiently expressed in HEK cells (Setola et al., 2005) and 5HT2C receptors were transiently expressed in CHO cells (Porter et al., 1999). HEK cells were grown to 90-95% confluence in 100 mm dishes and transfected with 24 µg of plasmid DNA for the wild type 5-HT2A or 5-HT2B receptor sequences using 40 µl of Lipofectamine 2000 (Invitrogen, Carlsbad, CA) per dish. Transfection proceeded for 24 hrs, then, medium was replaced by fresh growth medium and cells were allowed to express 5HT2A or 5HT2B receptors for another 24 hrs. CHO cells were grown to 40% confluence in 100 mm dishes and transfected with 12 µg of plasmid DNA for the wild type 5HT2C receptor sequence and 32 µl of Lipofectamine 2000, then, transfection and expression proceeded as above.

Radioreceptor assays (Booth et al., 2009). Radioreceptor saturation and competition binding assays were performed using membrane homogenates prepared from transfected CHO cells cells, similar to methods reported previously (Booth et al., 2002; Moniri et al., 2004). [^{3}H]-Ketanserin was used to radiolabel serotonin 5HT2A receptors and [^{3}H]-mesulergine was used to label serotonin 5HT2B and 5HT2C receptors (Knight et al., 2004). Forty-eight hours following transfection, cells were harvested and homogenized in 50 mM Tris-HCl containing 0.1 % ascorbic acid and 4.0

mM calcium chloride at pH 7.4 (assay buffer). The homogenate was centrifuged at 35,000 x*g* for 25 min and the resulting membrane pellet was re-suspended in assay buffer. Protein concentration was determined by the method of Lowry et al. (Lowry, 1951). For saturation binding assays, membrane suspension containing 20 μg (for 5HT2A receptor), 50 μg (for 5HT2B receptor) or 100 μg (for 5HT2C receptor) protein was incubated with 0.1 – 5.0 nM [^{3}H]-ketanserin (5HT2A receptors) or 0.1 – 20 nM [^{3}H]-mesulergine (5-HT$_{2B}$ and 5-HT$_{2C}$ receptors) in a total assay buffer volume of 250 μl. Non-specific binding was determined in the presence of 10 μM methysergide (5HT2A receptors) or 1.0 μM mianserin (5HT2B and 5HT2C receptors). Competition binding assays were conducted under the same conditions using 1.0 nM [^{3}H]-ketanserin (5HT2A receptors), 5.0 nM [^{3}H]-mesulergine (5HT2B receptors), or 1.0 nM [^{3}H]-mesulergine (5HT2C receptors) (~K_d concentration). Incubation of radioreceptor binding assay mixtures was for 1.0 h at 37°C, with termination by rapid filtration through Whatman GF/B filters using a 96-well cell harvester (Tomtec, Hamden, CT). The membrane-bound [^{3}H]-radioligand retained on the filter discs was quantified by liquid scintillation spectrometry. Data were analyzed by nonlinear regression using the sigmoidal curve-fitting algorithms in Prism 4.03 (GraphPad Software Inc., San Diego, CA). Ligand affinity is expressed as an approximation of K_i values by conversion of the IC_{50} data to K_i values using the equation $K_i = IC_{50}/1 + L/K_d$ where L is the concentration of radioligand having affinity K_d (Cheng, 1973). Each experimental condition was performed in triplicate and each experiment was performed a minimum of three times to determine S.E.M.

Assay for activation of PLC and [^{3}H]-IP formation. Functional activation of PLC was measured as [^{3}H]-IP formation in HEK cells transiently expressing serotonin -HT2A or 5HT2B receptors or CHO cells transiently expressing serotonin 5HT2C receptors, as previously reported (Moniri et al., 2004). HEK cells expressing serotonin 5-HT2A or 5-HT2B receptors, or, CHO cells expressing 5HT2C receptors were seeded at 10^5 cells per well in 12-well plates in inositol-free Dulbecco's modified Eagle's medium (DMEM) for 12 – 24 hours with 1.0 μCi/ml myo-[2-^{3}H]-inositol, the radiolabeled precursor of the PLC-β substrate phosphatidylinositol (with addition of 5% dialyzed fetal bovine serum to DMEM for HEK cells). Cells then were washed and incubated in inositol-free DMEM containing 10 mM lithium chloride, 10 μM pargyline, and various concentrations of test ligand for 45 – 60 min at 37 °C and 5% CO_2. After aspiration of media, wells were lysed by incubation with 50 mM formic acid (15 – 60 min). Formic acid was neutralized with ammonium hydroxide and contents from each well were added to individual AG1-X8 200-400 formate resin anion exchange columns. Ammonium formate/formic acid (1.2 M/0.1 M) was used to elute [^{3}H]-IP directly into scintillation vials for counting of tritium by liquid scintillation spectrometry. Resulting data were analyzed using the nonlinear regression algorithms in Prism 4.03 and are expressed as mean percentage of basal control [^{3}H]-IP formation, with potency expressed as concentration required to stimulate (EC_{50}) or inhibit (IC_{50}) maximal basal (constitutive) [^{3}H]-IP formation by 50% ± S.E.M. ($n \geq 3$).

LIST OF REFERENCES

Adams DR, Bentley JM, Benwell KR, Bickerdike MJ, Bodkin CD, Cliffe IA, Dourish CT, George AR, Kennett GA, Knight AR, Malcolm CS, Mansell HL, Misra A, Quirk K, Roffey JR, Vickers SP. Pyrrolo(iso)quinoline derivatives as 5-HT(2C) receptor agonists. Bioorg Med Chem Lett. 2006; 16:677-80.

Adrian, GP. Givors. Preparation of 4-(disubstituted aryl)-1-tetralones as intermediates for serotonin antagonists. Eur Pat Appl 1989; US5019655.

Allerton CMN, Andrews MD, Blagg J, Ellis D, Evrard E, Green MP, Liu KKC, McMurray G, Ralph M, Sanderson V, Ward R, Watson L. Design and synthesis of pyridazinone-based 5-HT2C agonists Bioorg Med Chem Lett 2009; 19: 5791–95.

Andersson PG, Schink HE, Österlund K**.** Asymmetric total synthesis of (+)-tolterodine, a new muscarinic receptor antagonist, via copper-assisted asymmetric conjugate addition of aryl grignard reagents to 3-phenyl-prop-2-enoyl-oxazolidinones**.** J Org Chem 1998; 8067-70.

Berg KA, Harvey JA, Spampinato U, Clarke WP. Physiological and therapeutic relevance of constitutive activity of 5-HT2A and 5-HT2C receptors for the treatment of depression. Prog Brain Res 2008; 172:287-305.

Bickerdike MJ, Vickers SP, Dourish CT. 5-HT2C receptor modulation and the treatment of obesity. Diabetes Obes Metab 1999; 1(4):207-14.

Browning J, Young K, Hicks P. The antipsychotic-like action of a 5-HT2C agonist on conditioned avoidance response behavior in rats. Abstr Soc Neurosci 1999; 25: 2075-87.

Boger DL, Mckie JA, Boyce CW. Asymmetric synthesis of the CBI alkylation subunit of the CC-1065 and duocarmycin analogs. Synlett 1997; 515-517.

Boger DL. Morden organic synthesis. TSRI Press 1999 P114.

Booth RG, Fang L, Wilczynski A, Sivendren S, Sun Z, Bruysters M, Sansuk K, and Leurs R. Molecular determinants of ligand-directed Gq versus Gs signaling for the histamine H_1 receptor. Abstracts of the Histamine Research Society 2007; 36:32, submitted for publication to Inflamm Res. June, 2007.

Booth RG, Baldessarini RJ. (+)-6,7-benzomorphan sigma ligands stimulate dopamine synthesis in rat corpus striatum tissue. Brain Res 1991; 557:349-52.

Booth RG, Baldessarini RJ. Adenosine A2 stimulation of tyrosine hydroxylase in rat striatal minces is reversed by dopamine D2 autoreceptor activation. Eur J Pharmacol 1990; 185:217-22.

Booth RG, Moniri NH. Novel Ligands Stabilize Stereo-Selective Conformations of the Histamine H1 Receptor to Activate Catecholamine Synthesis. Inflamm Res 2007; 56:1-12.

Booth RG, Moniri NH, Bakker RA, Choksi NY, Nix WB, Timmerman H, Leurs R. A novel phenylaminotetralin radioligand reveals a subpopulation of histamine H(1) receptors. J Pharmacol Exp Ther 2002; 302:328-36.

Bromidge SM, Duckworth M, Forbes IT, Ham P, King FD, Thewlis KM, Blaney FE, Naylor CB, Blackburn TP, Kennett GA, Wood MD, Clarke SE. 6-Chloro-5-methyl-1-[[2-[(2-methyl-3-pyridyl)oxy]-5-pyridyl]carbamoyl]- indoline (SB-242084): the first selective and brain penetrant 5-HT2C receptor antagonist. J Med Chem 1997; 40:3494-96.

Bubar MJ, Cunningham KA. Serotonin 5-HT2A and 5-HT2C receptors as potential targets for modulation of psychostimulant use and dependence. Curr Top Med Chem 2006; 6:1971-85.

Bucholtz EC, Brown RL, Tropsha A, Booth RG, Wyrick SD. Synthesis, Evaluation and Comparative Molecular Field Analysis of 1-Phenyl-3-amino-1,2,3,4-tetrahydronaphthalenes as Ligands for Histamine H1 Receptors. J Med Chem 1999; .42:3041-54

Bucholtz EC, Wyrick SD, Owens CE, Booth RG. 1-Phenyl-3-dimethylaminotetralins (PATs): Effect of stereochemistry on binding and function at brain histamine receptors. Med Chem Res 1998; 8:322-32.

Celine M, Patrick M, Jacques M.Synthesis of Oxa-Bridged Analogs of Farnesyltransferase Inhibitor RPR 115135. J Org Chem 2001; 3797-805.

Chanrion B, Mannoury la Cour C, Gavarini S, Seimandi M, Vincent L, Pujol JF, Bockaert J, Marin P, Millan MJ. Inverse agonist and neutral antagonist actions of antidepressants at recombinant and native 5-hydroxytryptamine2C receptors: differential modulation of cell surface expression and signal transduction. Mol Pharmacol 2008; 73: 748-57.

Chen CY, Reamer RA. Efficient enantioselective synthesis of sertraline, a potent antidepressant, via a novel intramolecular nucleophilic additonto imine. Org let 1999; 293-4.

Choksi NY, Nix WB, Wyrick SD, Booth RG. A novel phenylaminotetralin (PAT) recognizes histamine H1 receptors and stimulates dopamine synthesis in vivo in rat brain. Brain Res 2000; 852: 151–60.

Dale JA, Dull DL, Mosher HS. α-Methoxy-α-trifluoromethylphenylacetic acid, a versiatile reagent for the determination of enantiomeric composition of alcohols and amines. J Org Chem 1969; 34: 2543-49.

Dale JA, Mosher HS. Nuclear magnetic resonance enantiomer reagent. Configurational correlations via nuclear magnetic resonance chemical shift of diastereomeric mandelate, O-methylmandelate and α-Methoxy-α-trifluoromethylphenylacetate (MTPA) esters. J Am Chem Soc 1973; 95: 512-19.

Davies MA, Sheffler DJ, Roth BL. Aripiprazole: a novel atypical antipsychotic drug with a uniquely robust pharmacology. CNS Drug Rev 2004; 10:317-36.

DiMauro EF, Kozlowski MC. Salen-derived catalysts containing secondary basic groups in the addition of diethylzinc to aldehydes. Org Lett 2001;19:3053-6.

Di Matteo V, De Blasi A, Giulio C, et al. Role of 5-HT(2C) receptors in the control of central dopamine function Trends Pharmacol Sci 2001; 22: 229-32.

Dunlop J, Sabb AL, Mazandarani H, Zhang J, Kalgaonker S, Shukhina E, Sukoff S, Vogel RL, Stack G, Schechter L, Harrison BL, Rosenzweig-Lipson S.WAY-163909 [(7bR,10aR)-1,2,3,4,8,9,10,10a-octahydro-7bH-cyclopenta-b][1,4]diazepino[6,7,1hi]indole], a novel 5-hydroxytryptamine 2C receptor-selective agonist with anorectic activity. J Pharmacol Exp Ther 2005; 313:862-9.

Egami H, katsuki T. Fe(salan)-catalyzed asymmetric oxidation of sulfides with hydrogen peroxide in water. J Am Chem Soc. 2007; 129:8940-1.

Eltayb A, Wadenberg ML, Schilström B, Svensson TH. Antipsychotic-like effect by combined treatment with citalopram and WAY 100635: involvement of the 5-HT2C receptor. Int J Neuropsychopharmacol 2007;10:405-10.

Esposito E. Serotonin-dopamine interaction as a focus of novel antidepressant drugs. Curr Drug Targets 2006; 7:177-85.

Fitzgerald LW, Burn TC, Brown BS, Patterson JP, Corjay MH, Valentine PA, Sun JH, Link JR, Abbaszade I, Hollis JM, et al. Possible role of valvular serotonin 5-HT(2B) receptors in the cardiopathy associated with fenfluramine. Mol Pharmacol 2000; 57: 75–81.

Fink KB, Goethert M. 5-HT receptor regulation of neurotransmitter release. Pharmacol Rev 2007; 59:360-417.

Fletcher PJ, Chintoh AF, Sinyard J, Higgins GA. Antipsychotic-like effect by combined treatment with citalopram and WAY 100635: involvement of the 5-HT2C receptor. Int J Neuropsychopharmacol 2007;10:405-10.

Fletcher PJ, Grottick AJ, Higgins GA. Differential effects of the 5-HT(2A) receptor antagonist M100907 and the 5-HT(2C) receptor antagonist SB242084 on cocaine-induced locomotor activity, cocaine self-administration and cocaine-induced reinstatement of responding. Neuropsychopharmacology 2002; 27:576–86.

Fletcher PJ, Sinyard J, Higgins GA. The effects of the 5-HT(2C) receptor antagonist SB242084 on locomotor activity induced by selective, or mixed, indirect serotonergic and dopaminergic agonists. Psychopharmacology (Berl) 2006; 87:515-25.

Foguet M, Hoyer D, Pardo LA, Parekh A, Kluxen FW, Kalkman HO, Stuhmerr W, Luebbert H. Cloning and functional characterization of the rat stomach fundus serotonin receptor. EMBO J 1992; 11: 3481-87.

Frank MG, Stryker MP, Tecott LH. Sleep and sleep homeostasis in mice lacking the 5-HT2c receptor. Neuropsychopharmacology 2002; 27:869-73.

Gatti G, Piersanti G, Spadoni G. Conformation by NMR of two tetralin-based receptor ligands. Il Farmaco 2003; 58:469-76.

Giorgioni G, Accorroni B, Stefano AD, Marucci G, Siniscalchi A and Claudi F. Benzimidazole, Benzoxazole and Benzothiazole Derivatives as 5HT2B Receptor Ligands. Synthesis and Preliminary Pharmacological Evaluation. Med Chem Res 2005; 14:57-73.

Glennon, R.A. Do classical hallucinogens act as 5-HT_2 agonists or antagonists? Neuropsychopharmacology 1990; 3:509–17.

Goldstein J. Wall Street Journal March 30, 2009; http://blogs.wsj.com/health/2009/03/30/obesity-drug-development-is-tough-just-ask-arena/tab/article/

Grauer S, Brennan J, Piesla M, Comery T, Sabb A, Marquis K, Rosenzweig-Lipson S WAY-909, a 5-HT_{2C} agonist, exhibits an atypical-like antipsychotic profile in a battery of rodent behavioral models. Abstr Soc Neurosci 2004; 349-57.

Gray JA, Roth BL. Molecular targets for treating cognitive dysfunction in schizophrenia. Schizophr Bull 2007; 33:1100-19.

Grottick AJ, Fletcher PJ, Higgins GA. Studies to investigate the role of 5-HT(2C) receptors on cocaine- and food-maintained behavior. J Pharmacol Exp Ther 2000; 295:1183–91.

Gruender G, Hippius H, Carlsson A. The 'atypicality' of antipsychotics: a concept re-examined and re-defined. Nat Rev Drug Discov 2009; 8:197-202.

Halford JC, Harrold JA, Lawton CL, Blundell JE. Serotonin (5-HT) drugs: effects on appetite expression and use for the treatment of obesity. Curr Drug Targets 2005; 6:201-13.

Hayashi A, Suzuki M, Sasamata M, Miyata K. Agonist diversity in 5-HT(2C) receptor-mediated weight control in rats. Psychopharmacology (Berl) 2005; 178:241-49.

Heisler LK, Chu HM, Tecott LH, Epilepsy and obesity in serotonin 5-HT2C receptor mutant mice. Ann N Y Acad Sci 1998; 861:74-8.

Heisler LK, Cowley MA, Tecott LH, Fan W, Low MJ, Smart JL, Rubinstein M, Tatro JB, Marcus JN, Holstege H, et al. Activation of central melanocortin pathways by fenfluramine. Science (Wash DC) 2002; 297:609–11.

Heisler LK, Jobst EE, Sutton GM, Zhou L, Borok E, Thornton-Jones Z, Liu HY, Zigman JM, Balthasar N, Kishi T, Lee CE, Aschkenasi CJ, Zhang CY, Yu J, Boss O, Mountjoy KG, Clifton PG, Lowell BB, Friedman JM, Horvath T, Butler AA, Elmquist JK, Cowley MA. Serotonin reciprocally regulates melanocortin neurons to modulate food intake. Neuron 2006; 51:239-49.

Heisler LK, Zhou L, Bajwa P, Hsu J, Tecott LH Serotonin 5-HT(2C) receptors regulate anxiety-like behavior. Genes Brain Behav 2007; 6:491-6.

Herve D, Pickel VM, Joh TH, Beaudet A. Brain Reserch 1987; 435:71-83.

Hoyer D, Clarke DE, Fozard JR, Hartig PR, Martin GE, Mylecharane EJ, Saxena PR, Humphrey PP. International Union of Pharmacology classification of receptors for 5- hydroxytryptamine (Serotonin). Pharmacol Rev 1994; 46:157-203.

Horacek J, Bubenikova-Valesova V, Kopecek M, Palenicek T,Dockery C, Mohr P, Höschl C. CNS Drugs 2006; 20: 389-411.

Ho GJ, Mathre DJ. Lithium-initiated imide formation. A simple method for N-acylation of 2-Oxazolidinone and bornane-2,10-sultam. J Org Chem 1995; 2271-73.

Hutson PH, Barton CL, Jay M, et al. Activation of mesolimbic dopamine function by phencyclidine is enhanced by 5-HT(2C/ 2B) receptor antagonists: neurochemical and behavioural studies. Neuropharmacology 2000; 39: 2318-28.

Itoh T, Mase T, Nishikata T, Iyama T, Tachikawa H, Kobayashi Y, Yamamoto Y, Miyaura N.1,4-Addition of arylboronic acids to β-aryl-α,β-unsaturated ketones and esters catalyzed by a rhodium(I)–chiraphos complex for catalytic and enantioselective synthesis of selective endothelin A receptor antagonists. Tetrahedron 2006; 9610-21.

Julius D, Huang KN, Livelli TJ, Axel R, Jessel TM. The 5HT2 receptor defines a family of structurally distinct but functionally conserved serotonin receptors. Proc Natl Acad Sci 1990; 87:928–32.

Julius D, MacDermott AB, Axel R, Jessell TM. Molecular Characterization of a functional cDNA encoding the serotonin 1c receptor. Science 1988; 241:558–64.

Jun-Xu L, Unzeitig A, Javors MA, Rice KC, Koek W, France CP. Discriminative stimulus effects of 1-(2,5-dimethoxy-4-methylphenyl)-2-aminopropane (DOM), ketanserin, and (R)-(+)-.alpha.-(2,3-dimethoxyphenyl)-1-[2-(4-fluorophenyl)ethyl]-4-pipidinemethanol (MDL100907) in rats. J Pharmacol Exp Ther 2009; 331: 671-79.

Kehne JH, Moser PC, Moran PM, Frank RA. Reversal of amphetamine-induced behaviours by MDL 100,907, a selective 5-HT2A antagonist. Behav Brain Res 1996; 73:163-7.

Kimura Y, Hatanaka K, Naitou Y, Maeno K, Shimada I, Koakutsu A, Wanibuchi F, Yamaguchi T. Pharmacological profile of YM348, a novel, potent and orally active 5-HT2C receptor agonist. Eur J Pharmacol 2004; 483:37-43.

Knight AR, Misra A, Quirk K, Benwell K, Revell D, Kennett G, Bickerdike M. Pharmacological characterisation of the agonist radioligand binding site of 5-HT(2A), 5-HT(2B) and 5-HT(2C) receptors. Naunyn Schmiedebergs Arch Pharmacol 2004; 370:114-23.

Kroeze WK, Hufeisen SJ, Popadak BA, Renock SM, Steinberg S, Ernsberger P, Jayathilake K, Meltzer HY, Roth BL. 2003. H1-histamine receptor affinity predicts short-term weight gain for typical and atypical antipsychotic drugs. Neuropsychopharmacology 28, 519–526.

Kroeze WK, Kristiansen K, Roth BL. Molecular Biology of Serotonin Receptors - Structure and Function at the Molecular Level. Curr Top Med Chem 2002; 22: 507-28.

Kursar JD, Nelson DL, Wainscott DB, Baez M. Molecular cloning, functional expression, and mRNA tissue distribution of the human 5-hydroxytryptamine2B receptor. Mol. Pharmacol 1994; 46: 227-34.

Lam DD, Heisler LK. Serotonin and energy balance: molecular mechanisms and implications for type 2 diabetes. Expert Rev Mol Med 2007; 9:1–24.

Lamberts, JJ, Cuppen, TJ, Laarhoven, WH. Thermolysis of phenyl-substituted 1,2-dihydronaphthalenes. Evidence for diphenylbutadienes as intermediates. J Chem Soc Perkin Trans I 1985; 9:1819-27.

Launay JM, Herve P, Peoc'h K, Tournois C, Callebert J, Nebigil CG, Etienne N, Drouet L, Humbert M, Simonneau G, et al. Function of the serotonin 5-hydroxytryptamine 2B receptor in pulmonary hypertension. Nat Med 2002; 8:1129–35.

Leff P, Scaramellini C, Law C, McKechnie K. A three-state receptor model of agonist action. Trends Pharmacol Sci 1997; 18: 355–62.

Liu KKC, Cornelius P, Patterson TA, Zeng Y, Santucci S, Tomlinson E, Gibbons C, Maurer TS, Marala R, Brown J, Kong JX, Lee E, Werner W, Wenzel Z, Vage C. Design and synthesis of orally-active and selective azaindane 5HT2c agonist for the treatment of obesity. Bioorg Med Chem Lett 2010; 20:266–71.

Lucero MJ,Houk KN. Torsional Control of Epoxidation Stereoselectivity in 1,2-Dihydronaphthalenes. Transition State Modeling with Semiempirical Quantum Mechanics. J Org Chem 1998; 63: 6973-77.

Lubbert H, Hoffman BJ. Snutch TP, van Dyke T, Levine AJ, Hartig PR, Lester HA, Davidson N. cDNA cloning of a serotonin 5-HT1C receptor by electrophysiological assays of mRNA-injected Xenopus oocytes. Proc Natl Aca Sci USA 1987; 84:4332–36.

Maeda K, Brown JM. Efficient kinetic resolution in hydroboration of 1,2-dihydronaphthalenes. Chem Commum. 2002; 310-11.

Mai A, Massa S, Valente S, Simeoni S, Ragno R, Bottoni P, Scatena R, Brosch G. . Aroyl-pyrrolyl hydroxyamides: influence of pyrrole C4-phenylacetyl substitution on histone deacetylase inhibition. ChemMedChem 2006; 2: 225-37.

Marquis KL, Sabb AL, Logue SF, Brennan JA, Piesla MJ, Comery TA, Grauer SM, Ashby CR Jr, Nguyen HQ, Dawson LA, Barrett JE, Stack G, Meltzer HY, Harrison BL, Rosenzweig-Lipson S. WAY-163909 [(7bR,10aR)-1,2,3,4,8,9,10,10a-octahydro-7bH-cyclopenta-[b][1,4]diazepino[6,7,1hi]indole]: A novel 5-hydroxytryptamine 2C receptor-selective agonist with preclinical antipsychotic-like activity. J Pharmacol Exp Ther 2007; 320:486-496.

Martinelli MJ,Peterson BC,Khau VV,Hutchison DR,Leanna MR,Audia,JE, Droste JJ. Stereoselective Epoxidations and Electrophilic Additions to Partial Ergot Alkaloids and Conformationally-Fixed Styrenes. Experimental and Theoretical Modeling Evidence for the Importance of Torsional Steering as a Stereocontrol Element. J Org Chem 1994; 59: 2204-10.

Meltzer HY, Li Z, Kaneda Y, et al. Serotonin receptors: their key role in drugs to treat schizophrenia. Prog Neuropsychopharmacol Biol Psychiatry 2003; 27:1159-72.

Meltzer HY, Arvantis L, Bauer D, Rein W. Placebo-controlled evaluation of four novel compounds for the treatment of schizophrenia and schizoaffective disorder. Am J Psychiatry 2004; 161:975-84.

Miller, Lisa J, Michael E. Atypical antipsychotic drug-induced weight gain: focus on metformin. Pharmacotherapy 2009; 29: 725-35.

Mogi M, Fugi K, Node M. Asymmetric reduction of methoxy substituted β-tetralones using hydrogenation. Tetrahedron Asymmetry 2004; 15:3715-17.

Monguchi Y, Kume A, Hattori K, Maegawa T, Sajiki H. Pd/C–Et_3N-mediated catalytic hydrodechlorination of aromatic chlorides under mild conditions. Tetrahedron 2006; 62: 7926–33.

Moniri NH, Booth RG. Role of PKA and PKC in histamine H1 receptor-mediated activation of catecholamine neurotransmitter synthesis. Neurosci Lett 2006; 407: 249–53.

Moniri NH, Covington-Strachan D, Booth RG. Ligand-directed functional heterogeneity of histamine H1 receptors: Novel dualfunction ligands selectively activate and block H1-meditated phospholipase C and adenylyl cyclase signaling. J Pharmacol Exp Ther 2004; 311: 274–8.

Navarra R, Comery TA, Graf R, Rosenzweig-Lipson S, Day M.The 5-HT(2C) receptor agonist WAY-163909 decreases impulsivity in the 5-choice serial reaction time test.Behav Brain Res 2008; 188:412-5.

Nichols DE. Hallucinogens. Pharmacol Ther 2004 ; **101**:131–81.

Nilsson BM. 5-Hydroxytryptamine 2C (5-HT2C) receptor agonists as potential antiobesity agents. J Med Chem 2006; 49:4023-34.

Nocjar C, Roth BL, Pehek EA. Localization of 5-HT(2A) receptors on dopamine cells in subnuclei of the midbrain A10 cell group. Neuroscience 2002; 111:163-76.

Noyori E. Pioneering perspectives on asymmetric hydrogenation. Acc Chem Res 2007; 40:1238–1239.

Palucki M, Pospisil PJ, Zhang W, Jacobsen EN. Highly enantioselective, low temperature epoxidation of terminal olefins. J Am Chem Soc 1994; 116: 9333–34.

Palvimaki E, Roth BL, Majasuo H, Laakso A, Kuoppamaki M, Syvalahti E, Interactions of selective serotonin reuptake inhibitors with the serotonin 5-HT2C receptor. Psychopharmacology 1996; 126: 234–40.

Poissonnet G, Parmentier JG, Boutin JA, Goldstein S. The Emergence of selective 5-HT2B antagonists structures, activities and potential therapeutic applications. Mini rev med chem 2004; 4: 325-30.

Porter RH, Benwell KR, Lamb H, Malcolm CS, Allen NH, Revell DF, Adams DR, Sheardown MJ. Functional characterization of agonists at recombinant human 5-HT2A, 5-HT2B and 5-HT2C receptors in CHO-K1 cells. Br J Pharmacol 1999; 128:13-20.

Powell CM, Miyakawa T. Schizophrenia-relevant behavioral testing in rodent models: a uniquely human disorder? Biol Psychiatry 2006; 59: 1198-207.

Raymond JR. Mukhin YV. Gelasco A. Turner J. Collinsworth G. Gettys TW. Grewal JS. Garnovskaya MN. Multiplicity of mechanisms of serotonin receptor signal transduction. Pharmacol Ther 2001; 92:179-212.

Reynolds GP, Templeman LA, Zhang ZJ. The role of 5-HT2C receptor polymorphisms in the pharmacogenetics of antipsychotic drug treatment. Prog Neuropsychopharmacol Biol Psychiatry 2005; 29:1021-28.

Rowland NE, Crump EM, Nguyen N, Robertson K, Sun Z, Booth RG. Effect of (-)-trans-PAT, a novel 5-HT2C receptor agonist, on intake of palatable food in mice. Pharmacol Biochem Behav 2008; 91:176-80.

Rosenzweig-Lipson S, Zhang J, Mazandarani H, Harrison BL, Sabb A, Sabalski J, Stack G, Welmaker G, Barrett JE, Dunlop J. Antiobesity-like effects of the 5-HT2C receptor agonist WAY-161503. Brain Res 2006; 1073-74.

Rosenzweig-Lipson S, Sabb A, Stack G, Mitchell P, Lucki I, Malberg JE, Grauer S, Brennan J, Cryan JF, Sukoff Rizzo SJ, Dunlop J, Barrett JE, Marquis KL. Antidepressant-like effects of the novel, selective, 5-HT(2C) receptor agonist WAY-163909 in rodents. Psychopharmacology (Berl) 2007; 192:159-70.

Roth BL, Willins DL, Kristiansen K, Kroeze WK. 5- hydroxytryptamine2-family receptors (5-hydroxytryptamine2A, 5-hydroxytryptamine2B, 5-hydroxytryptamine2C): where structure meets function. Pharmacol Ther 1998; 79:231–57.

Roth BL. Drugs and valvular heart disease. N Engl J Med 2007; 356: 6-9.

Rothman RB, Baumann MH, Savage JE, Rauser L, McBride A, Hufeisen SJ, and Roth BL. Evidence for possible involvement of 5-HT(2B) receptors in the cardiac valvulopathy associated with fenfluramine and other serotonergic medications. Circulation 2000; 102: 2836–41.

Röver S, Adams DR, Bénardeau A, Bentley JM, Bickerdike MJ, Bourson A, Cliffe IA, Coassolo P, Davidson JE, Dourish CT, Hebeisen P, Kennett GA, Knight AR, Malcolm CS, Mattei P, Misra A, Mizrahi J, Muller M, Porter RH, Richter H, Taylor S, Vickers SP.Identification of 4-methyl-1,2,3,4,10,10a-hexahydropyrazino[1,2-a]indoles as 5-HT2C receptor agonists. Bioorg Med Chem Lett 2005;15:3604-8.

Sabb AL, Vogel RL, Welmaker GS, Sabalski JE, Coupet J, Dunlop J, Rosenzweig-Lipson S, Harrison B.Cycloalkyl[b][1,4]benzodiazepinoindoles are agonists at the human 5-HT2C receptor. Bioorg Med Chem Lett. 2004; 14:2603-7.

Saltzman AG, Morse B, Whitman MM, Ivanshchenko Y, Jaye M, Felder S. Cloning of the human serotonin 5-HT2 and 5-HT1C receptor subtypes. Biochem Biophys Res Commun. 1991 181:1469-7148.

Sard H, Kumaran G, Morency C, Roth BL, Toth BA, He P, Shuster L. SAR of psilocybin analogs: discovery of a selective 5-HT 2C agonist. Bioorg Med Chem Lett 2005; 15:4555-59.

Seifert R, Wenzel-Seifert K, Burckstummer T, Pertz HH, Schunack W, Dove S, Buschauer A, Elz S. Multiple differences in agonist and antagonist pharmacology between human and guinea pig histamine H1-receptor. J Pharmacol Exp Ther 2003; 305:1104–15.

Siuciak JA, Chapin DS, McCarthy SA, Guanowsky V, Brown J, Chiang P, Marala R, Patterson T, Seymour PA, Swick A, Iredale PA.CP-809,101, a selective 5-HT2C agonist, shows activity in animal models of antipsychotic activity. Neuropharmacology 2007; 52:279-90.

Shimada I, Maeno K, Kondoh Y, Kaku H, Sugasawa K, Kimura Y, Hatanaka K, Naitou Y, Wanibuchi F, Sakamoto S, Tsukamoto S.Synthesis and structure-activity relationships of a series of benzazepine derivatives as 5-HT2C receptor agonists. Bioorg Med Chem 2008; 16:3309-20.

Shimada I, Maeno K, Kazuta K, Kubota H, Kimizuka T, Kimura Y, Hatanaka K, Naitou Y, Wanibuchi F, Sakamoto S, Tsukamoto S. Synthesis and structure-activity relationships of a series of substituted 2-(1H-furo[2,3-g]indazol-1-yl)ethylamine derivatives as 5-HT2C receptor agonists. Bioorg Med Chem 2008;16:1966-82.

Shimada Y, Kondo S, Ohara Y, Matsumoto K, Katsuki T. Titanium-catalyzed asymmetric epoxidation of olefins with aqueous hydrogen peroxide: remarkable effect of phosphate buffer on epoxide yield. Synlett 2007; 2445-47.

Siuciak JA, Chapin DS, McCarthy SA, Guanowsky V, Brown J, Chiang P, Marala R, Patterson T, Seymour PA, Swick A, Iredale PA. CP-809,101, a selective 5-HT2C agonist, shows activity in animal models of antipsychotic activity. Neuropharmacology. 2007; 52:279-90.

Smith BM, Smith JM, Tsai JH, Schultz JA, Gilson CA, Estrada SA, Chen RR, Park DM, Prieto EB, allardo CS, Sengupta D, Thomsen WJ, Saldana HR, Whelan KT, Menzaghi F, Webb RR, Beeley NR. Discovery and SAR of new benzazepines as potent and selective 5-HT(2C) receptor agonists for the treatment of obesity. Bioorg Med Chem Lett 2005; 15:1467-70.

Smith S, Prosser W, Donahue D, Anderson C, Shanahan W. 66th Annu Meet Sci Sess Am Diabetes Assoc 2006; Abst 344.

Sung Jin Cho, Jensen NH, Kurome T, Kadari S, Manzano ML, Malberg JE, Caldarone B, Roth BL, Kozikowski AP. Selective 5-Hydroxytryptamine 2C Receptor Agonists Derived from the Lead Compound Tranylcypromine: Identification of Drugs with Antidepressant-Like Action. J Med Chem 2009; 52:1885–902.

Tecott LH, Sun LM, Akana SF, Strack AM, Lowenstein DH, Dallman MF, Julius D. Eating disorder and epilepsy in mice lacking 5-HT2c serotonin receptors. Nature 1995; 374:542-6.

Thomsen WJ, Grottick AJ, Menzaghi F, Reyes-Saldana H, Espitia S, Yuskin D, Whelan K, Martin M, Morgan M, Chen W, Al-Shamma H, Smith B, Chalmers D, Behan D.Lorcaserin, a novel selective human 5-hydroxytryptamine2C agonist: in vitro and in vivo pharmacological characterization. J Pharmacol Exp Ther 2008; 325:577-87.

Turner JH, Raymond JR. Interaction of calmodulin with the serotonin 5-hydroxytryptamine2A receptor. A putative regulator of G protein coupling and receptor phosphorylation by protein kinase C. J Biol Chem 2005; 280:30741-50.

Vincek AS, Booth RG. New Approach to 4-Phenyl-β-aminotetralin from 4-(3-Halophenyl)tetralen-2-ol Phenylacetate. Tetrahedron Letters 2009; 50:5107-08.

Weiner DM, Burstein ES, Nash N, Croston GE, Currier EA, Vanover KE, Harvey S, Donahue E, Hansen HC, Andersson CM, et al. 5-Hydroxytriptamine$_{2A}$ receptor inverse agonists as antipsychotics. J Pharmacol Exp Ther 2001; 299: 268-76.

Wyrick SD, Booth RG, Myers AM, Kula NS, Baldessarini RJ. Synthesis of [*N*-C^3H_3]-racemic-*trans*-1-phenyl-3-dimethylamino-6-chloro-7-hydroxy-1,2,3,4-tetrahydronaphthalene (PAT-6). J Lab Comp. Radiopharm 1992; 31:871-4.

Wyrick SD, Booth RG, Myers AM, Owens CE, Bucholtz EC, Hooper PC, Kula NS, Baldessarini RJ, Mailman RB. 1-Phenyl-3-amino-1,2,3,4-tetrahydronaphthalenes and related derivatives as ligands for the neuromodulatory σ_3 receptor: Further structure-activity relationships. J Med Chem 1995; 38:3857-64.

Wyrick SD, Booth RG, Myers AM, Owens CE, Kula NS, Baldessarini RJ, Mailman RB. Synthesis and pharmacological evaluation of 1-phenyl-3-amino-1,2,3,4-tetrahydronaphthalenes as ligands for a novel receptor with sigma-like neuromodulatory activity. J Med Chem 1993; 36: 2542-51.

BIOGRAPHICAL SKETCH

Mr. Zhuming Sun was born in Yangzhou, China. He received his bachelor degree in China Pharmaceutical University. He completed his graduate research in the Deptment.of Medicinal Chemistry University of Florida in the summer of 2010.